

**Numerical Simulation of Enhanced Heat Transfer of PVT
Unit Under Condensation and Cooling Conditions**

冷凝与冷却工况下 PVT 组件强化传热数值模拟研究

by

Pie Basalike

11706114

to

Institute of Building Energy, School of Civil Engineering

in partial fulfillment of the requirements

for the degree of

Doctor of Philosophy

in the subject of

Heating, Ventilation and Air Conditioning Engineering

on

September, 2022

Dissertation Supervisors

Prof. Jili Zhang

And Dr. Peng Wang

大连理工大学

Dalian University of Technology

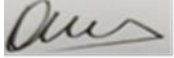
Dalian University of Technology Dissertation

Originality Declaration

I declare that this thesis dissertation is the result of an independent research I have made under the supervision of my supervisor. It does not contain any published or unpublished works or research results by other individuals or institutions apart from those that have been referenced in the form of references or notes. All individuals and institutions that have made contributions to my research have been acknowledged in the Acknowledgement.

I am fully aware that I myself will bear all the legal responsibility arising from violation of the above declaration.

Dissertation Title: Numerical Simulation of Enhanced Heat Transfer of PVT Unit Under
Condensation Condition and Cooling Conditions

Author Signature:  Date: 19/09/2022

大连理工大学学位论文独创性声明

作者郑重声明：所呈交的学位论文，是本人在导师的指导下进行研究工作所取得的成果。尽我所知，除文中已经注明引用内容和致谢的地方外，本论文不包含其他个人或集体已经发表的研究成果，也不包含其他已申请学位或其他用途使用过的成果。与我一同工作的同志对本研究所做的贡献均已在论文中做了明确的说明并表示了谢意。

若有不实之处，本人愿意承担相关法律责任。

学位论文题目：冷凝与冷却条件下 PVT 组件强化传热数值模拟研究

作者签名： 日期：2022年09月19日

Abstract

In order to cope with energy related sustainability issues, it is urgent to reduce building energy consumption. Developing and using clean energy is an effective way to solve this problem. In recent years, solar photovoltaic thermal (PVT) heat pump system is being developed at the rapid pace. It can provide a variety of energy and resources such as heat, electricity, cold and domestic hot water, while realizing the conversion and utilization of a variety of renewable energy. With research advancement, a novel of Photovoltaic Thermal (PVT) heat pump system that can operate both during day and night in summer is currently under development. In the daytime, PVT heat pump system uses PVT unit as evaporator, that can not only generate electricity and heat, but also effectively cool the solar cells, so that the temperature of the solar cells can be maintained in the range of high power generation and therefore, improvement in the power generation efficiency of the system is achieved. At night, the PVT unit will act as a condenser to release the condensation heat of the heat pump system in the form of long wave cold radiation and natural convection of the surrounding air. The heat pump system will realize the night cooling process to produce the chilled water or ice (ice storage) required by the building.

Specifically, the PVT unit is composed of a roll bond heat exchange plate added behind the PV unit. A serpentine refrigerant channel is arranged inside the inflatable heat exchange plate. In daytime, the refrigerant vapor-liquid two-phase fluid flows into the inflatable heat exchanger plate, evaporates in its serpentine channel and then flows out. At night, the refrigerant vapor flows into the inflatable heat exchanger plate, cools, condenses and releases condensation heat in its serpentine channel, and then flows out. In the process, the condensation heat of the PVT heat pump system is continuously released to the ambient and the sky by convection, radiation and conduction through different layer materials of the PVT unit. Therefore, the heat released by the PVT unit under condensation condition will directly affect the cooling capacity of PVT heat pump system at night. The condensation and heat release characteristics of PVT unit are closely related to the shape of serpentine channel structure, the shape of surface structure, the flow and heat transfer state of refrigerant in channel, the thermal conductivity between the plate and PV unit, and the sky effective temperature. In order to improve the night cooling performance of PVT heat pump system, it is necessary to study the condensation and heat transfer characteristics of PVT units at night in summer. In addition, PVT units can participate in the heat exchange of the system in the form of the above condenser at night in summer, and can also realize the natural cooling operation with the sky and air in the form of radiation heat exchange cooler alone. At this time, the working medium flowing through the PVT channel can be water, glycol solution and nano fluid. This sensible heat

exothermic cooling technology has been applied in building roof cooling systems, its cooling and heat transfer performance also needs to be further improved. Therefore, this thesis uses numerical simulation method to study the condensation and cooling enhanced heat transfer characteristics of PVT unit at night in summer, in order to optimize the design of PVT unit channel and improve its heat transfer performance.

In order to achieve this goal, this paper has carried out numerical modeling and simulation research in ANSYS fluent 18 on four types of PVT units: the existing serpentine channel PVT unit condenser (model 1), the serpentine channel PVT unit condenser with fins (model 2), the PVT unit condenser with hexagonal grid channel coupled with fluid channel with serpentine arrangement (model 3), and the PVT unit with water- $\text{Al}_3\text{O}_2/\text{Ag}$ as the fluid medium (model 4). The purpose of this thesis is to develop and propose alternative methods to enhance the heat transfer characteristics of PVT units. Therefore, firstly, the existing system experimental for studying PVT unit condenser is introduced in details and then followed the description of other used representative numerical models of PVT units. For the sake of simplicity and less computational time, the models are scaled down before being solved. In addition, the mathematical equations of fluid heat transfer process in PVT unit materials are described in details. In the research process, the refrigerant used in the existing serpentine channel PVT unit condenser and the serpentine channel PVT unit condenser with fins is R407C, and the refrigerant used in the PVT unit condenser with hexagonal grid channel coupled with fluid channel with serpentine arrangement is R134a.

Then, simulation assumptions and model verification are carried out to better solve mathematical equations. First, before simulation, this thesis studies and sets up appropriate model solving methods, operating conditions, assumptions and grid quality that can capture the solution. The accuracy of the model is determined by comparing the simulation results of this paper with the existing research results. In this process, the main parameters compared are performance coefficient, heat dissipation, outlet temperature, condenser surface temperature, temperature, speed and vapor volume fraction. Secondly, in the process of simulation, this thesis verifies the model. The verification model of the existing serpentine channel PVT unit condenser is helpful to determine the optimal size of the component channel structure and optimize the heat transfer characteristics of the PVT unit condenser. The influence of fins on the heat transfer characteristics and overall performance coefficient of PVT unit condenser is realized through the validation model of PVT unit with fins. In order to further find an alternative method to improve the night cooling performance of PVT unit condenser, a PVT unit condenser model integrating hexagonal grid channel coupled with fluid channel with serpentine arrangement is proposed and verified in this thesis. Furthermore, a model of nanofluid based PVT unit is solved to study the influence of using new fluid medium of nanofluid on the heat transfer characteristics of PVT unit under cooling condition.

On the basis of validated models, this thesis conducts numerical simulation for the specific application conditions of various PVT unit condensers. First, in order to design and optimize the PVT unit condenser, model 1 is established and verified, and then the PVT unit condenser is designed and optimized. In the PVT unit condenser, the heat flux of the outer surface largely depends on the heat conduction through the material. Increasing/decreasing heat transfer through conduction will increase/decrease the heat dissipation flux, while the Nusselt number will decrease/increase. In this case, through the correlation between the maximum heat dissipation flux and the average fluid Nusselt number, the optimal size of the PVT unit can be obtained. The calculation results of the model show that, except the dimensions of inner diameter and outer diameter which increase by 0.36mm and 0.35mm respectively, the rest of structural parameters of PVT unit show reduction in size. Second, compared with the existing serpentine channel PVT unit condenser, the optimal size of the two channel spacing, transverse distance and longitudinal distance are reduced by 5.3mm, 137.76mm and 63mm. Secondly, in consideration to the new size, a representative model of PVT unit condenser with a size of 160.56mm x 388.56mm is established and solved, and the effects of different internal and external factors on heat transfer characteristics are analyzed. The calculation results of the model show that the heat dissipation flux of the optimized model is 12.5% higher than that of the existing model. The above research has important theoretical significance for determining the structure size of PVT unit condenser and predicting the heat transfer characteristics and overall performance of PVT unit condenser under different time lengths and specific weather conditions.

In order to further improve the heat transfer characteristics and overall performance coefficient of PVT module condenser, fins and new channel structure are adopted in the existing serpentine channel PVT unit condenser. Under the experimental average condition, the numerical model of PVT unit condenser with four kinds of fins and ribs, including straight rectangle, straight triangle, rectangular pin and parabolic pin, was solved. For comparative analysis, this thesis derives from the results of other related research, and determines the reference cases of fin size and fin position parameters (width, height and angle), in which the fin structure parameters depend on the size and type of radiator. First of all, a comparative study of temperature distribution and heat dissipation is carried out, in order to determine the corresponding results as compared with those of the PVT unit condenser without finned serpentine channel, so as to determine the improvement effect of heat transfer characteristics. Secondly, based on the PVT unit condenser model with fins of straight rectangular and triangular, the heat dissipation and overall fin efficiency under different fin numbers are studied to determine the most suitable fin number. Finally, based on the optimal working condition model of PVT unit condenser with fins of straight rectangular and triangular, the effects of fin

size and fin position on the coefficient of performance, heat dissipation, total fin efficiency and pressure drop are studied. The results show that the heat dissipation and performance of the PVT unit condenser can be improved to 5.079 by installing heat sinks on the outer surface of the flow channel. In order to solve the PVT unit condenser model with hexagonal grid channel coupled with fluid channel with serpentine arrangement, volume of fluid (VOF) and $k-\epsilon$ models are used to simulate the two-phase refrigerant R134a and deal with the turbulence problem during the phase change at different temperatures, respectively. The maximum coefficient of performance obtained is 4.66, which is 0.419 smaller than that obtained by the PVT unit condenser with fins. The above results show that the PVT unit condenser with fins and new channel structure can speed up the cooling process and meet the cooling load demand in a short time.

In order to determine the influence of other fluids other than refrigerant on heat transfer characteristics, this thesis also uses ANSYS FLUENT software to solve a PVT unit cooler model with nanofluid under cooling conditions. Firstly, it is assumed that the two kinds of nanofluids in the tube are single-phase, incompressible laminar fluids. Secondly, PVT unit models of Al_3O_2 water and Ag- water nanofluids were solved in steady state. Thirdly, under different nanoparticle fractions, weather conditions and flow coefficients, the research results are discussed in terms of Nusselt number, entropy generation (Δs), outlet temperature and coefficient of performance (COP). When the PVT unit operates with Ag-water as the fluid medium, the maximum coefficient of performance can reach 3. This means that in addition to the existing common working fluids, using nanofluids, especially Ag-water, has a great potential to improve the heat transfer characteristics and overall performance coefficient of PVT units under night cooling conditions.

The research in this thesis provides numerical simulation methods and specific enhanced heat transfer methods for improving the condensation heat transfer and sensible heat cooling heat transfer performance of PVT units, which has important theoretical significance. It provides theory, method and data support for the development of new PVT units, and has important practical value.

Key Words: PVT unit components; Structural design; Condensation heat exchange; Night natural cooling; Numerical enhanced heat transfer; Use of nanofluids

摘 要

为了实现能源环境的可持续性发展，迫切需要降低建筑能耗，而开发利用清洁能源是解决这一问题的有效途径。近年来，太阳能光伏光热（Photovoltaic thermal, PVT）热泵技术得到了快速发展，不仅可以为建筑提供热、电、冷和生活热水等多种形式的能源，而且可同时实现对太阳能、空气能、土壤热能等多种可再生能源的转化利用。随着研究的不断发展，最新的研究已经提出一种可以在夏季白天和晚上都可以运行的新型 PVT 热泵热电冷综合能源系统。白天，PVT 热泵系统采用 PVT 组件作为蒸发器，在实现发电与产热的同时，还可以有效地冷却 PVT 组件的太阳能电池，使太阳能电池的温度保持在高发电量范围内，提高光伏系统的发电效率。夜间，该热泵系统的 PVT 组件又可作为冷凝器，同时以长波冷辐射和天空之间实现辐射放热、以自然对流换热和周围空气之间实现对流换热，释放热泵系统的冷凝热量，从而实现夜间制冷过程，产生建筑所需的冷冻水或冰（冰蓄冷），供建筑在白天空调降温使用。

PVT 组件是在 PV 组件背部压制了吹胀式换热板，吹胀式换热板内设蛇形或其它形状的工质流道。白天，制冷剂液态可在吹胀式换热板蛇形流道内蒸发、吸热；夜间，制冷剂蒸汽进入吹胀式换热板，在蛇形流道内冷却、冷凝，释放冷凝热。在冷凝过程中，PVT 热泵系统的冷凝热通过 PVT 组件不同结构层的对流、辐射和导热，不断释放到环境和天空中。因此，PVT 组件释放的冷凝热将直接关系到 PVT 热泵系统的夜间制冷量。PVT 组件的冷凝放热特性与蛇形流道形状、流道表面形状、流道内制冷剂的流动和传热状态、换热板与 PV 组件之间的热导率、天空有效温度等因素密切相关。为提高 PVT 热泵系统的夜间制冷性能，非常必要深入研究 PVT 组件在夏季夜间的冷凝传热特性。

另外，PVT 组件在夏季夜间除了以上述冷凝器的形式参与系统换热外，还可以单独以辐射换热冷却器的方式实现与天空和空气之间的自然冷却运行，此时，流经 PVT 流道的工质可以是水、乙二醇溶液及纳米流体等，这种显热放热的冷却技术在建筑屋面冷却系统等已有应用，其冷却换热性能也需要进一步提高。为此，本文采用数值模拟方法，研究了 PVT 组件在夏季夜间的冷凝和冷却强化传热特性，以优化 PVT 组件流道设计，提高其传热性能。

为实现这一目标，本文针对现有蛇形流道 PVT 组件冷凝器（模型 1）、带翅片蛇形流道 PVT 组件冷凝器（模型 2）、六角网格流道和蛇形流道相结合的 PVT 组件冷凝器（模型 3）、以及以水- $\text{Al}_3\text{O}_2/\text{Ag}$ 作为流体介质的 PVT 组件（模型 4）四种类型 PVT 组件，在 ANSYS Fluent 18 中进行了数值建模和模拟研究。本文研究旨在开发和提出增强 PVT 组件传热特性的替代方法，因此，首先详细介绍了现有研究 PVT 组件冷凝器的系统实验装置，描述了 PVT 各部件的代表性数值模型，并简化上述模型；详细描述了上

述四种模型所使用的几何形状以及 PVT 组件材料中流体传热过程的数学方程。在研究过程中, 现有蛇形流道 PVT 组件冷凝器和带翅片蛇形流道 PVT 组件冷凝器使用的制冷剂为 R407C, 六角网格流道和蛇形流道结合的 PVT 组件冷凝器使用的工质为 R134a。

随后, 为更好地求解数学方程而开展模拟假设和模型验证工作。首先在模拟前, 本文研究设置了适当的模型求解方法、操作条件、假设和创建能够捕获解决方案的网格质量。通过比较本文模拟结果和现有研究结果来确定模型精度; 在该过程中, 比较的主要参数有性能系数、散热量、出口温度、冷凝器表面温度以及温度、速度和蒸汽体积分数等。其次, 在模拟过程中, 本文对模型进行验证。现有蛇形流道 PVT 组件冷凝器的验证模型有助于确定组件流道结构的最佳尺寸, 有利于优化 PVT 组件冷凝器的传热特性。翅片对 PVT 组件冷凝器的传热特性和整体性能系数的影响, 是通过带翅片 PVT 冷凝器的验证模型来实现的。为了进一步寻找可以提高 PVT 组件冷凝器夜间冷却性能的替代方法, 本文提出并验证了六角网格流道和蛇形流道相结合的 PVT 组件冷凝器模型; 并进一步地使用纳米流体 PVT 组件的验证模型, 来研究使用新的纳米流体对 PVT 组件冷凝器传热特性的影响大小。

在验证模型的基础上, 本文针对各类 PVT 组件冷凝器具体应用工况进行了数值模拟。首先, 为了设计和优化 PVT 组件冷凝器, 建立并验证了模型 1, 进而设计和优化了 PVT 组件冷凝器。在 PVT 组件冷凝器中, 到外表面的热通量很大程度上取决于通过材料的热传导量。通过传导增加/减少热传递会增加/减少散热通量, 而努塞尔数会减少/增加。在这种情况下, 通过散热通量最大值与平均流体努塞尔数之间的关联式, 即可获得 PVT 组件流道结构最佳尺寸。模型的计算结果表明, 一是, 除了最佳内径和外径尺寸分别增加 0.36mm 和 0.35mm 外, 其余 PVT 组件结构参数呈现尺寸减小的特点。二是, 最佳尺寸相对于现有蛇形流道 PVT 组件冷凝器的两个流道间距、横向距离和纵向距离分别减少了 5.3mm、137.76mm 和 6.3mm。其次, 针对新的尺寸, 建立并求解了尺寸为 160.56mm x 388.56mm 的 PVT 组件冷凝器的代表模型并求解, 分析了不同内外因素对传热特性的影响。模型计算结果显示, 优化后的模型的散热通量比现有模型提高了 12.5%。上述研究对确定 PVT 组件冷凝器的流道结构尺寸, 对预测 PVT 组件冷凝器在不同时间长度、特定天气条件下的传热特性和整体性能, 具有重要的理论意义。

为进一步提高 PVT 组件冷凝器的传热特性和整体性能系数, 本文在现有蛇形流道 PVT 组件冷凝器上采用了翅片和新型流道结构。在实验平均工况下, 求解了流道外表面为直矩形、直三角形、矩形销和抛物线销四种翅片肋型的 PVT 组件冷凝器数值模型。为对比分析, 本文源于其他相关研究的成果, 确定了翅片尺寸和翅片位置参数(宽度、高度和角度)的参考案例, 其中, 翅片结构参数具体取决于散热器的尺寸和类型。首先, 进行了温度分布和散热量的比较研究, 目的是确定与没有翅片蛇形流道 PVT 组件冷凝器的相应结果进行对比, 以确定传热特性的改进效果。其次, 在 PVT 组件冷凝器模型的基础上, 以直矩形和三角形翅片为基础, 研究了不同翅片数量下的散热量和整体翅片效率, 以确定最适合的翅片数量。最后, 基于直矩形和三角形翅片 PVT 组件冷

凝器最佳工况模型，研究了翅片尺寸和翅片位置对性能系数、散热量、翅片总效率和压降的影响。研究表明，在流道外表面安装散热片可将 PVT 组件冷凝器的散热量和性能提高到 5.079。为了求解六角网格流道和蛇形流道相结合的 PVT 组件冷凝器模型，分别使用分数体积 (VOF) 和 $k-\epsilon$ 模型来模拟两相制冷剂 R134a 和处理在不同温度下相变过程中发生的湍流问题，获得的最大性能系数为 4.66，比带翅片的 PVT 组件冷凝器获得的性能系数小 0.419。上述结果表明，带翅片的 PVT 组件冷凝器可加快冷却过程并在短时间内满足冷却负荷需求。

为了确定除制冷剂以外其他流体对传热特性的影响，本文还在冷却条件下使用 ANSYS Fluent 软件求解了一个带有纳米流体的 PVT 组件冷却器模型。首先假设了管内两种纳米流体均是单相、不可压缩的层流流体；其次，在稳态下分别求解了 Al_3O_2 -水和 Ag-水两种纳米流体的 PVT 组件模型；第三，在不同的纳米粒子分数、天气状况和流量系数条件下，根据努塞尔数、熵生成 (ΔS)、出口温度和性能系数 (COP) 讨论了研究结果。当 PVT 组件以 Ag-水作为流体介质运行时，最大性能系数可达到 3；这意味着除了现有的常用工质外，使用纳米流体特别是 Ag-水，提高 PVT 组件在夜间冷却条件下的传热特性和整体性能系数是具有很大潜力的。

本文的研究对提高 PVT 组件冷凝换热和显热冷却换热性能，提供了数值模拟方法和具体强化换热方法，具有重要的理论意义；对开发新型 PVT 组件提供了理论、方法和数据支持，具有重要的实用价值。

关键词：PVT 组件；结构设计；冷凝换热；夜间自然冷却；数值增强传热；纳米流体的用途

CONTENTS

Abstract	I
摘 要.....	v
CONTENTS	viii
List of Figures	xi
List of Tables.....	xv
Table of Major Symbols and Units	xvi
1. Introduction	1
1.1 Research Background, Problems and Significance.....	1
1.1.1 Energy consumption and its detrimental impacts	1
1.1.2 Significance of the research.....	3
1.2 Operating principle and research development of PVT heat pump	4
1.2.1 Operating principle of PVT heat pump	4
1.2.2 Water/air based PVT unit	7
1.2.3 Integration of various channels arrangements in PVT unit	11
1.2.4 PVT unit incorporating fluids medium with special properties.....	13
1.3 Cooling of PVT unit with natural cold of the sky	15
1.3.1 Modes of cooling with natural cold of the sky	15
1.3.2 Influencing factors of cooling with natural cold of the sky.....	17
1.3.3 Coupling NNC with PVT unit	19
1.3.4 Research progress of PVT unit under night cooling.....	21
1.4 Strategy to study PVT heat pump systems using CFD method	24
1.4.1 Model establishment	24
1.4.2 Solution methods	29
1.5 Research Contents and Research Route	31
1.5.1 Knowledge gaps.....	31
1.5.2 Research objectives and methods	32
1.5.3 Research contents and route	36
2. Physical and mathematical models of the PVT unit under condensation and cooling conditions	38
2.1 Physical models of PVT unit under condensation and cooling conditions.....	38
2.1.1 Introduction of experimental set up of PVT heat pump system	38
2.1.2 Four types of physical models of PVT unit under condensation and cooling conditions	40

2.2 Analysis of working fluid characteristics in PVT unit under condensation and cooling conditions	44
2.2.1 Analysis of refrigerant flow characteristics	45
2.2.2 Analysis of nanofluids characteristics	45
2.3 Mathematical models for PVT unit under condensation and cooling conditions	46
2.3.1 Numerical model of flow and energy of working fluid in PVT unit	47
2.3.2 Thermal modelling of PVT unit under condensation and cooling conditions	49
2.4 Summary	51
3. Solution strategy for the numerical models of PVT unit and proposal of evaluation indexes	53
3.1 The inputs, methods and assumptions to the simulation	54
3.1.1 Operating conditions of weather and flow	54
3.1.2 Numerical methods and solution assumptions	55
3.2 Proposal of evaluation indexes of PVT unit	56
3.2.1 Overall fin efficiency of the PVT unit	56
3.2.2 Heat dissipation flux and percentage discrepancy	57
3.2.3 Ratio of heat dissipation flux to flow resistance of PVT unit	58
3.2.4 Refrigeration coefficient of performance of PVT heat pump	58
3.3 Mesh creation and model validation of numerical simulation	60
3.3.1 Preparation for existing PVT unit condenser model	60
3.3.2 Preparation for PVT unit condenser with fins	62
3.3.3 Preparation for PVT unit condenser incorporating a novel channel	65
3.3.4 Preparation for PVT unit with nanofluids	68
3.2 Summary	71
4. Numerical analysis of existing PVT unit condenser	73
4.1 Design of PVT unit condenser	73
4.1.1 Temperature and velocity distribution in both PVT unit layers and channels	75
4.1.2 Effect of lateral and longitudinal distance on heat transfer characteristics	77
4.1.3 Effect of channel parameters on heat transfer characteristics	78
4.2 Investigation of optimized model of PVT unit condenser	80
4.2.1 Distribution of internal flow properties	80
4.2.2 Effect of internal factors on the heat characteristic of optimized PVT unit condenser	82
4.2.3 Effect of external factors on the heat characteristic of optimized PVT unit condenser	84
4.2.4 Heat dissipation flux of optimized PVT unit condenser	87

4.3 Summary	88
5. Numerical study of PVT unit condenser with fins and novel channel.....	90
5.1 Numerical study of PVT unit condenser with fins.....	90
5.1.1 Comparative study of PVT unit condenser with and without fins.....	90
5.1.2 Heat transfer characteristics of PVT unit condenser with fins of different shapes	92
5.2 Characteristics analysis at different fins number and fin parameters	95
5.2.1 Impact of fins number on heat transfer characteristics of PVT unit condenser	95
5.2.2 Effect of fin size and position on the operation of PVT unit condenser.....	96
5.2.3 Optimization process of PVT unit condenser with fins.....	99
5.3 PVT unit condenser incorporating a novel channel	100
5.3.1 Distribution of vapor fraction in novel channel.....	100
5.3.2 Impact of change in flow conditions	101
5.3.3 Impact of change in weather conditions	102
5.4 Summary	104
6. Numerical simulation of nanofluid-based PVT unit for cooling.....	105
6.1 Description and contours inside of nanofluid-based-PVT unit.....	105
6.2 Effect of nanoparticles fraction on the PVT unit cooling	107
6.3 Effect of flow conditions on the PVT unit cooling	109
6.4 Effect of weather conditions on the PVT unit cooling.....	112
6.5 Summary	113
7. Conclusions and Outlook	115
7.1 Conclusions.....	115
7.2 Innovative points.....	118
7.3 Future Outlook	119
References	121
Publications and projects during PhD Period.....	132
Acknowledgement.....	133
Curriculum Vitae.....	134
Dalian University of Technology Doctoral Dissertation Copyright Use Authorization.....	135
大连理工大学学位论文版权使用授权书.....	136

List of Figures

Fig.1.1 Working principle of heat pump	5
Fig.1.2 Schematic diagram of conventional PVT heat pump ^[29]	7
Fig.1.3 Schematic diagram of PVT unit collector ^[30]	7
Fig.1.4 Types of PVT system based on collector type, coolant type and material type ^[34]	8
Fig.1.5 Schematic of water PVT collector ^[38, 39]	9
Fig.1.6 Schematic diagram of air PVT collectors with; (a) channels holes and (b) V-corrugated ^[43, 46]	10
Fig.1.7 Sub-types of PVT collectors using water, air and a combination of water-air ^[47, 48]	10
Fig.1.8 Conservative (left) and bifurcation (right) flow arrangements ^[56]	12
Fig.1.9 Different layouts of channels flow ^[57]	12
Fig.1.10 Cooling process by the NNC	16
Fig.1.11 Cooling of house room long-wave radiation	16
Fig.1.12 Schematic of possible cooling of house room by night air cooling	17
Fig.1.13 Schematic diagram of PVT heat pump for heating (a) and cooling modes (b) ^[16]	20
Fig.1.14 Schematic diagram of (a) PVT unit , (b) Composition of PVT unit and (c) structure of serpentine channel inside heat exchanger ^[16]	21
Fig.1.15 Illustration of the heat exchange to turn unused thermal energy of tank 1 into cooling load of tank 2 by the PVT unit	22
Fig.1.16 Schematic diagrams of water PVT collector	25
Fig.1.17 PVT system with fins (a) and the corresponding mesh (b).....	26
Fig.1.18 Schematic of PVT system (a), its front view (b) , parallel channels with different groove profiles (c) and mesh patterns (d).....	26
Fig.1.19 PVT system with water layer on top (a) and mesh distribution patterns (b)	27
Fig.1.20 Different tubing layout at the back side of PVT collector (A) (a. Continuous, b. longitudinal and c. lateral) and mesh distribution (B).....	27
Fig.1.21 Different flow channel patterns (a-d) and mesh (e) ^[144]	28
Fig.1.22 PVT unit integrated with TE (a) and pipe mesh patterns (b).....	29
Fig.1.23 Geometry of Al ₃ O ₂ -water/PVT system (a) and its corresponding mesh (b).....	29
Fig.1.24 Heat transfer mechanisms in fluid channels and materials of the PVT unit condensation and cooling conditions at night	32
Fig.1.25 Strategy to solve the considered PVT unit models in CFD/ANSYS Fluent software	35

Fig.1.26 Research roadmap of the PhD thesis	37
Fig.2.1 Schematic diagram of experimental set up of PVT heat pump system	39
Fig.2.2 Process of ice formation inside ice storage tank ^[138]	39
Fig.2.3 Representative 3D simulation model of existing PVT unit condenser	41
Fig.2.4 Simplified model geometry of PVT unit condenser with fins	42
Fig.2.5 Schematic diagram of the existing PVT unit (a), simplified model of existing PVT unit (b) and simplified of newly PVT unit (c).....	43
Fig.2.6 Model geometry of the PVT unit with nanofluids	44
Fig.2.7 Schematic diagram of PVT unit condenser	49
Fig.2.8 Thermal resistance circuit of PVT unit under condensation and cooling conditions	50
Fig.3.1 Step by step procedure to get solution results from ANSYS Fluent.....	53
Fig.3.2 Base case of weather conditions, COP and heat dissipation flux	54
Fig.3.3 Four different types of fins used at the outer surface of PVT unit channel	57
Fig.3.4 Schematic diagram of Vapor-Compression refrigeration cycle.....	59
Fig.3.5 Local views of mesh for the CDF model of PVT unit without fins.....	61
Fig.3.6 Grid independent study for PVT unit without fins	61
Fig.3.7 Comparison between simulation and experimental results.....	61
Fig.3.8 Local views of mesh for RB-PVT unit model with fins	63
Fig.3.9 Grid independent study for PVT unit with fins	63
Fig.3.10 Comparison of two models (experimental and simulation) in terms of heat dissipation flux	64
Fig.3.11 Comparison of two models (experimental and simulation) in terms of COP....	64
Fig.3.12 Nusselt number at different meshes of PVT unit condenser.....	65
Fig.3.13 Comparison between temperature contours of ^[144] and current study.....	66
Fig.3.14 Comparison between velocity contours of ^[144] and current study	67
Fig.3.15 Comparison between vapor fraction contours of ^[144] and current study	67
Fig.3.16 Mesh patterns of different components of water/nanofluids based PVT unit ...	68
Fig.3.17 Wall pipe temperature at five mesh of Ag-water/ PVT unit and Al ₃ O ₂ -water/PVT unit.....	69
Fig.3.18 Comparison between of the outlet water temperature of the current study and that of Selmi et al. ^[188]	70
Fig.3.19 Comparison between the absorber temperature of the Ag-water/PVT unit for current study and that of Khanjari et al. ^[157]	71
Fig.3.20 Comparison between the absorber temperature of the Al ₃ O ₂ -water/PVT unit for current study and that of Khanjari et al. ^[157]	71
Fig.4.1 Design parameters of existing physical model of PVT unit condenser	74
Fig.4.2 Design parameters of existing simulation model of PVT unit condenser	75

Fig.4.3 Temperature distribution in PVT unit material at distance $x=250\text{mm}$ and considering the first 2 channels	76
Fig.4.4 Temperature distribution inside 3D channels	76
Fig.4.5 Temperature distribution at the top surface of the PVT unit condenser	76
Fig.4.6 Velocity distribution in channel of the PVT unit condenser.....	77
Fig.4.7 Effect of PVT unit parameter distance on heat transfer characteristics.....	78
Fig.4.8 Effect of channel parameters on heat transfer characteristics.....	79
Fig.4.9 Distribution patterns of molecular viscosity at 0.12m/s	80
Fig.4.10 Distribution patterns of molecular viscosity at 0.14m/s	81
Fig.4.11 Distribution patterns of Prandtl number at 0.12m/s	81
Fig.4.12 Distribution patterns of Prandtl number at 0.14m/s	82
Fig.4.13 Influence of inlet flow temperature on heat characteristics	83
Fig.4.14 Influence of inlet flow velocity on heat characteristics	84
Fig.4.15 Influence of inlet flow fraction on heat characteristics.....	84
Fig.4.16 Effect of emissivity change on the heat characteristics of the PVT unit	86
Fig.4.17 Effect of ambient temperature on the heat characteristics of the PVT unit	86
Fig.4.18 Effect of wind speed on the performance of the PVT unit	87
Fig.4.19 Comparison of heat dissipation flux between optimized and experiment	88
Fig.5.1 Temperature distribution at the top face of PVT unit condenser.....	91
Fig.5.2 Temperature distribution in PVT unit materials at the lateral cross-section ($X=50\text{mm}$).....	92
Fig.5.3 Temperature distribution in 5 fins of straight rectangular shape	93
Fig.5.4 Temperature distribution in lateral cross-section materials of PVT unit condenser, at $X=135\text{mm}$	93
Fig.5.5 Temperature distribution in longitudinal cross-section materials of PVT unit condenser, at $Z=16\text{mm}$	93
Fig.5.6 Comparison in terms of heat dissipation flux of PVT unit condenser with and without fins.....	95
Fig.5.7 PVT unit condenser with 3 and 5 fins of straight rectangular profile.....	96
Fig.5.8 PVT unit condenser with 3 and 5 fins of straight triangular profile	96
Fig.5.9 Effect of fin length on heat dissipation, overall fins efficiency , pressure drop and performance.....	98
Fig.5.10 Effect of fin width on heat dissipation, overall fins efficiency , pressure drop and performance.....	98
Fig.5.11 Effect of fins positions on heat dissipation flux (q), overall fins efficiency , pressure drop and performance	98

Fig.5.12 Variation of vapor volume fraction in the channel 101

Fig.5.13 Impact of mass flow rate on the heat dissipation flux (q), average vapor fraction (α_{aver}) and refrigeration coefficient of performance (COP) of PVT condenser..... 102

Fig.5.14 Impact of flow temperature on the heat dissipation flux (q), average vapor fraction (α_{aver}) and refrigeration coefficient of performance (COP) of PVT condenser..... 102

Fig.5.15 Impact of ambient temperature on the heat dissipation flux (q), average vapor fraction (α_{aver}) and refrigeration coefficient of performance (COP) of PVT condenser 103

Fig.5.16 Impact of radiation intensity on the heat dissipation flux(q), average vapor fraction (α_{aver}) and refrigeration coefficient of performance (COP) of PVT condenser 103

Fig.6.1 Temperature distribution at the pipe outlet of the PVT unit with a. Al₃O₂-water and b. Ag-water used as fluids medium 106

Fig.6.2 Velocity distribution at the pipe outlet of the PVT unit with a. Al₃O₂-water and b. Ag-water used as fluids medium 107

Fig.6.3 Effect of incrementing nanoparticles fraction of Al₃O₂ in the Al₃O₂-water through the pipe of the PVT unit 108

Fig.6.4 Effect of incrementing nanoparticles fraction of Ag in the Ag-water through the pipe of the PVT unit 109

Fig.6.5 Effect of applying different mass flow rates of Al₃O₂-water at the pipe inlet of the PVT unit 110

Fig.6.6 Effect of applying different mass flow rates of Ag-water at the pipe inlet of the PVT unit 110

Fig.6.7 Effect of applying different temperatures of Al₃O₂-water at the pipe inlet of the PVT unit 111

Fig.6.8 Effect of applying different temperatures of Ag-water at the pipe inlet of the PVT unit..... 112

Fig.6.9 Impact of operating Al₃O₂-water/PVT unit at various ambient temperatures ... 113

Fig.6.10 Impact of operating Ag-water/PVT unit at various ambient temperatures..... 113

List of Tables

Tab.2-1 Specifications of the main components of the experimental system ^[138]	40
Tab.2-2 Thermo-physical properties of PVT unit layer materials and their dimensions .	40
Tab.2-3 Details for reference cases of fins.....	42
Tab.2-4 Thermo-physical properties of refrigerants ^[154]	45
Tab.2-5 Thermo-physical properties of nanoparticles	46
Tab.3-1 Parameter variables for weather, refrigerant flow and surface emissivity	54
Tab.3-2 Testing devices and their corresponding specifications ^[138]	55
Tab.3-3 Summary results of Yao et al. ^[144] and current study	67
Tab.3-4 Summary information of the validated PVT unit models under consideration ..	72
Tab.4-1 Summary optimum dimensions of the PVT unit condenser for experiment and simulation models	79
Tab.5-1 Maximum obtained results from PVT unit condenser with 3 fins of straight rectangular shape, at different fin parameters change	100

Table of Major Symbols and Units

Symbol	Name of Measure	Unit Symbol
C	Control surface	m^2
COP	Coefficient of Performance	-
C_p	Specific heat capacity	$J/(kg \cdot K)$
d	Tube width	m
D_h	Hydraulic diameter	m
e	Internal energy	joule
Ep	Turbulent dissipation rate	m^3/s^3
F	Force	N
F	Flow resistance	$kg/s \cdot m^4$
g	Gravity	m/s^2
H	Heat flux to flow resistance	$W \cdot s \cdot m^2/kg$
J	Generation of turbulent kinetic energy	m^2/s^2
k	Thermal conductivity	$W/(m \cdot K)$
ke	Turbulent kinetic energy	m^2/s^2
L	Length	m
\dot{m}	Flowrate	kg/s
Nu	Nusselt number	-
p	Pressure	Pa
q	Heat dissipation flux	W/m^2
Q_{conv}	Heat due to convection	kW
Q_{rad}	Heat due to radiation	kW
R	Heat resistance	$(m^2 \cdot K)/W$
Re	Reynold number	-
S_E	Energy source term	$J/(s \cdot m^3)$
T	Temperature	K
T_a	Ambient temperature	K
T_{flow}	Refrigerant flow temperature	K
T_{PVT}	Average surface temperature of PVT unit	K
T_{sky}	Sky temperature	K
U	Overall heat transfer coefficient	$W/(m^2 \cdot K)$
u	Refrigerant flow velocity	m/s

V	Air speed	m/s
W	Tube pitch	m
Y	Fluctuating dilation incompressible turbulence	-
λ	Surface tension	N/m
α	Absorptivity	-
β	Angle	degree
ε	Emissivity	-
μ	Viscosity	kg/(m·s)
ρ	Density	kg/m ³
σ	Stefan-Boltzmann constant	W/(m ² ·K ⁴)
α	Flow fraction	-
δ	Thickness	m
η_{over}	Overall efficiency	-
ω	Inverse effective Prandtl Number	-

1. Introduction

1.1 Research Background, Problems and Significance

1.1.1 Energy consumption and its detrimental impacts

Energy is the keystone of modern civilization and one of the principal driving factors for the overall economic growth of any country. As a result, the world's energy consumption has been rising rapidly due to an increase in both industrial development and population growth, and approximately 80% of the world's energy demand is supplied by fossil energy sources^[1]. Excessive consumption of fossil fuels consumes the reserves day by day, and at the time releases a huge amount of greenhouse and pollutant gases that causing serious environmental problems. According to International Energy Agency (IEA), energy related CO₂ emissions has elevated more than 37% from 1990 to 2018, and it is estimated to reach a rise of 42% by 2040 (IEA,2019). The CO₂ as a greenhouse gas is highly responsible for global warming, which is currently about 1.0°C above pre-industrial levels, and if CO₂ emissions continue to increase at the current rate, this value is expected to rise above 1.5°C between 2030 and 2052^[2]. This trend has urged the United Nations Paris Agreement to set the direction for a more energy-efficient future with lower CO₂ emissions by declaring ambitious international climate targets^[3].

In fact, the rate of increase in CO₂ emissions depends on the type of energy resources, methods of converting resources into final energy and the efficient ways of using energy in different socioeconomic activities. These activities have resulted in substantial greenhouse gases (GHG) emitted into the atmosphere, causing climate change and related detrimental impacts on marine ecosystems^[4], agriculture^[5], tourism^[6], and transportation^[7]. Much of those environmental problems are due to the energy that fuel buildings and activities within them^[8, 9]. More concretely, global building sector accounts for nearly 38% of global greenhouse gas emissions and 39% of global energy consumption, which therefore represents an important focus for energy efficiency improvements and a move to closer climate targets^[10].

In order to sustainably cope with the rapid increase in energy consumption of the building and reduce its related CO₂ emissions, an effort is being made by many researchers and organizations. In its annual summit, international Energy Agency (IEA) evaluates and elaborates the strategic plans which will further reduce future energy demand as well as the concentration of CO₂ emissions in the atmosphere. The assessment made by IEA in 2019 showed that overall reductions have been achieved in energy intensity for lighting, appliances, cooking and water heating thanks to technological improvements. However, space Cooling, Ventilation, and Air-Conditioning (HVCA) energy intensity has increased as a result of greater HVCA load demand in many hot climatic areas. In view of the above reasons, there is an urgent

need to reduce the use of fossil fuel energy and vigorously develop renewable energy to reduce greenhouse gas emissions.

The efficient operation of HVAC systems is of critical importance considering that people spend more than 80% of their time indoors^[11]. Typically, the main function of HVAC system is to satisfy the thermal comfort of occupants by adjusting and changing the outdoor conditions to the desired conditions of occupied buildings^[12]. Therefore, sustainability considerations and innovations in HVAC systems are necessary to provide a remarkable, healthy, productive, and sustainable built environment for occupants while reducing energy consumption and costs^[13]. The energy usage of HVAC systems accounts for 15% of the world's total energy consumption^[14], which in turns contributes to a big share of greenhouse gas emissions and costs. These facts inspired researchers, industries and policymakers to find alternatives to reducing energy consumption of HVAC systems.

Nowadays, an attempt is being made to allow a higher proportion of on-site and off-site renewable energy development and utilization technologies to emerge in energy mix of HVAC system. Considering the climate and geographical conditions, the use of various heating and cooling technologies that utilize renewable energy sources in HVAC systems in the building are very important options in improving sustainability. It can be achieved either by improving existing methods of energy saving or through emerging of new renewable energy development and utilization technologies. Among them, the photovoltaic thermal (PVT) heat pump is a new technology which is very suitable for solving the energy demand of building heat, electricity and domestic hot water^[15]. The PVT heat pump systems are mostly operated during summer daytime when the heating demand of the building is relatively low and can be met within a short time. In addition, the cooling load demand is highly needed in that particular season but it cannot be produced from the traditional PVT heat pump system. Therefore, in order to increase the system performance and meet the cooling load demand, the same system of PVT heat pump has been made to operate both during daytime and nighttime, with the latest technology^[16]. In particular, to the recently incorporated system of PVT heat pump working in the nighttime, its main role is to convert unused thermal energy into cooling load especially by taking advantages of the night natural cold (NNC) of the sky and long-wave radiation. The PVT heat pump system of this kind can use refrigerants and nano-fluids as fluids medium through the channels, to absorb and release heat of thermal energy to the ambient environment. For PVT heat pump system with refrigerants as fluids through the channels, two phase change is considered. During heat absorption of the thermal energy storage tank, refrigerant becomes vapor and while the vapor volume fraction reduces as the condensations heat release to the ambient environment. Therefore, it is of utmost importance to determine methods which further optimize the design of the PVT unit and further improve its condensation heat transfer performance. On the other hand, nano-fluid is taken single phase and pumped in the circulation

loop to reduce the temperature of thermal energy storage of tank to that required by the cooling load demand.

In this PhD thesis, the methods to further enhance the heat transfer characteristics of PVT heat pump system operating during nighttime to produce cooling load demand, are numerically investigated and proposed using ANSYS Fluent 18. The research is conducted considering only PVT unit as the most influential component in the system of PVT heat pump. The refrigerants (R407C and R134a) and nano-fluids (water- Al_3O_2 and water-Ag) are used as fluids medium to release the heat of thermal energy storage of the tank. The PVT units with both refrigerants and nano-fluids are operated in nighttime with the objective to produce cooling load demand from unused thermal energy but with two different operating principles. The night PVT unit with refrigerant works as a condenser and while the one with nano-fluid works as a PVT unit for cooling. Four models of PVT unit including three models of PVT unit condenser and one model of PVT unit with nano-fluids are solved. The models are solved after being validated with those of previous studies. Based on the validated models, further results are obtained to investigate different case studies.

1.1.2 Significance of the research

Based on the research literature of the sections 1.1.1, the proportion of CO_2 emissions in the atmosphere is increasing as a result of increasing energy for cooling load demand, in hot climatic zones. This is because of use of non-renewable resources for production and satisfaction of energy required by a big number of occupants. Alternative solutions to cope with this problem have been proposed and implemented by many researchers and organizations but there are still some problems to be addressed. Among them, the recovery of thermal energy obtained from PVT heat pump system during daytime as well as extension of the operating time for the system are the prominent solutions to sustainably meet the cooling load in the buildings. This can be realized by operating the conventional PVT heat pump both during daytime and nighttime. During nighttime, PVT heat pump system will release the heat of thermal energy to the ambient environment, especially by taking advantages of the night natural cold (NNC) of the sky and long-wave radiation. More specifically, the heat is transferred to the PVT unit component by the fluids inside channel and continuously released to the ambient environment by different modes, until the required temperature is reached inside cooling load storage tank. Apart from the channel structure and the surface roughness of the back side which can influence the heat transfer characteristics of the unit, the performance will also be affected depending on the fluid carrier inside channel. The refrigerant has the ability to absorb and release heat whenever needed. In case refrigerant is used as fluid medium, the PVT unit will act as a condenser to release the condensations heat to the ambient. On the other hand, nano-fluid as a fluid medium with enhanced thermal conductivity will increase the heat transfer due to

conduction in PVT unit materials. For PVT unit condenser, a compressor is needed to bring the refrigerant (s) (R407C and R134a) to the required conditions and while for PVT unit with nano-fluid(s) (water- Al_3O_2 and water-Ag), a pump is required to keep the flow in a circulation loop.

Therefore, in this thesis, the methods to enhance the heat transfer characteristics of the PVT unit under condensation and cooling conditions are numerically investigated and proposed, using ANSYS Fluent 18. As the heat of newly developed unit is dissipated to ambient environment from the channels at the bottom surface, the methods to enhance the heat transfer characteristics are applied with much emphasis on the fluid inside channels and at the back surface of the PVT unit. First, a research is performed to deeply study the condensation heat transfer characteristics of the existing PVT unit condenser. The method is realized considering the experimental data from the experiment and the physical conditions from the actual validation experiment such as; model parameters, initial conditions and boundary conditions as the inputs to the computational model. The experiment about PVT unit condenser was conducted during summer nighttime under the weather conditions of Dalian University of Technology, building of Heat and Gas supply, Ventilation and Air Conditioning (6th floor). Next, the strategies to improve the heat transfer characteristics are introduced and studied using previous studies and approaches from various disciplines of engineering. Those include the use of fins at the outer surface of the channel, integration of new channel and incorporation of nano-fluids as fluid medium in the channel of PVT unit under cooling condition.

Successfully implementation of those methods would minimize or eliminate the aforementioned problems (see sections 1.1.1). In addition, the unused heat of solar thermal energy will be fully recovered as a results of enhancing the heat transfer characteristics of the PVT unit. Moreover, improving the heat transfer characteristics of the unit will speed up the cooling process and leads to obtaining cooling load within a very short time. This will in turns reduce the actual area occupied by the units or depending on the decision of operator, the number of units on the same area will be increased/decreased. On the other hand, the costs will be minimized as a results of reducing both area and the number of the PVT units. Furthermore, the cooling system will be extended not only to serve one place or one room but also to be used in the entire building and the region as a whole. This self-reliance in energy for cooling will limits the external supports thereby reducing some amount of money used to be spent. It will also be a basic framework model for future researchers willing to further improve the system.

1.2 Operating principle and research development of PVT heat pump

1.2.1 Operating principle of PVT heat pump

Heat pumps are machines capable of transferring heat from the area with low temperature to the area with high temperature or vice versa, by using electricity to power the compressor/pump. Heat pumps have been found to be alternative way to deal with both high carbon

emission and energy consumption of the building and thereby enhancing the overall efficiency of HVAC system ^[17-19]. Conventional heat pump works similar to PVT heat pump system but differ in energy sources used to operate them. Conventional heat pump can be used both to warm up and cool the room. In cooling mode (Fig.1.1. b), the heat absorbed by the room coil is released by blowing a fan across the coil. Cool air will be generated and the heat from the room is sink into the air, water or the ground. During winter, heating mode is activated and the direction of the flow is reversed after leaving the compressor/pump. This reversal of flow is achieved by a reversing valve. The change of flow causes the room coil to become a heat sink and the outdoor coil a heat source. The fan that blows the room air across the heat sink coil causes heat to be released into the room (Fig.1.1. a). The outside/indoor air and water which can be either from the sea or ground are the heat sources of the system. For water as a source, the problems such as fouling of heat exchanger unit, high investment cost and health related issues were identified ^[20]. Moreover, the installation of electrical work, pipes in the ground and some other miscellaneous can form a big part of the total costs ^[21]. Therefore, in order to alleviate all these problems associated with the operation of heat pump systems, solar energy is one of the most effective alternatives to aid/replace the already existing heat sources of air, water and underground. The importance of integrating heat pumps with solar PV panel has been proven by different authors in perspectives of environment, financial, performance and life cycle cost ^[22-24].

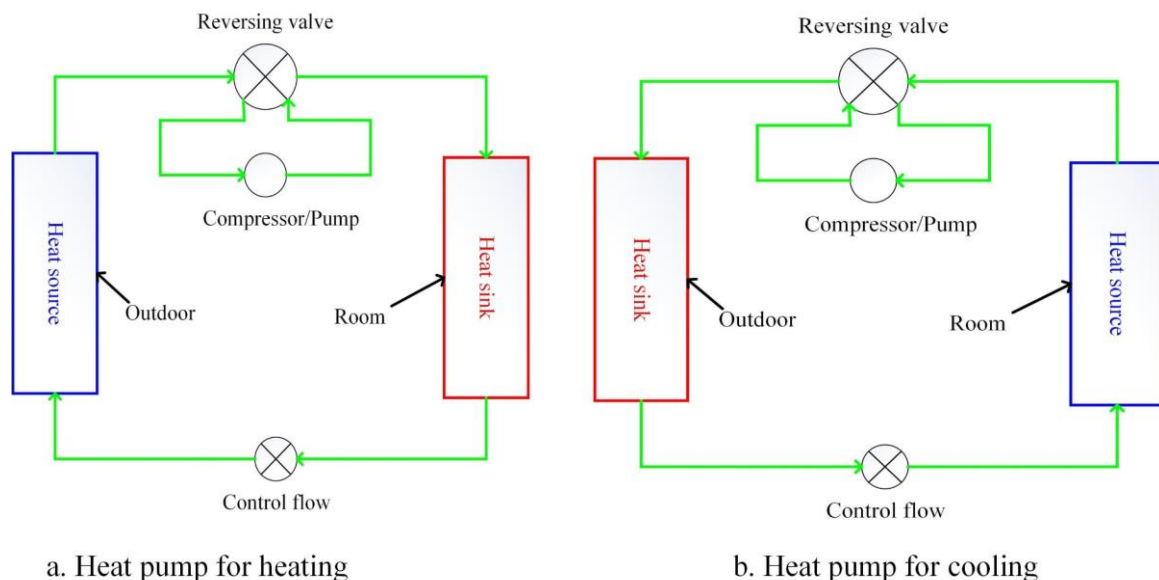


Fig.1.1 Working principle of heat pump

The PVT heat pump is an innovative system introduced and investigated in recent decades, to utilize renewable energy of sun as a heat source in the heat pump systems. With this technology, the primary energy source (coal, gas, and electricity) is reduced or even eliminated and therefore as a result, further improvement in energy performance as well as reduction in electricity consumption, carbon emissions, and operation cost of heat pumps can be achieved. The working principle of a conventional PVT heat pump system is similar with that of Fig.1.1, a where solar energy represents the heat source of the outdoor and PVT unit collector the heat sink of room coil. The conventional PVT heat pump systems commonly use water and air as fluids medium to absorb solar energy striking the flat plate solar collector (Fig.1.2). A part of energy is transformed into useful electricity and while the rest is converted into thermal energy for hot water demand and heat of space air conditioning. With this system, different devices such as flow meter, pressure meter, thermocouple, valve and pump are used to ensure the fluid flow characteristics in a circulation loop meets the required conditions for better performance of the PVT heat pump system. In fact, the performance of PVT heat pump system will depend on the effective operation of the PVT unit collector and the amount of heat removed from the PV cells. Increasing the heat removal enhances both thermal and electrical efficiencies as well as prevents the deterioration of the PV cell materials. The concept of PVT unit collector was developed by ^[25], after realizing that more than half of the sunlight incident on the solar cell is converted into heat and may cause structural damage to the cell if it remains on the PV cell surface for a longer period. In addition, commercial PV cells were only converting between 6 and 8% of the incident radiation into electrical energy and balance remains as a lost either by reflection or as heat that penetrated into the PV cell ^[26]. The importance of PVT unit collector such as increases in electrical efficiency due to the cooling effect, more architectural uniformity by aesthetical design and minimization of both space usage and payback period were notified in the studies of ^[27, 28]. Since then, alternative methods to further reduce the cell temperature were proposed and implemented. In fact, to realize the task, a complete PVT unit collector is typically composed by seven important parts (Fig.1.3). Except solar PV-cell which converts sun light into useful electricity, the rest of layers play the role to protect PV-cell materials from being damaged as well as to refine the absorbed heat of solar radiation. The heat exchanger (absorber) plays a big role in PVT unit as it cools down the PV cell or module, at the same time collecting the thermal energy in the form of hot water or hot air. While this process occurs, the efficiency of the PV cell or module increases.

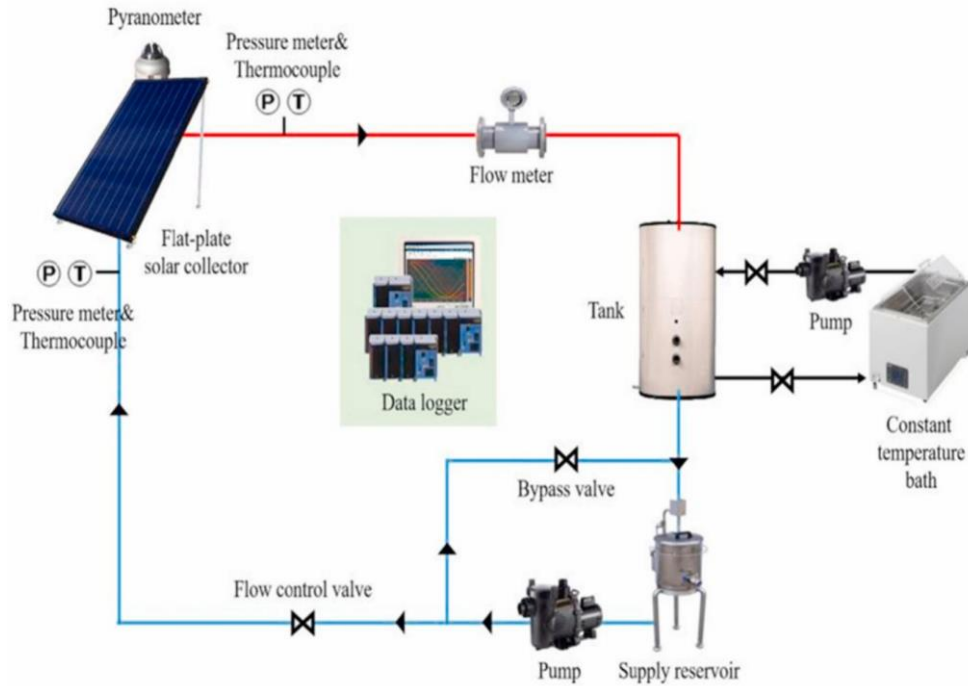


Fig.1.2 Schematic diagram of conventional PVT heat pump^[29]

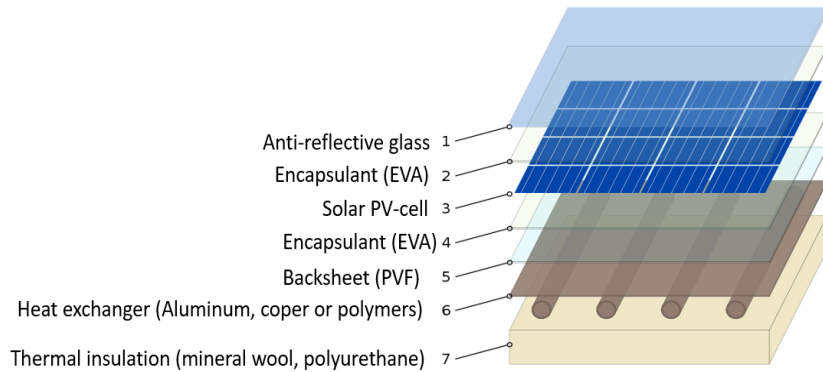


Fig.1.3 Schematic diagram of PVT unit collector^[30]

1.2.2 Water/air based PVT unit

Depending on weather conditions and the type of; collector, coolant and PV-cell materials, PVT unit collector can be operated differently and achieve different results. PVT unit is mainly classified in three categories according to the collector type, coolant type and material type (Fig.1.4). There are two types of collectors (i.e. Flat plate or Concentrator) and each one has its own advantages and drawbacks. Flat plate collector is easy to design and control^[31] as compared to concentrator collector. Even though the concentrator collector is costly due to its system complexity^[32], but it is the best in extracting higher energy as compared to the flat plate

PV collector ^[33] and therefore makes it best suitable for industrial applications where a huge amount of heat is needed. In the next sections of this PhD thesis, analyses will be carried out based on flat plate collector as a commonly used collector type. The performance of PVT system varies depends on fluid mass flow rate, type of collector, modifications in the absorber such as adding fins and thin metallic sheets in the coolant channel, sheet and tube absorber, roll-bond absorber, temperature at the inlet and on the basis of fluid flow paths (single channel/double channel).

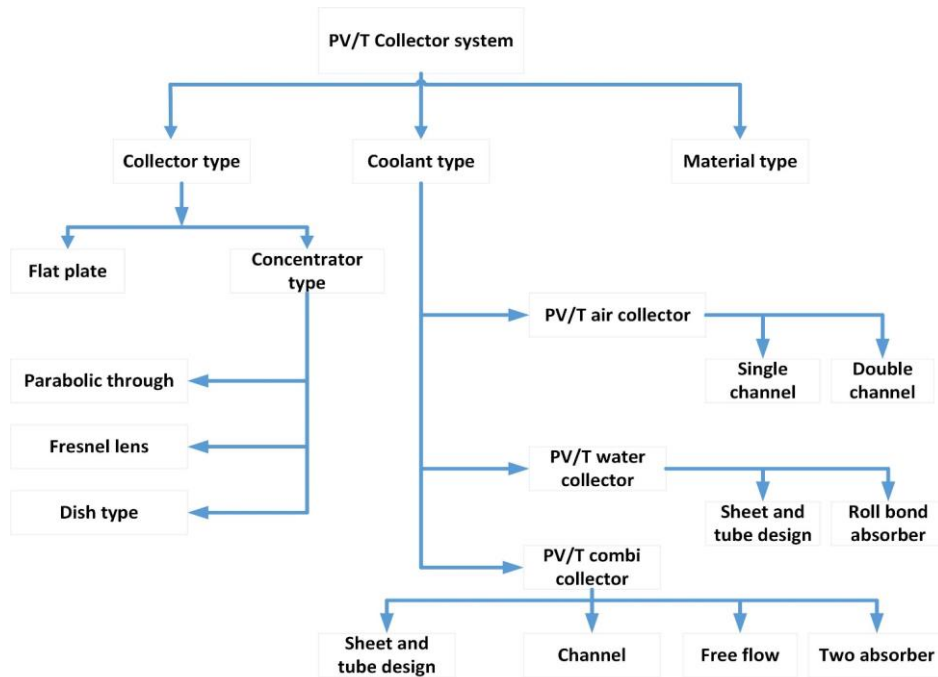


Fig.1.4 Types of PVT system based on collector type, coolant type and material type ^[34]

The most commonly and long back ago used method is cooling of PV cells with air, water and a combination of air/water. The first works on water PVT collectors were performed by ^[25, 35] comparing five hybrids solar heating and cooling system such as, baseline solar heating system, parallel heat pump system, series heat pump system, absorption-cycle chiller and high-performance series advanced heat pump. The aim of the study was to analyze and determine the merits of these systems in four climatic regions of USA (Boston, Miami, Phoenix and Ft. Worth). The results were discussed in terms of energy saving and economic. In all four geographic regions, the greatest energy savings potential was provided by an advanced heat pump system. On the other hand, the hybrid systems were shown to be the most economical in northern climates dominated by high-heat demands and whereas for the regions with balanced heating and cooling loads, PV systems appeared to be most economical. An experimental work was carried out by ^[36] to determine the performance of hybrid PVT systems operating under Soudi Arabia climate. In their findings, PVT system was not suitable due to a high ambient temperature during summer. The performance of a water PVT collector (Fig.1.5) was

evaluated by^[37, 38]. Two types of tube-in-sheet heat-collecting plates of $W/D=6.2$ and $W/D=10$ was compared with a polycarbonate multichannel structure with $W/D=1$ by^[37]. A higher performance was found for a PVT collector with polycarbonate multichannel structure with $W/D= 1$. A good thermal performance and a low temperature difference of 4°C between water in tank and PV module, were obtained from experimental work of ^[38], using PVT collector made from corrugated polycarbonate panel.

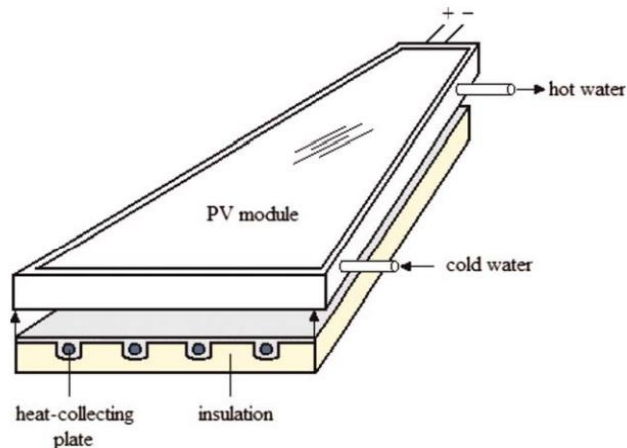


Fig.1.5 Schematic of water PVT collector ^[38, 39]

Several steady-state and dynamic simulation models for water PVT collectors were developed and validated with experiment, in the studies of ^[28]. The simulation was done considering 1D, 2D and 3D models. From the calculations of the daily yield, the simple one dimensional (1D) steady-state model performed almost as good as the much more time-consuming 3D dynamical model. They also concluded that the 2D and 3D models provide more detailed information for design improvement. An explicit dynamic model based on the control-volume finite-difference approach for a single-glazed flat-plate water PVT collector was proposed by ^[40]. The introduced model enabled to generate results for the performance assessment of the PV/T collector including instantaneous energy outputs.

Sometime later, the first studies about air PVT collectors were carried out theoretically and experimentally by ^[41, 42]. The air PVT collector design varies from each other based on the channel position. To this, a number of air PVT collectors were designed and studied by different authors. Two configurations shown in Fig.1.6 were proposed by ^[43]. For the first design (Fig.1.6 a), air flows through the holes of 0.25 cm diameter in the secondary absorber and impinges on the primary absorber. With this system, thermal and electrical efficiencies were determined to be 42 and 8.9%, respectively. The second design (Fig.1.6b) consists of a V-corrugated secondary absorber in which the tips of the V's are in contact with the primary absorber. Thermal and electrical efficiencies of this second configuration were determined to be 40 and

7.8%, respectively. A comparative study in terms of overall performance of unglazed and glazed hybrid PVT air collector with or without tedlar was numerically conducted by [44], under weather conditions of New Delhi, India and the glazed hybrid PVT without tedlar was selected as a best option. The impact of collector area, length, mass flow rate and duct depth on the efficiency of the conventional hybrid PVT collector of single and double-glass covers of PVT air heating system was studied by [45], using steady-state simulation.

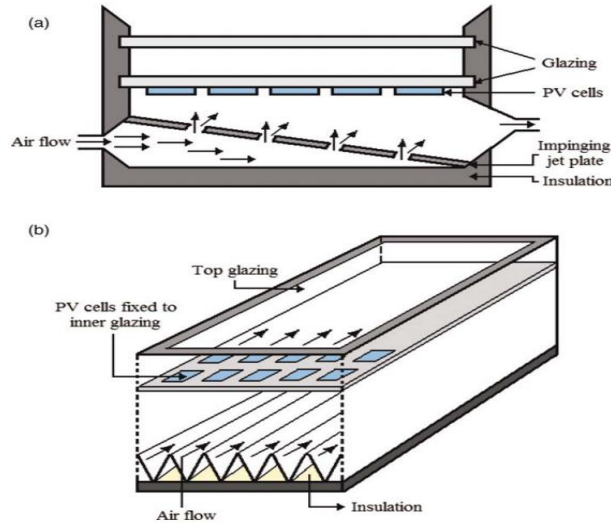


Fig.1.6 Schematic diagram of air PVT collectors with; (a) channels holes and (b) V-corrugated [43, 46]

To further optimize the performance of the PVT collector, different arrangements combining air/water into one collector were developed. The combination of air/water PVT collector was classified according to Zondag et al. [47] as (A) tube and sheet, (B) channel, (C) free flow and (D) two-absorber (Fig.1.7).

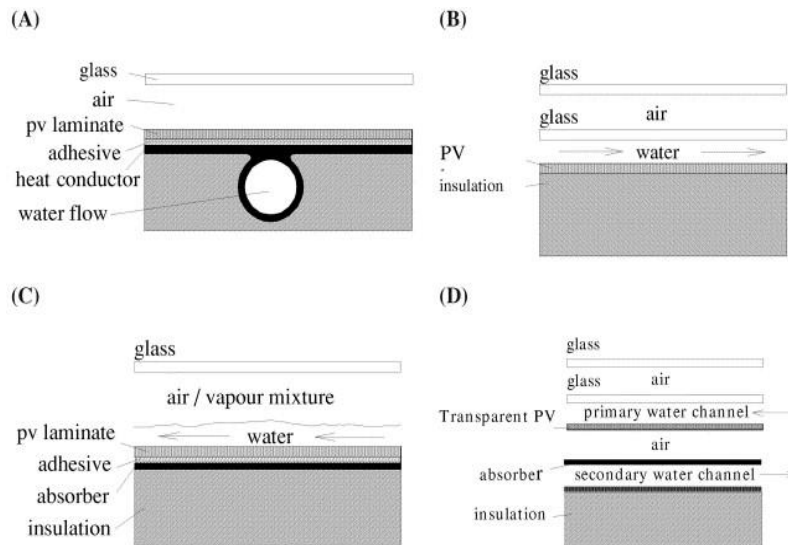


Fig.1.7 Sub-types of PVT collectors using water, air and a combination of water-air [47, 48]

The thermal efficiency of sheet-and-tube, channel PVT, free flow and two-absorber PVT-collectors was investigated by ^[47]. For the studied cases, thermal efficiencies of 52%, 58% and 65% were obtained for uncovered collector, single cover sheet and tube design, and channel above the PV design, respectively. A comparative experiment of hybrid PVT consisting of photovoltaic modules with thermal collectors was conducted by ^[49] to determine the effect of two PV module materials (pc-Si and a-Si) on the electrical efficiency. Furthermore, a parametric analysis in terms of PV and water, PV and air, PV water with glazing and PV air with glazing, was performed. The results of the experiment revealed a PV/water system efficiency of 13.3%, which was higher than other systems and while a higher electrical efficiency was acquired for pc-Si material. The thermal and electrical efficiencies of a combined water and air PVT collector incorporating thin flat metal sheet with finned back wall of air channel, suspended in the middle of the system were investigated by ^[50] considering different parameters such as channel depth, channel length and mass flow rate. Due to the high thermo-physical properties of water compared to air, a PVT water based collector resulted in total efficiency of about 61-62%, 9-10% and 52% for electrical and thermal efficiencies, respectively. An air and water PVT collector system incorporating channel and free flow absorber was experimentally investigated in the study of ^[51], based on four configurations such as unglazed with tedlar, glazed with tedlar, unglazed without tedlar and glazed without tedlar. The results showed that the daily efficiency of the water PVT system was higher than air for all configuration excepted glazed without tedlar. In addition, the results showed that the overall thermal efficiency of the system during summer and winter conditions was approximately 65% and 77%.

A substantial work has been carried out to determine the performance of PVT heat pump systems with air and water as cooling fluids medium and by use of various absorber arrangements. However, with research advancement, different channel structures as well as fluids with special properties are being developed and incorporated with the objective to maximize the heat removal from PV cell materials and enhance both thermal and electrical efficiencies.

1.2.3 Integration of various channels arrangements in PVT unit

In the past, complex channels structures heat sinks were entirely the cooling technology in electronic devices. Within time, the technology got application in the PV system due to its highest effectiveness in removing excessive heat of the surface with high temperature. This is due to the fact that the contact surface is increased with help of small size pipes networking whereby the fluid upon entering the network, it gets distributed within the heat exchanger so as to augment its contact surface area. The flow arrangements and channels materials, play an

important role to maximize both heat removal and heat transfer coefficient. The exceeded heat energy of the solar collector is transferred to the channels surface and to the fluid and therefore the three mediums form a heat exchanger ^[52]. An adequate choice of channels configuration, reduces pressure drop which is a characteristic of uniformity and thereby enhancing the heat transfer ^[53]. Although channel heat exchangers are able to dissipate higher heat flux densities but the slow flow rate creates a larger increase in the temperature alongside the direction of the coolant flow in both channel material and the coolant. In the study of ^[54, 55], it was shown that in addition to channel dimension, surface roughness also affects the heat transfer characteristics and the drop of pressure of coolant flow in a channel. Channels flow arrangements are mainly classified in two different configurations; conservation and bifurcation (Fig.1.8). These classes might have varying layouts as presented in (Fig.1.9, a-h).

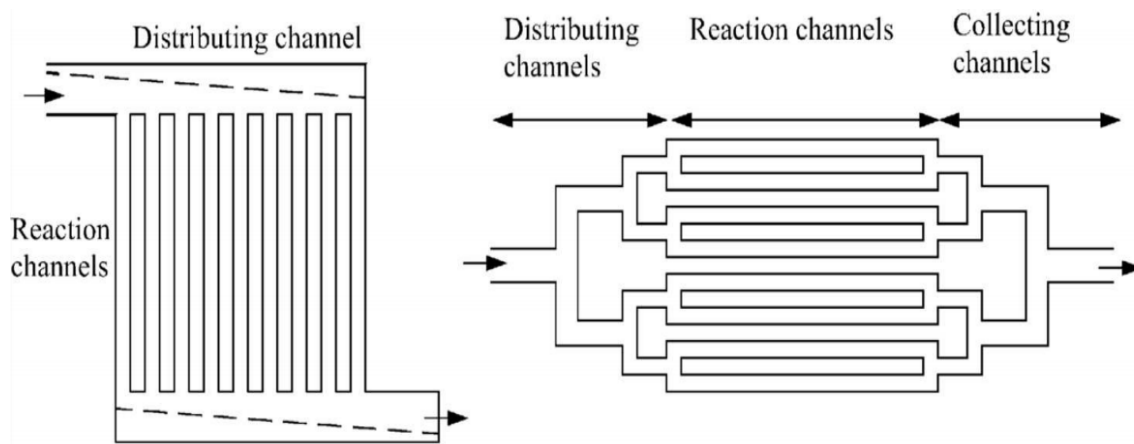


Fig.1.8 Conservative (left) and bifurcation (right) flow arrangements ^[56]

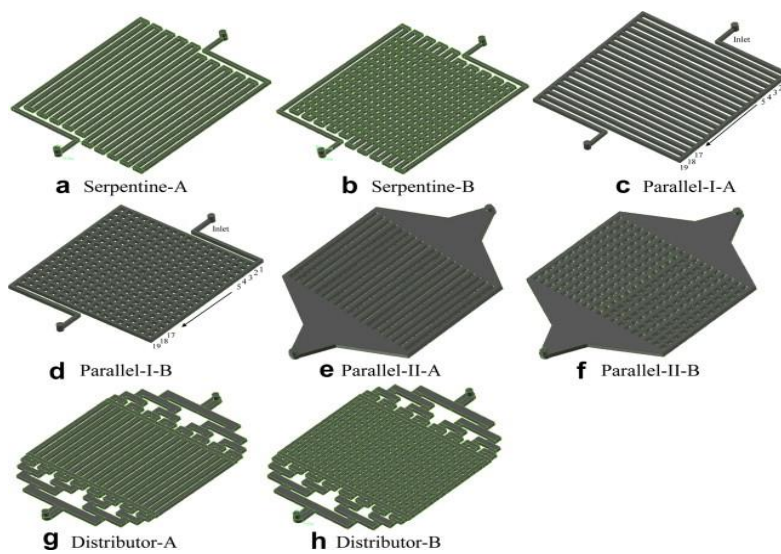


Fig.1.9 Different layouts of channels flow ^[57]

Many authors carried out their studies about the effective use of different channels configurations. With help of electrical resistance analogy for conservative and bifurcation networks, a model was developed by ^[57] to study the difference in characteristics of flow through the stated two networks. The main purpose was to reduce the pressure drop as well as to attain a constant pressure in all channels by utilization of two channels shape; rectangular and circular. The results showed that the minimum pressure drop acquired when Reynold number is low and whereas for high value of Reynold number, a pressure uniformity was achieved in channels. The comparison in terms of flow uniformity and flow distribution between rounded corners and circular bifurcation channels was carried out in the work of ^[58]. It was found that the longer the length of the channel after the bend, the more the flow is uniform. Moreover, a better flow distribution was observed when the length was five times the diameter. In summary to the previous literatures, the authors had as objective to enhance the fluid flow distribution in channels which is an indication of better heat transfer, temperature control and low pressure loss. It further results in minimization of pumping power, vibrations, noises, stresses and corrosions which might occur due to bad flow uniformity. This is also an obvious indicator that the performance of the PVT heat pump system will depend on the type of channel configuration employed.

1.2.4 PVT unit incorporating fluids medium with special properties

With the recent research, the heat transfer characteristics can be improved by enhancing thermo-physical properties of fluids. More specifically, this is realized by adding solid particles to the base fluid such as water, glycol ethylene, kerosene, oils and ionic liquids ^[59-61]. The concept of enhancing fluids properties was provided in nineteen centuries by Maxwell ^[62] but the technique didn't gain much attention due to large size of particles which was found to cause problems such as agglomeration, clogging and erosion^[63]. Later alone in 1995, new types of fluids known as nanofluids were developed by dispersing nanometer-sized particles in base liquids^[64]. In comparison to the conventional fluids, nanofluids have resulted superior thermal properties due to Brownian motion, thermophoresis, liquid-layering, clustering, and Ballistic transport induced by solid nanoparticles ^[65]. Therefore, this fact paves way for them towards different applications. In this view, utilization of nanofluids would increase the amount of absorbed incident solar energy, which was found to be only 13% when using a commonly fluid of water^[66]. Several investigations have reported successful application of nanofluids in solar energy application. The performance of flat plate collector and direct absorption solar collector with nano-fluid in the channel was analyzed by ^[67]. It was observed that nanoparticle increases the absorption of solar radiation as compared to pure water and helps in achieving a better efficiency. In the study of ^[68], the effect of nanoparticles size, concentration, and types of nanoparticles on the overall performance of the PVT system was studied. It was reported that

the performance of Al_2O_3 nanoparticles with water as a base fluid is better than TiO_2 nanoparticles. A number of authors reported a performance improvement when using different nano-fluids in the channel of PVT unit collector^[69-71]. In the experimental study of^[72], an increase in electrical and thermal efficiency of 3.03% and 12.4% were respectively attained. By use of two types of nanoparticles ($\text{CuO} + \text{Fe}$ and CuO) in a base fluid of water, the maximum increase in electrical and thermal efficiency of 2.14% and 5.4% were respectively achieved, in numerical study of^[73].

Meanwhile, refrigerants have the ability to absorb and release heat of solar when it is needed and vice versa. Therefore, using them in the system of PVT heat pump would be one of the most prominent solutions to deal with solar intermittence. The application of refrigerants as fluids medium through channels is attracting attention of many researchers due to the fact that they undergo phase change at different temperatures and considered to be high energy-saving, more stable and environmental friendly^[74]. For the first time in 1955, a system of direct expansion PVT heat pump using refrigerant to maximize the heat removal of the PV cells was proposed by^[75]. With this system, the refrigerant circulating in solar collector, changes its phase from liquid to vapor as it absorbs the heat of solar energy and becomes a heat source of the heat pump integrated in the same unit^[76, 77]. Following studies were focused on the system performance investigation when using different refrigerants and integration with some other heat sources. In this perspective, the experimental study of refrigerant-based PVT heat pump under real conditions was investigated by^[78]. The rig consisted of forty-eight solar panels arranged in two rows on a pre-coated steel support structure with R134a refrigerant fluid in copper tubes adhered to a thermal absorber and polystyrene foam insulator, and a 200L water tank. The experiment was conducted each day of June from 12:00 to 13:00. During this month, an average solar irradiance of almost 1 kW/m^2 was reached. The PV output current was between 30A and 37A and the output power between 800 and 900 W. The water temperature reached 50°C at the end of the experiment. Another experimental work was conducted by^[79] to study the performance of solar Rankine system using CO_2 as a working fluid. The system which produces both electricity and heat/refrigeration achieved a high thermal efficiency of 70% and electrical efficiency of 9.45%. Theoretical and experimental study was performed by^[80] to validate the model predictions and also to simulate a commercial collector and improved double-glazed flat plate collector using R134a, R227ea and R365mfc as working fluids to operate between the solar collector and a fixed temperature sink. It was found from the study that the net mechanical power which is strongly depend on mass flow rate and solar radiation attained a maximum efficiency of 11%. The performance of PVT heat pump using R-134a refrigerant was investigated both experimentally and analytically by^[77], at different valve openings. The study achieved a maximum COP of 3.7 at water temperature of 60°C . A similar study was carried out by^[81] under weather conditions of Singapore, to determine the impact of variable speed compressor on the system performance. For this study, COP, collector efficiency

and condenser tank temperature were respectively obtained in the range 4-9, 40-70% and 30-50°C. A solar collector efficiency of 62.7% and a COP of 2.6 were achieved in the experimental study conducted by [82]. In this study, a water-based collector loop was used and while the water heat source was employed in heat pump. By utilizing another type of refrigerant (R-22) in the PVT heat pump, the same COP of about 3.1 was achieved in the studies of [83] and [84] even though operated under different climatic conditions. In the former, the purpose was to heat up water in the tank capacity of 150L by use of electric expansion valve and under weather conditions of Shanghai, China. Whereas in the later, the author had the same purpose but in the West of Turkey. On the other hand, integrating PVT heat pump with ground heat source resulted a higher performance as studied by many authors. For the first time, the performance of the combined system of SGHP was evaluated by [85], considering both vertical double-spiral coil ground heat exchanger (GHX) and conventional heat exchanger of single-pipe vertical heat exchanger. In their findings, the maximum COP of 4.235 was reached. Further, they provided a reference model of solar-ground source heat pump and heat exchangers (GHXs). Many other works about similar study were performed and reported a good COP as can be consulted from [86-89].

In fact, from the above research studies about the use of nano-fluids and refrigerants, it is clearly demonstrated that a significant improvement in both thermal and electrical efficiencies of the PVT heat pump system have been achieved. The increase in thermal efficiency will increase the amount heat waste during daytime. This heat can be recovered by using the same two types of fluids medium (refrigerant and nano-fluid) to release it to the ambient, especially by taking advantages of the night natural cold of the sky.

1.3 Cooling of PVT unit with natural cold of the sky

1.3.1 Modes of cooling with natural cold of the sky

The natural night cooling (NNC) method utilizes night cold air and long-wave radiation to cool down and reduce the temperature of the surface's absorbed heat gains during daytime [90-92], Fig.1.10. For NNC to happen, the upper part surface should be interconnected to the heat capacity storage by the walls and internal partitions [93] and also when the surface temperature is greater than that of the ambient air [92, 94]. With this technique, the surface's absorbed heat gain is cooled down and as a result, the temperature of the heat storage capacity is minimized [91, 92]. This process is realized when the temperature of ambient air reaches the same temperature as the thermal mass [92]. The NNC technique can be applied in many climatic zones throughout the world. However, its efficacy differs depending upon urban morphology [95], meteorological conditions and some other microclimatic variables such as the urban heat island effect [96, 97]. The effectiveness of NNC technique lowers due to urban poor quality air and its

associated changes in urban microclimatic caused by the urban heat [98]. Some useful techniques such as the utilization of cool coating and green rooves were utilized by [99] and [100], respectively to reduce these impacts.

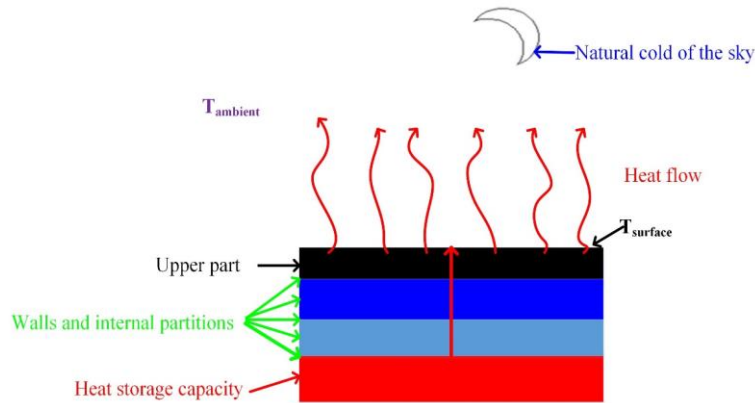


Fig.1.10 Cooling process by the NNC

In fact, this technique has been mostly employed to cool the rooms of building. Like for instance, the heat generated by the light inside house can be released to the ambient environment through rooftop, during nighttime, Fig.1.11. Alternatively, the night cooling air maybe allowed to enter the house through duct, cools down the room and warm air/heat is released through outlet duct, walls, windows and other opening gaps (Fig.1.12). Therefore, in additions to the aforementioned factors, the NNC is influenced by some other parameters such as; air flow, cooling load, building (shape, function location and construction), temperature differential, convective-heat-transfer-coefficient and algorithmic parameters for simulation and thermal storages. Besides, the cooling is more effective in non-residential buildings since the absence of personnel at night allows the achievement of higher air change rates.

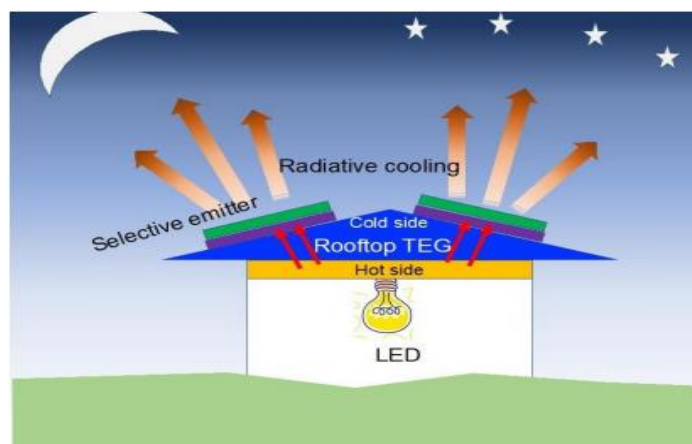


Fig.1.11 Cooling of house room long-wave radiation

whereas the airflow benefits of the per unit air change rate per hour of NNC significantly decreased at higher airflow rates, especially when the energy performance of NNC per unit of airflow change is limited to 3.3, 2.5, 1.8, 1.2 and 0.7 kWh/m²/y, for 2, 5, 10, 20 and 30 ACH of air flow. To further explore the influence of parameter on the NNC, Leenknecht et al. ^[107] performed a numerical study and use weighted overheating hours (WOH) to compare 1008 cases. It was found that the ACH increased for each instance that the WOH was added; however, this increase plateaus at higher air change rates. The impact of NNC in addition to the building envelopes factors (shape, size, type and location of the windows) was studied by Gratia et al. ^[108] considering moderate climatic of Belgium. In order to obtain a specific ventilation rate, the opening area of windows and the type of ventilation differed based on wind protection and wind orientation. The authors ascertained that single-sided ventilation was as efficient as cross night ventilation, in that with 8 ACH, both reduced the cooling load by approximately 40%. The performance of NNC in terms of indoor environmental conditions, adaptive comfort, and heat removed was assessed by Landsman et al. ^[109]. From their results, the NNC performance of each building varied mainly due to the differences in their typology and functionality. Moreover, NNC strategies in combination with each building's physical construction attributes affect the overall performance. Geros et al. ^[110] analyzed the effectiveness of NNC when a single-sided ventilation inside and outside was used in urban environment (urban canyons). The airflow between the two locations was ranged from 0.2 to 10ACH and the air flow rate for the two data sets ranged from 4 to 69 ACH. In their findings, the impact of wind velocity and direction became more evident for cross-ventilation. Furthermore, the ranges for temperature difference of 0.02°C- 2.6°C and 0.2°C-3.5°C were found for zone indoor inside the canyons and zone indoor of cross ventilation, respectively. The study concluded that the zone inside canyons significantly impacted the single- sided ventilation due the obtained both lower wind and temperature as compared to the outside. Givoni ^[111, 112] in his study found that the efficacy of NNC was maximized in desert and arid regions with night-time temperatures below 20°C, a summer diurnal temperature fluctuation of 15–20°C, and a maximum daytime temperature between 30 and 36°C. By use of tool capable of predicting indoor summer temperature required NNC air change rates and quantity of thermal mass, Shaviv et al. ^[113] found that the decline in maximum indoor temperature was reliant on the main parameters of thermal inertia, the diurnal and nocturnal temperature range of the site, and air change rate, and that the prediction of indoor temperature was a function of these stated parameters.

(3) Convective heat transfer coefficient

Convective heat transfer coefficients (CHTC) is another parameter having a great impact on the NNC as pointed out in the study of ^[114]. The cooling performance of conventional NV is reliant on the CHTC from the exposed building mass and the cool night-time air flow; the thermal inertia is recharged by the infrared and solar radiation through the air-to-room convective process in the daytime ^[115]. Several studies disclose that the convective cooling of

the air in the space and thermal inertia have a considerable impact on the predicted performance [107, 116, 117]. In the studies conducted by [118-120], they obtained limited results because of use of arbitrary values which were not dependent on the interior of NNC system. The influence of the CHTCs on the energy balance of buildings under heating and free-floating conditions was reported in the International Energy Agency (IEA) [121]. For NNC to be effective, CHTCs require increased air change rates; however, this requirement may not always apply. The simulation study conducted by Blondeau et al. [122] noticed no substantial difference in the indoor air temperature predictions derived from several increased convective coefficients at night-time. In fact, the cooling potential of NNC technique is limited because it is only dependent on thermal mass of the structure to decrease the air temperature [123]. Hence, in order to enhance the effectiveness of NNC, other energy technologies such PVT heat pump systems have to be coupled with.

1.3.3 Coupling NNC with PVT unit

To boost the effectiveness of NNC and enhance the performance of conventional PVT heat pump, PVT unit has been integrated with NNC. This is to mean that PVT unit which is considered as a heat source releases its heat to the ambient environment. The cooling of PVT unit with NNC is realized following the Fig. 1.1. b of heat pump system for cooling mode and Fig.1.12 of cooling process by NNC. The PVT unit represents the heat source of the room and while NNC shows the heat sink of the outdoor. Alternatively, the heat of refrigerant or other alternative fluids like nanofluids in the channels represents the heat storage capacity and while different layers' materials on top of channels configuration (Fig.1.14) represent walls, internal partitions and upper surface.

Nowadays, most of PVT heat pump systems are in operation during daytime to generate electrical and thermal energies. However, thermal energy is less needed and produced for the purpose to cool down the PV cells and thereby enhancing electrical efficiency of the system. This is an obvious indicator that a huge amount of heat is wasted and make the cogeneration system not as much profitable as expected. With research development, researchers realized that combining the natural night cooling with PVT heat pump system, could be a best solution to the above mentioned problem. In this perspective, PVT units are being modified to serve both as an evaporator during daytime and as a condenser in the night. In particular to the PVT unit condenser as a recently incorporated component, its main function is to recover the waste heat of solar energy, by taking advantages of natural cold of the sky and long-wave radiation, which can even attain a temperature of below -10°C [124].

The newly developed PVT heat pump system is mainly composed by five components; roll bond (RB)-PVT unit, compressor, storage tanks (thermal/ice), electronic expansion valve and four reversing valve (Fig.1.13) [16]. Here it should be notified that RB was introduced

(Fig.1.13) in order to overcome high thermal resistance which would incur due to small contact area between the most commonly used absorber of sheet-and-tube and pipes ^[125]. Otherwise, the notation of PVT unit will only be used in the next sections of this thesis. The heat exchange occurs between storage tank and PVT unit. During daytime, the solar radiation which is not transformed into electricity by PV cells is absorbed by PVT unit and transported to the thermal storage tank via the fluid carrier inside pipes. The reversed process is performed during nighttime whereby the unused heat of solar thermal energy from the storage tank is transported to the PVT unit by the fluid inside pipe, for rejection to the ambient environment. In both processes, compressor and electronic valve regulate the flow to the required conditions and while reversing valves change the direction of refrigerant flow. For the former process, PVT unit acts as an evaporator (Fig.1.13. a) whereas in the later process, PVT unit serves as a condenser (Fig.1.13. b). It is therefore understandable that the PVT unit plays a big role in a PVT heat pump system due to its dual-functionality. On top of that it is directly exposed to the ambient and hence highly effects the performance of the whole system of PVT heat pump. Even though most of the researchers investigated the performance of PVT heat pump with much emphasis on PVT unit evaporator as the most popular system, the similar approaches can also be applied to the PVT heat pump system with PVT unit as a condenser but with some modifications. It is worth noting that the common objective in both two PVT units is to speed up the cooling process and attain a desired temperature of either PV cell surface or water in ice storage tank. However, there are still some problems which need to be addressed for higher performance of the PVT heat pump system.

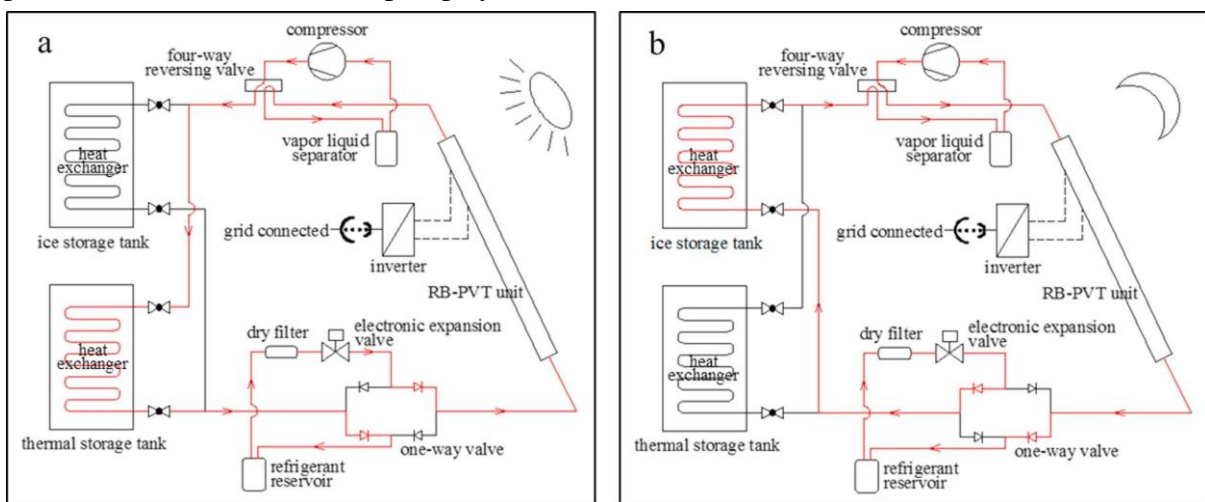


Fig.1.13 Schematic diagram of PVT heat pump for heating (a) and cooling modes (b)^[16]

More specifically, at night, the PVT unit will act as a condenser to release the condensation heat of the heat pump system in the form of long wave cold radiation and natural convection of the surrounding air. The heat pump system will realize the night cooling process to produce the chilled water or ice (ice storage) required by the building. Specifically, the PVT unit (Fig.1.14.

a) is composed of a heat exchanger plate added behind the PV unit (Fig.1.14. b). A serpentine refrigerant channel (Fig.1.14.c) is arranged inside the inflatable heat exchange plate. The refrigerant vapor flows into the inflatable heat exchanger plate, cools, condenses and releases condensation heat in its serpentine channel, and then flows out. In the process, the condensation heat of the PVT heat pump is continuously released to the ambient and the sky by convection, radiation and conduction through different layer materials of the PVT unit (Fig.1.5 b), until the required temperature of chilled water/ice is reached inside tank.

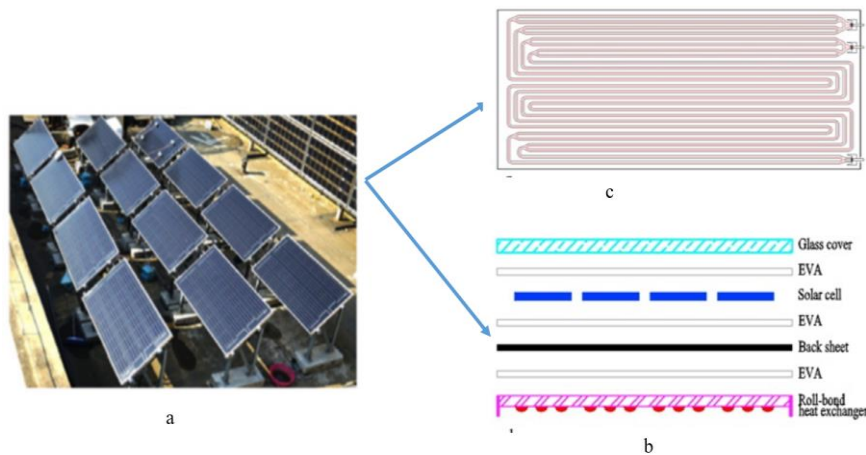


Fig.1.14 Schematic diagram of (a) PVT unit , (b) Composition of PVT unit and (c) structure of serpentine channel inside heat exchanger ^[16]

Therefore, the heat release performance of PVT unit under condensation condition will directly affect the cooling capacity of PVT heat pump system at night. The condensation and heat release characteristics of PVT unit are closely related to the shape of serpentine channel structure, the shape of surface structure, the flow and heat transfer state of refrigerant in channel, the thermal conductivity between the plate and PV unit, and the sky effective temperature. In order to further improve the night cooling performance of PVT heat pump system, it is necessary to deeply study the condensation heat transfer characteristics and enhance heat transfer methods of PVT unit working in the condenser at night in summer.

1.3.4 Research progress of PVT unit under night cooling

The natural conditions depend on both water content of atmosphere and the distance from the ground surface, whereby 90 % of sky radiation comes from the first kilometer above ground and 40 % from only 10 meters above ground ^[126]. Radiative cooling is based on heat loss by long-wave emission towards the sky. The mechanism is realized when the surface of the object is warmer than its surrounding. Radiative cooling is a new method as the first experiments based

on radiative cooling of air flowing in narrow channel started in Israel about 50 years ago. As time went on, different radiative cooling applications such as; movable insulation, air based systems and open or closed water-based systems were investigated. In the years 1981, radiative cooling water based system was applied for the first time to cool water inside tank and by using a standard flat plate collector coupled with a storage tank ^[127]. Eleven years later in 1992, the same approach as ^[127] was applied in Israel by ^[128] to assess the net cooling power of the previous system without cover. In 2005, radiative cooling based movable insulation was tested for the first time by ^[129] and a specific cooling power in range of 20-80W/m² was measured. From to 2006 to 2010, the method was mainly applied in buildings to assess the magnitude of the resource and the variations in cooling potential for different locations ^[130, 131].

In the latest technology of PVT heat pump, PVT unit is being served both as an evaporator and as a condenser. Fig.1.15 illustrates the process of cooling load formation. In fact, the thermal energy stored in a tank 1 during daytime becomes a cooling load (ice) storage tank 2 in night and while PVT unit which was operating as an evaporator to absorb solar thermal energy is switched to the condenser to release heat of unused thermal storage of tank 1. During this particular time, the heat exchangers (in form of coils) embedded into tank work as evaporator. The liquid refrigerant (Flow refrigerant out T₂) is supplied to the heat exchangers inside tank, absorbs heat and changes its phase from liquid to vapor. The vapor refrigerant (Flow refrigerant in T₁) is sent to the PVT unit to start a new cycle as well as to release heat to the ambient (Q_{ambient}). While this process occurs, a heat exchange between hot water (Q_{hot water}) and PVT unit (Q_{PVT}) continuously takes place until the required cooling temperature is reached inside cold storage tank 2.

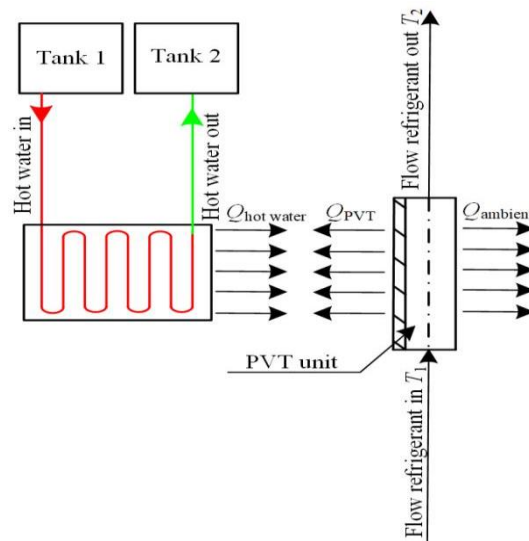


Fig.1.15 Illustration of the heat exchange to turn unused thermal energy of tank 1 into cooling load of tank 2 by the PVT unit

Recently, some others authors improved energy usage by natural cooling strategy. Development and performance evaluation using TRNSYS of a novel ceiling ventilation system integrated with PVT collectors and PCMs, has been conducted by ^[132]. In their findings, the indoor thermal comfort of passive buildings without air conditioning systems can significantly be improved with maximum air temperature rise of 23.1⁰C from the PVT collectors during winter. They also found that using the mentioned system but with only PCM materials, enhanced indoor thermal comfort through night-time sky radiative cooling. A combined system of both solar heating and radiative cooling based on composite surface, and which is mounted together with traditional flat plate solar heating system, have been compared experimentally by ^[133] in terms of thermal performances both at daytime and nighttime. The results showed that, solar heating-radiative cooling during nocturnal collector testing mode had a net radiative cooling powers of 50.3 W/m² and 23.4 W/m² on clear and overcast nights, respectively. In the study conducted by ^[134], a transient CFD method was performed to predict the energy consumption of school building by considering both 2D and 3D of its geometry and when night cooling strategy is used instead of normal cooling loads. It was found that using free cooling energy of the sky saves energy by 50 %. The study about nighttime radiative cooling of unglazed and PVT collectors has been also conducted by ^[134] to compare the results obtained using three methods; simulation with TRNSYS, experiment and theoretical. The main target was to evaluate the performance of the system in terms of cooling power, cooling performance per night and coefficient of performance (COP). In all three cases, a good agreement was observed and the ranges of; 20-75 W/m², 0.2-0.9 kWh/m² and 19 -59 were respectively obtained. An investigation of finite element analysis of the dynamic performance of a hybrid flat plate solar collector/nocturnal radiator for water heating and cooling in five Nigerian cities, was carried out by ^[135]. The study results showed that the minimum temperatures of water attained during nocturnal period were; 20.21⁰C, 20.12⁰C, 21.9⁰C, 20.95⁰C and 22.01⁰C for Owerri, Portharcourt, Ikeja, Maiduguri and Sokoto respectively. Development of mathematical model, testing and experimental works have been conducted by ^[136] to assess the performance of the system incorporating; Solar PV, Solar thermal and radiative sky cooling. It was found that the annual electrical, heat and cooling gain of the system in Eastern China are 479.67, 2369.07 and 1432.49 MJ respectively.

PVT unit to produce tri-energy generation (i.e. heat, electricity, and cooling load) has been developed and studied by ^[16], to determine both practical feasibility and performance. In particular, to the refrigeration performance, study results showed that both COP and cooling power decreased by 1.4 and 1.4kW for the water process respectively, and whereas for the ice process, a constant COP of 2.3 was obtained during the whole period of the experiment. Besides,

18.5kWh and 6.7kWh were obtained for refrigeration capacity and power consumption, respectively. An experimental study of PVT heat pump operating under nighttime has been conducted by ^[137], to investigate the refrigeration performance and operating characteristics of the system. They concluded that, the system can fulfill the cooling demand of the building and also be a basic framework model for the whole region of North China. An experiment and simulation with MATLAB have been carried out by ^[138] to analyze refrigeration characteristics of a hybrid heat dissipation photovoltaic-thermal heat pump system under various weather conditions in summer night. For the analyzed system, PVT unit acted as a condenser to reject heat to the ambient while storage tank served as an evaporator. The results of the study showed that the maximum COP and average heat dissipation obtained were 2.1 and 420 W/m² respectively. It further proved that the change in ambient air temperature and wind velocity less than 1 m/s, have a great impact on both system performance and heat dissipation of the PVT modules.

Existing research studies on PVT unit condenser were focused on the performance and feasibility of the system under different weather conditions. In addition, most of them were conducted using experiments and software other than ANSYS Fluent/CFD. With its ability to present thermal behavior of the material without having to build an experiment, ANSYS Fluent/CFD can be employed both to deeply study the condensation heat transfer characteristics and to propose new strategies to enhance heat transfer mechanisms of PVT unit under cooling condition, during summer nighttime.

1.4 Strategy to study PVT heat pump systems using CFD method

The performance of the PVT heat pump system has been investigated using different methods such as experiment and numerical. For numerical results to be accredited, they first have to be compared with the previous similar studies either carried out experimentally or numerically. In this perspective, a number of authors performed their studies about PVT unit by numerical method and their results were discussed considering different parameters. This section presents different models of PVT unit and various strategies employed by authors to study the heat transfer characteristics and overall COP of the PVT unit, by use of ANSYS Fluent/CFD method. Here it should be notified that only recent numerical studies with ANSYS Fluent/CFD are considered so as to serve as guidelines for the current PhD thesis. For more clarification, model establishment is first described and then follows the methods to solve these models.

1.4.1 Model establishment

Alternative cooling strategies are being developed day by day and numerically investigated to determine their effect on the overall efficient of PVT unit. Therefore, in this section, the models as well as the methods of mesh creation proposed by different authors are briefly

explained. It should be mentioned that some of the studies did not provide mesh contours and therefore, they are not presented here alongside with the physical models. One of the ways to enhance the cooling of PV cells is to improve the functionality of channels. For instance, in the study of ^[139], a model of PVT system was solved and validated with experiment, under weather conditions of Malaysia. The key research issue was to design, develop and study the water based PVT system integrating a dual oscillating absorber copper pipeline flow, by use of ANSYS 19.2. From Fig.1.16, a. represents the full model and while the b. shows the components comprising the model utilized in the study. During mesh creation, structured mesh with hexahedral elements were created to improve the temperature gradient and natural convection at the boundary layer (Fig.1.16, c).

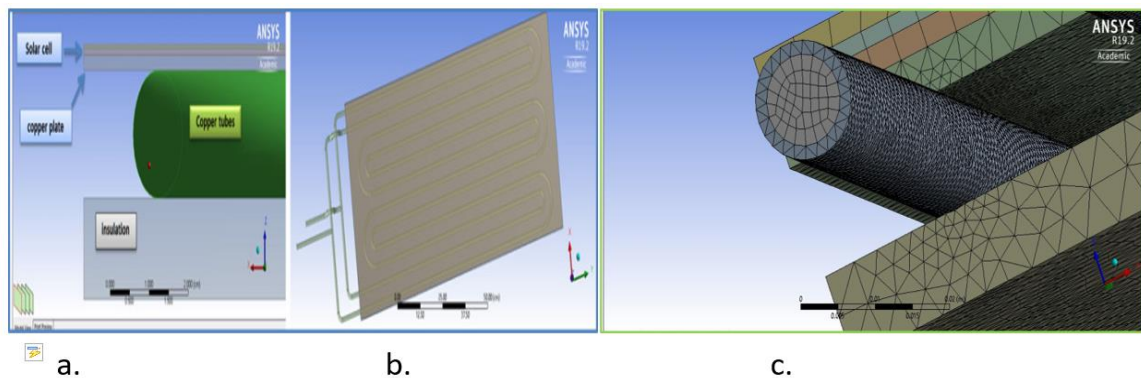


Fig.1.16 Schematic diagrams of water PVT collector

Even though low thermal conductivity, efficient use of air depends on the structure of channel through it is passing. A simulation with ANSYS Fluent was carried out by ^[140] to predict the temperature distribution of the PVT unit with fins, Fig.1.17, (a). The flow channels at the bottom face of the PVT system were created by incorporating the rectangular fins on the longitudinal distance. The air was used as a cooling fluid medium through the channels in order to quantify its harvesting energy at the outlet air, without having to build an experiment. A structural mesh was created with much emphasis being put on the mesh of ducts, where further refinement was performed, Fig.1.17, (b).

In order to avoid overheating and thermal failure of PV modules, it is of paramount importance to extend extra surfaces which further remove heat. The effect of incorporating periodic grooves in parallel channels of PVT system was numerically investigated in the study of ^[141], Fig.1.18 (a-c). Due to complexity of heat transfer process in the parallel cooling channel with periodic expanded grooves, the mesh near the wall of channels was refined, Fig.1.18 (d).

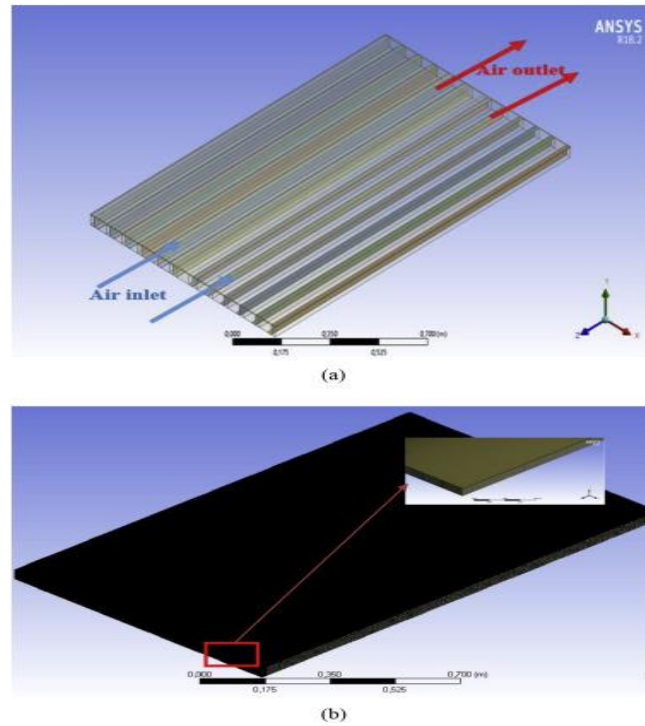


Fig.1.17 PVT system with fins (a) and the corresponding mesh (b)

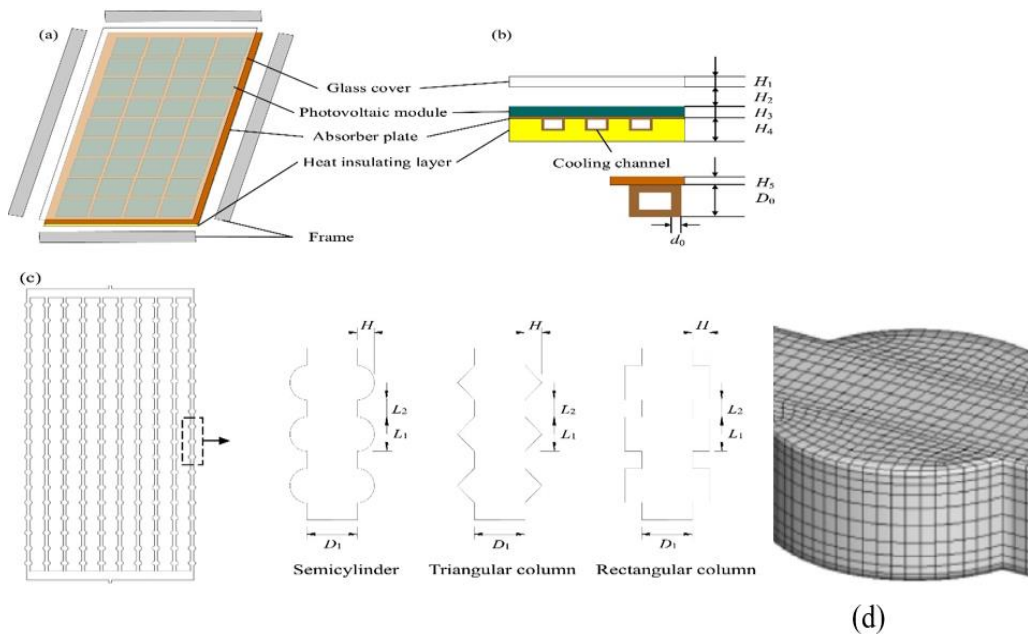


Fig.1.18 Schematic of PVT system (a), its front view (b), parallel channels with different groove profiles (c) and mesh patterns (d)

To further determine a better way of placing different components of PVT unit, a novel PVT unit (Fig.1.19, a) incorporating water layer at the top of PV module, to cool PV cells as well to filter the incoming of solar radiation was modeled and solved numerically in ANSYS

Fluent ^[142]. The model was meshed in ANSYS Fluent 16.2 using the built-in physics controlled mesh sequence and a model-free hexagonal mesh was set as a way to reduce residuals, Fig.1.19, b.

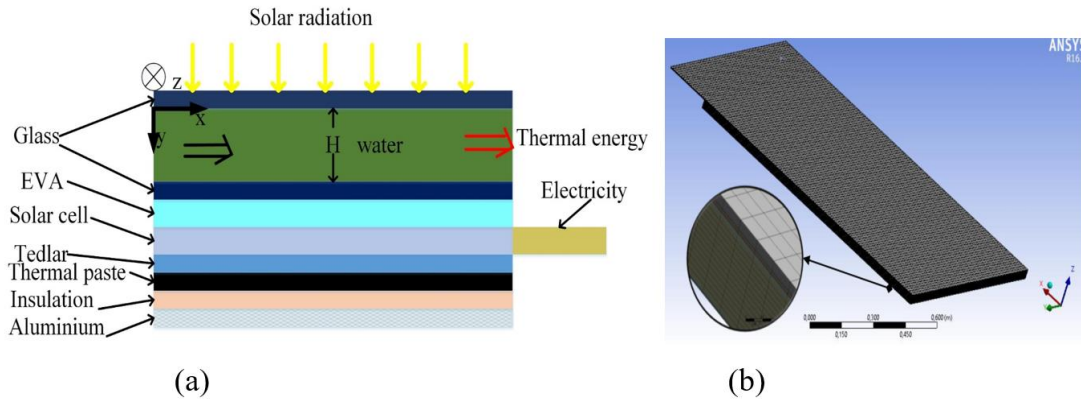


Fig.1.19 PVT system with water layer on top (a) and mesh distribution patterns (b)

The impact of flow channel arrangements, diameters and flow rates on the water based PVT unit was numerically studied, by use of ANSYS Fluent ^[143]. The system was simulated considering three arrangements (a. continuous, b. longitudinal and c. lateral), Fig.1.20 A. The model was first built in SOLIDWORKS and imported in ANSYS meshing. During mesh creation, triangular mesh was applied to pipes and while the rest of parts were meshed in a similar way by tetrahedral method, Fig.1.20 B.

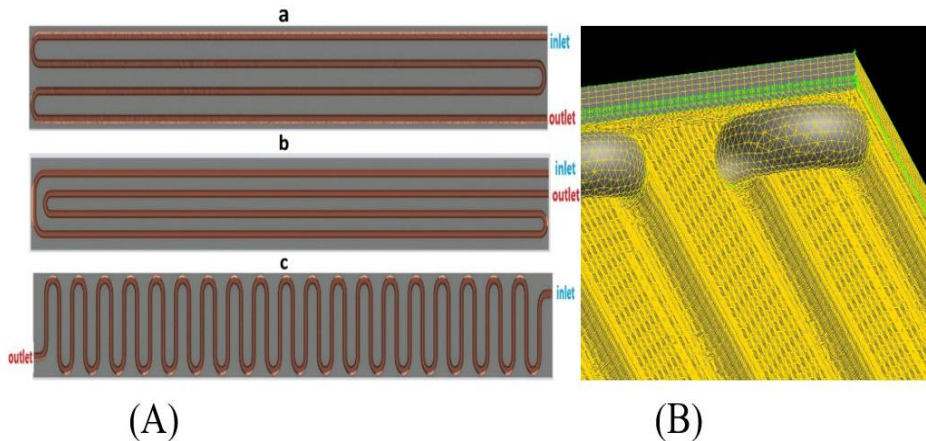


Fig.1.20 Different tubing layout at the back side of PVT collector (A) (a. Continuous, b. longitudinal and c. lateral) and mesh distribution (B)

To further optimize fluid channel pattern, the characteristics of two phase change roll-bond were investigated in the study of ^[144] using different flow channel arrangements of hexagon, grid, rectangle and linear types , Fig.1.21, a-d. A numerical simulation with CFD was performed

to determine the distribution behaviors of different parameters in the four stated flow channels. The 3D structured grids were adopted inside the computational domain for both solid and fluid due to the fact that they have better convergence in CFD solution algorithms and solvers compared with unstructured grids, Fig.1.21, e.

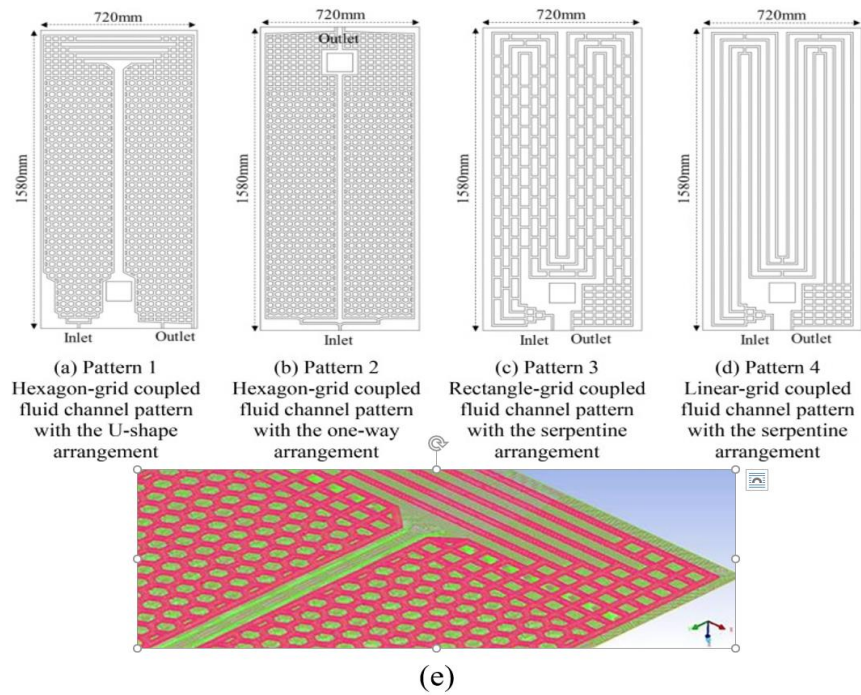


Fig.1.21 Different flow channel patterns (a-d) and mesh (e) [144]

In case when solar is not enough to provide the required energy for PVT system, thermoelectric (TE) can be integrated with PVT system to overcome the problem. TE is taken as a heat sink to provide energy to the inlet water in riser and to the layers on top of it. In this circumstance, a numerical study of PVT unit integrated with thermoelectric (TE) generator module was conducted by [145], Fig.1.22 (a). The best mesh to properly capture the solution was first selected among 6 created meshes based on both outlet temperature and velocity attained for each mesh, Fig.1.22 (b).

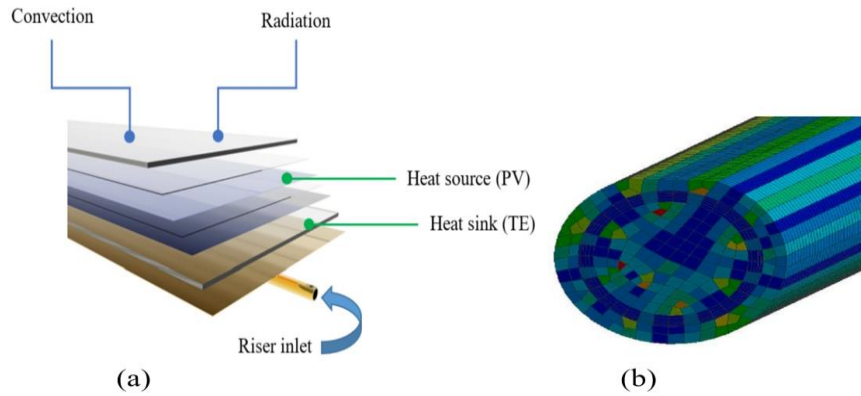


Fig.1.22 PVT unit integrated with TE (a) and pipe mesh patterns (b)

The heat transfer enhances depends on the thermal conductivity of cooling fluid medium used. The thermal conductivity of existing fluids can be improved by addition of nanoparticles to the base fluid. In this perspective, the effect of solar radiation and inlet temperature of Al_2O_3 -water nanofluid on the performance of PVT system with, was analyzed by [146]. The model is composed by serpentine pipe, insulation layer at the back side and 4 different layers on top, Fig.1.23(a). Different meshing methods were applied at different components of Al_3O_2 -water/PVT system, Fig.1.23(b). The rectangular geometries were meshed by the number of divisions option and while edges were divided into thinner sections. Meanwhile, tetrahedron method and curvature size function option were respectively activated for pipe and fluid domain.

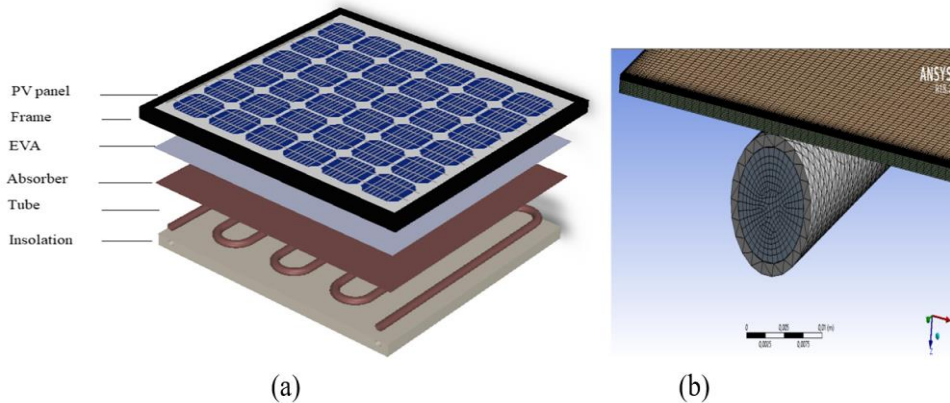


Fig.1.23 Geometry of Al_3O_2 -water/PVT system (a) and its corresponding mesh (b)

1.4.2 Solution methods

The methods of solving the above described models and their corresponding outcomes are illustrated in this section. The model of Fig.1.16 [139] was solved at steady state under constant inlet water temperature of 299.15K and various operating conditions of 600-1000W/m² for solar

radiation and mass flow rate of 2-6l/min. Maximum efficient of 59.6% and 11.7% was respectively attained for thermal and electrical, at higher mass flow rate of 6l/min.

Thermal and electrical efficiency, energy and exergy of the PVT system of Fig.1.17^[140] were analyzed at two mass flow rates of 0.031087kg/s and 0.04553kg/s. The mathematical equations related to the 3 D model of PVT unit with fins were first discretized by SIMPLE algorithm and solved by a second upwind scheme considering the walls to be adiabatic, constant inlet air velocity and pressure condition at the outlet. The required solution attained whenever the residuals for continuity and velocity were less than 10^{-6} and while those for energy were less 10^{-8} . As a results, the maximum thermal and electrical efficiency of 49.5 % and 13.98% was respectively achieved at mass flow rate of 0.04553kg/s.

During model solution of Fig.1.18^[141], the pressure, momentum and discrete ordinates were relaxed by under-relaxation factors of 0.3, 0.7 and 0.9 respectively. The results revealed that the heat transfer enhances due to thermal boundary layers and vertexes formed in the grooves. In addition, increasing groove length increases both convective heat transfers and flow resistance of the pump power of parallel cooling channels.

In the process of getting solution for model of Fig.1.19^[142], a quasi-steady state was assumed to reflect a constant solar radiation within 15 min. The flow of water which is temperature-dependent was considered laminar and fully-developed. At different boundary conditions, the 3D model was solved at steady-state and the average data of both cell surface and water outlet temperature were recorded and used to calculate the energetic and exegetic indexes of the PVT unit. The impact of channel height (H), inlet water and weather parameters on the aforementioned indexes were investigated and an excellent performance of the new system was determined as compared to the existing models of PVT systems with water channel at the back.

The mathematical equations (continuity, momentum, and energy) related to the PVT system of Fig.1.20^[143] were solved using Fluent discretization software and a Pressure-based solver in this software. For the sake of less computational time, wind speed (0m/s) and thermo-physical properties of the PVT unit materials were assumed constant. From their study, highest efficiency of 65.71% and 11.88% was achieved for thermal and electrical, respectively.

In the model of ^[144](Fig.1.21) , the modelling of phase change fluid of R134a was performed by multiphase and the evaporation-condensation mechanism was selected for phase interaction. Moreover, the turbulences were handled by k-epsilon viscous model. In their preliminary studies, hexagon type was selected as a best channel pattern. The obtained results after coupling hexagon grid type with one-way channel arrangement were 4.37, 16.7% and 47.6% for COP, electrical and thermal efficiency, respectively. The solution of the PVT system integrated with TE (Fig.1.22)^[145] by employing SIMPLE algorithm and pressure coupling method. At the same operating parameters, electrical efficiency of PVT/TE was found to be 2.25% higher than that of PVT. The nanofluid in the serpentine pipe of Al₃O₂-water/PVT

system (Fig.1.23) ^[146] was assumed single phase due to the existence of thermal equilibrium between water and nanoparticles. Conjugate heat transfer and least square cell based were set to deal with gradients of the solution at the cell center. The results revealed that increasing both solar radiation and inlet temperature reduces electrical efficiency and while thermal efficiency remained constant after first rise. Moreover, a higher improvement in both heat transfer coefficient and system efficiency was achieved when using Al₂O₃-water nanofluid as compared to pure water.

From the studies conducted, ANSYS Fluent/CFD has been employed to analyze the performance characteristics of PVT heat pump system, by applying various methods to increase the heat removal. However, the authors mostly focused on the PVT unit evaporator as the most commonly used units and it is rarely to find research conducted on the PVT unit condenser. However, it is believed that similar techniques to numerically study the performance of the PVT evaporator, can also be applied in PVT unit under condensation and cooling conditions with some modifications.

1.5 Research Contents and Research Route

This section presents the knowledge gaps from the already conducted research studies, objectives and methods of the PhD thesis, contents and a summary roadmap.

1.5.1 Knowledge gaps

A comprehensive literature studies has indicated that a great job has been done on the performance improvement of PVT unit component. However, the researchers mainly focused on the PVT unit collectors working at daytime, and there is relatively little research work on the enhanced heat transfer of PVT unit component under condensation and cooling conditions at night. It should be reminded that the PVT unit collector as a condenser is a recently developed component to convert unused solar thermal energy into cooling load demand. As a newly incorporated component, few existing research studies have been to determine the performance and practical feasibility of the unit under various weather conditions, mostly by using experimental method. In contrary to the conventional PVT unit where solar energy is absorbed and converted into useful energy of heat and electricity, the heat of fluid inside pipe of the PVT unit under condensation and cooling conditions at night is released to the ambient environment by different modes, especially by taking advantages of natural cold of the sky and long-wave radiation, Fig.1.24.

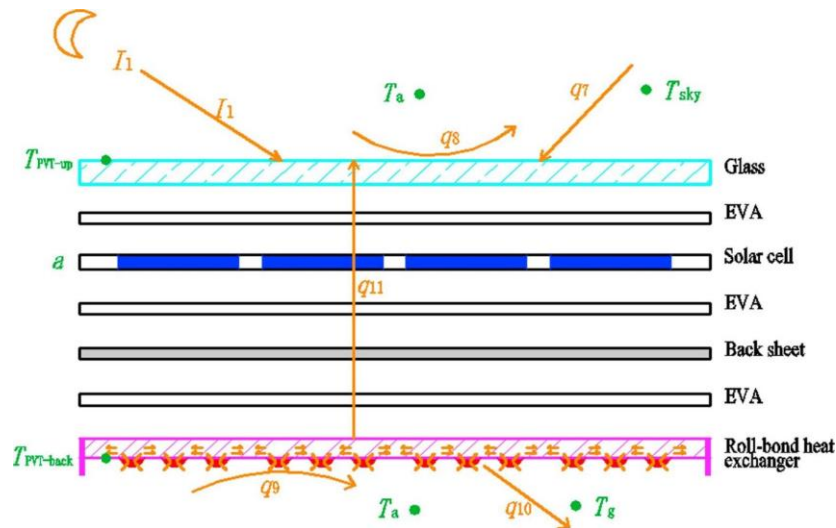


Fig.1.24 Heat transfer mechanisms in fluid channels and materials of the PVT unit condensation and cooling conditions at night

With this unit (Fig.1.24), the refrigerant vapor flows into the inflatable heat exchanger plate, cools, condenses and releases condensation heat in its serpentine channel, and then flows out. In the process, the condensation heat of the PVT heat pump is continuously released to the ambient and the sky by convection, radiation and conduction through different layer materials of the PVT unit, until the required temperature of cooling load is reached. The heat release performance of PVT unit under condensation condition will directly affect the cooling capacity of PVT heat pump system at night. The condensation and heat release characteristics of PVT unit are closely related to the shape of serpentine channel structure, the shape of surface structure, the flow and heat transfer state of refrigerant in channel, the thermal conductivity between the plate and PV unit, and the sky effective temperature. In order to further improve the night cooling performance of PVT heat pump system, it is necessary to deeply study the condensation heat transfer characteristics and enhance the heat transfer methods of PVT unit working as a condenser at night in summer. Moreover, proposal of new strategies to replace the already existing ones is of utmost importance in the research of PVT unit condenser.

1.5.2 Research objectives and methods

The main objective of this PhD thesis is to further improve the summer night cooling performance of PVT heat pump system, by proposing alternative methods to replace already existing ones. Only PVT unit is considered as the most important component to release the heat of thermal storage tank to the ambient environment. Moreover, a numerical simulation method was used to study the enhanced heat transfer of the PVT unit under the summer nighttime, with much focus on dimensions of existing PVT unit condenser, roughness of the bottom face, change in channel structure and incorporation of new fluid in the channel unit to absorb and

transfer the heat to the PVT unit. The physical and mathematical models are first established and then after solved to get and analyze the results of the particular cases under investigation. The specific research objectives and the solution methods are given as follows:

(1) To establish the mathematical equations related to each of the considered models of the PVT unit for cooling at night. The developed mathematical equations are for fluid inside channel and thermal energy in PVT unit materials. Thermo-physical properties of three types of fluids of water, refrigerant (R407C and R134a) and nanofluids are given as a function of temperature. Moreover, thermal energy equations are written taking into accounts heat conduction through different layers of the PVT unit and convection at both surfaces (top and bottom) and inside channel.

(2) To propose the solution method for the developed mathematical equations in ANSYS software and finalize simulation. The methods, assumptions, operating conditions as well indexes to assess the performance of the four considered models of PVT unit condenser are provided. To get an accurate solution, the model has to be well prepared. The preparation of the model includes creation of mesh able to capture solution and model validation.

(3) To analyze the heat transfer behavior of the PVT unit condenser at its different parameters change. The heat transfer is analyzed in terms of heat dissipation flux and outlet average fluid Nusselt number considering distance between two channels and lateral distance, longitudinal distance and the diameter of both internal and external of the channel. This is performed in order to determine optimum dimensions of the PVT unit condenser. The optimum dimensions are obtained by the intersection points between heat dissipation flux and outlet average fluid Nusselt number. Additional, the effect of internal and external factors as well as the heat transfer improvement of optimized model, are determined.

(4) To determine the heat transfer characteristics of the PVT unit with fins addition at the outer surface of channels, and put forward this new type of PVT unit. A set of studies are conducted to achieve a desired model of PVT unit condenser with fins. Initially four PVT unit condenser models with fins of different profiles are studied in terms of heat dissipation flux. On the basis of the models with highest heat dissipation flux, further studies are performed to determine the number of fins best fit on the outer surface of channel. This is carried out in terms of both heat dissipation flux and the overall fin efficiency. Having known the best fin profile and number, a sensitivity analysis is done to study the effect of different fin parameters (length, width and position) on the COP, heat dissipation, pressure drop and overall fin efficiency.

(5) To determine the effect of integrating news cooling strategies in the absorber of existing PVT unit. To realize this study, a model of PVT unit condenser integrating a novel channel of hexagon-grid coupled with fluid channel of serpentine arrangement in its absorber was solved and the results of COP, average vapor fraction and heat dissipation flux are discussed at both

different mass flow rates and ambient temperatures. In addition, PVT unit integrated with nanofluids as fluids medium is solved under cooling condition and the results are discussed in perspective of entropy generation, outlet temperature, Nusselt number of the fluid inside channel and the COP at different nanoparticle fractions, mass flow rates, inlet flow temperature and ambient temperature.

In fact, to achieve the above mentioned objectives, four different models were solved in ANSYS Fluent software and a step by step procedures was followed to get the solution results, Fig.1.25. A representative 3D model of each of the four considered models was built in ANSYS design modeler, meshed in ANSYS meshing and then after solved in ANSYS solution processor. In addition, in ANSYS solution processor, the accuracy was confirmed when the percentage discrepancy between the results of the considered models and those of previous studies was less than 20% , as in accordance with ^[147], and otherwise had to revise the whole simulation. In total 5 sets of simulation were carried out in ANSYS Fluent software. The first set of simulation were performed to determine the optimum dimensions of existing model of PVT unit condenser and analyze the heat transfer characteristics of optimized model. The second sets of simulation were to further improve the heat transfer characteristics of the unit by adding fins at the outer surface of the channels. The fourth sets of simulation were to investigate the effect of integrating PVT unit condenser with a novel channel. At last, a model of PVT unit with nanofluids as fluids medium in channel was solved under cooling condition in order to propose new fluid to replace refrigerant.

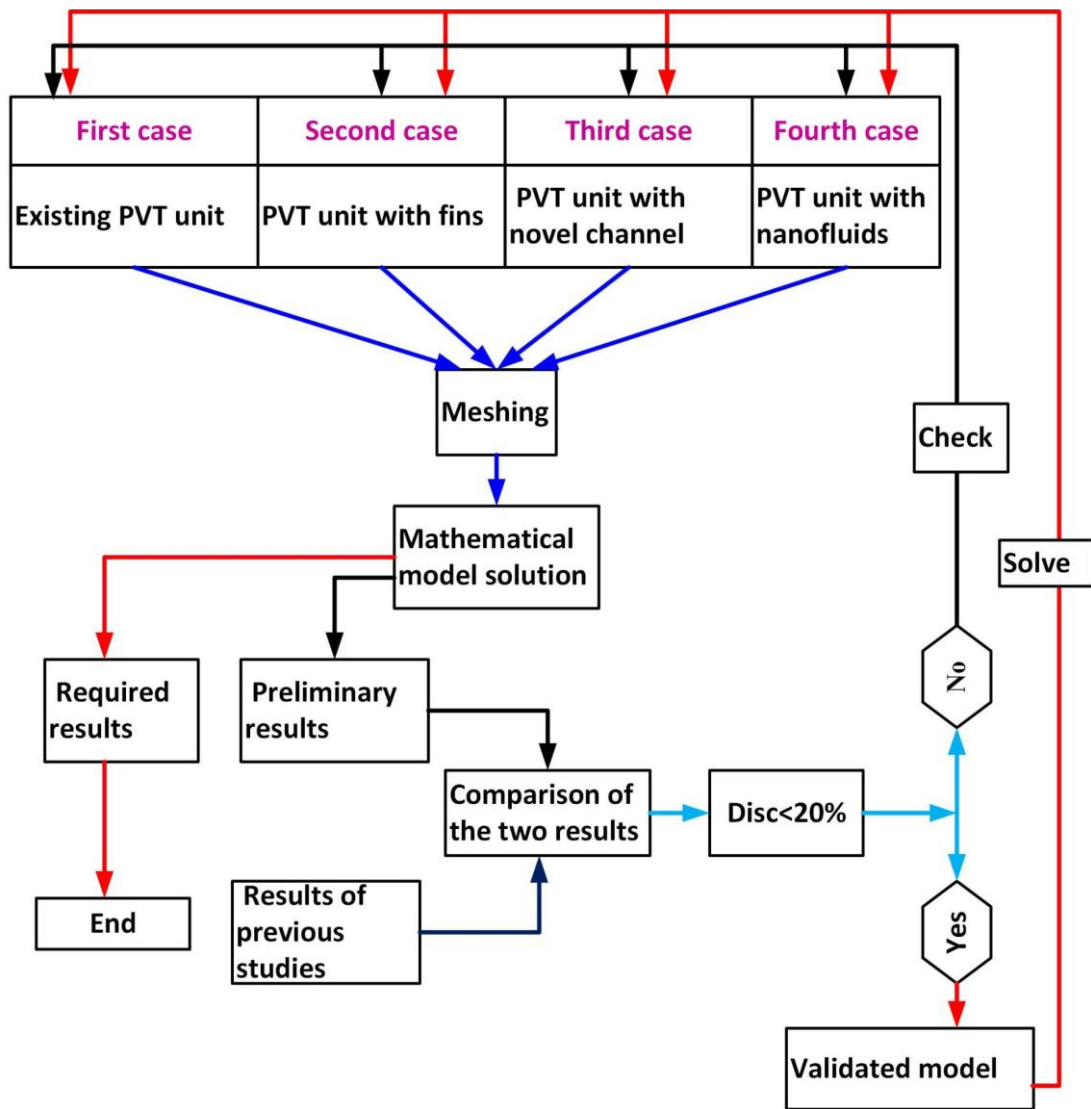


Fig.1.25 Strategy to solve the considered PVT unit models in CFD/ANSYS Fluent software

1.5.3 Research contents and route

(1) Research contents

Based on the above research ideas, objectives and methods, the work of the whole research is detailed in the following seven chapters.

In Chapter one, the existing methods as well as emerging technologies to improve the performance of PVT heat system are reviewed in more details in order to determine the problem to be solved, describe the significance of the current research, find out the knowledge gaps and also put forward the ways to overcome them. In addition, the objectives of the research and step by step procedures to achieve them, are given.

The used PVT unit models and their related mathematical equations are detailed in Chapter 2.

Creation of mesh, verification of simulation models, solution methods, operating conditions, assumptions and evaluation method of obtained results; are presented in Chapter three.

The determination of optimum dimensions of existing PVT unit condenser model as well as the impact of internal and external factors on the heat transfer characteristics of an optimized model, is carried out in Chapter four.

In Chapter five, the heat dissipation flux, pressure drop and refrigeration coefficient of performance (COP) of PVT unit model with fins of different shapes at the outer surface of channel are studied. Furthermore, the heat dissipation flux, vapor fraction and COP of PVT unit condenser incorporating a novel channel of hexagon-grid coupled with fluid channel of serpentine arrangement are investigated.

In Chapter six, the heat transfer characteristics and internal fluid phenomenon, which can influence the performance of PVT unit are investigated considering the model of nanofluid($\text{Al}_3\text{O}_2/\text{Ag}$) based PVT unit under cooling condition.

Finally, the conclusion, innovative points and future outlook are given in Chapter seven.

(2) Research route

The tasks of the whole PhD thesis are summarized in Fig.1.26.

At first, extensive literature study was carried out to determine the problem, knowledge gaps and set objectives of the current PhD research work.

These objectives were in turns achieved after performing a number of tasks. Those include the determination of suitable models and development of mathematical equations to be solved in ANSYS solution preprocessor.

After this step was realized, the considered models were prepared by both creating the mesh able to the solution of the mathematical equations and ensuring their accuracy. In addition, the methods to evaluate the obtained results were presented.

Having the models prepared, their corresponding results were obtained, presented and discussed in 3 different chapters (4,5 and 6).

Finally, on the basis of the discussions, conclusions, innovative points and future research were drawn.

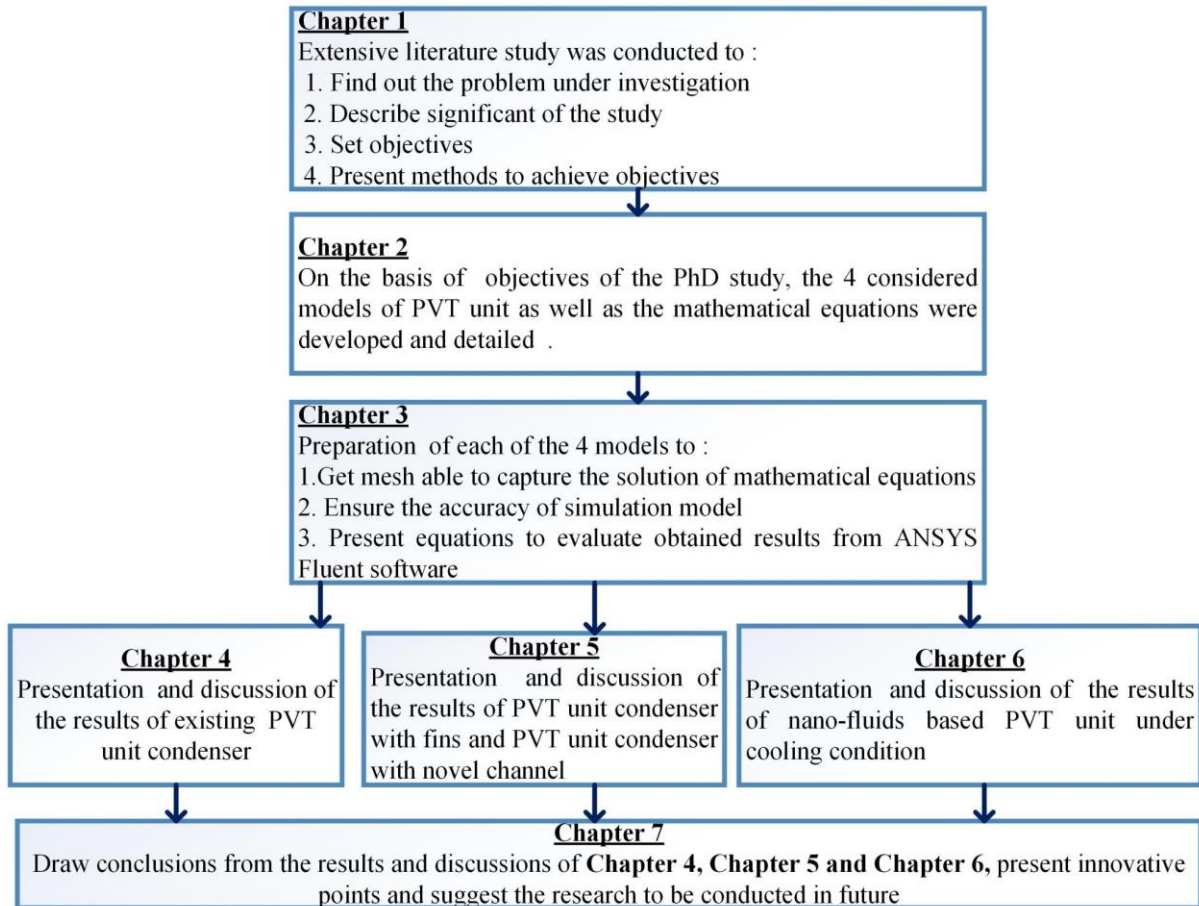


Fig.1.26 Research roadmap of the PhD thesis

2. Physical and mathematical models of the PVT unit under condensation and cooling conditions

In this chapter, the four mentioned model geometries of PVT unit (see section 1.5.2) as well as the corresponding mathematical equations for both fluids medium and thermal energy in PVT unit materials are described in more details. As the research seeks to develop and propose alternative methods to enhance the heat transfer characteristics of PVT unit under condensation and cooling conditions, the description for existing experimental set up of the experiment conducted about the PVT unit condenser is performed first and then followed by the details of other used models of PVT unit. For the sake of simplicity and less computational time, simulation models are reduced before they are solved in ANSYS Fluent software. The representative models considered are for existing PVT unit condenser (namely model 1), PVT unit condenser with fins (namely model 2), PVT unit condenser incorporating a novel channel (namely model 3) and PVT unit with nanofluids (water- $\text{Al}_3\text{O}_2/\text{Ag}$) as fluid medium through the channel (namely model 4). The four models operate during nighttime to exchange the heat of refrigerants condensation (R407C and R134a) and nanofluids inside channel with the natural cold of the sky (see section 1.3). The development of model geometries and the related mathematical equations is an initial and important step toward the solution of the particular case studies.

2.1 Physical models of PVT unit under condensation and cooling conditions

In this section, experimental set up of PVT heat pump system as well as the four considered models of PVT unit under condensation and cooling conditions are described.

2.1.1 Introduction of experimental set up of PVT heat pump system

The current PhD research study took reference to the experimental model of Fig.2.1. The experiment set up and components specifications are shown in Fig.2.1 and Table 2-1, respectively. The main aim of the experiment was to investigate the heat dissipation flux of the PVT heat pump system operating under various weather conditions of Dalian (China), during summer nighttime. For this system (Fig.2.1), the heat is exchanged in two main components (PVT modules or PVT unit and Cold storage tank) which are interconnected by pipes and devices (electronic expansion valve and compressor). In addition, the system is equipped with sensors to control the temperature (T), pressure (P) and mass flow rate (M) of the refrigerant. Moreover, PVT unit acts as a condenser to reject heat to the ambient and while cold storage tank acts as an evaporator. The PVT unit is composed by layer materials placed on top of special serpentine channels configuration, to allow an exchange of heat between fluid inside channels and top ambient environment. Top and bottom faces of the PVT unit release heat by both convection and radiation means, while the heat in layer materials is analyzed by conduction

mode. Thermo-physical properties and dimensions of layer materials are shown in Table 2-2. The heat of the storage tank is continuously absorbed by a phase change fluid of R407C and transferred to the PVT unit condenser for rejection to the ambient environment. Continuous heat removal of the storage tank results in ice formation (Fig.2.2), which serves as a cooling load during summer daytime. During simulation in ANSYS Fluent18, only PVT unit condenser/PVT modules as the most influential component is considered.

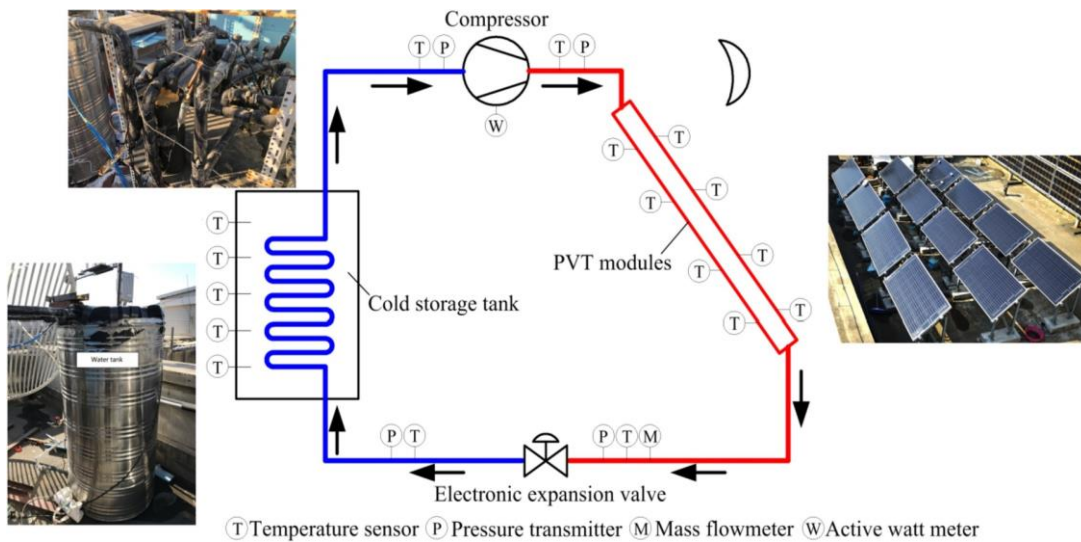


Fig.2.1 Schematic diagram of experimental set up of PVT heat pump system



a. During experiment **b.** After experiment

Fig.2.2 Process of ice formation inside ice storage tank ^[138]

Tab.2-1 Specifications of the main components of the experimental system ^[138]

Components	Specification	Value
Compressor	Displacement volume	41cc/rev
Cold storage water tank	Volume	600L
	Length	70m
Submerged coil	Outside diameter of pipe	12.7mm
	Inside diameter of pipe	11.1mm
PV modules	Length x Width	1560mm x 780mm
	Amount	12
	Total area	14.6m ²
Electronic expansion valve	Nozzle diameter	2.4mm

Tab.2-2 Thermo-physical properties of PVT unit layer materials and their dimensions

S/N	Layers materials	k (W/m.K)	C (J/kg.K)	ρ (kg/m)	Dimension (mm)
1	EVA ₁	0.23	2090	950	0.4
2	TPT	0.23	1250	1200	0.5
3	EVA ₂	0.23	2090	950	0.4
4	Cell	148	703	2300	0.2
5	EVA ₃	0.23	2090	950	0.4
6	Glass	0.98	750	2700	3.2

2.1.2 Four types of physical models of PVT unit under condensation and cooling conditions

(1) Existing PVT unit condenser model

The representative 3D model of existing PVT unit condenser (Fig.2.3) was used for validation with experimental model, acquisition of optimum dimensions and determination of heat transfer improvement. With this model (Fig.2.3), the heat of refrigerant (R407C) flow enters one inlet and leaves the two outlets, and therefore the properties of the fluid at the outlet were determined as the average value of the two outlets (outlet1 and outlet2). Top and bottom faces release heat by both convection and radiation modes, and while the heat in layer materials

is analyzed by conduction. During simulation, one-fourth of the existing PVT unit (195mm x 390mm) was considered for the sake of simplicity and less computational time, Fig.2.3.

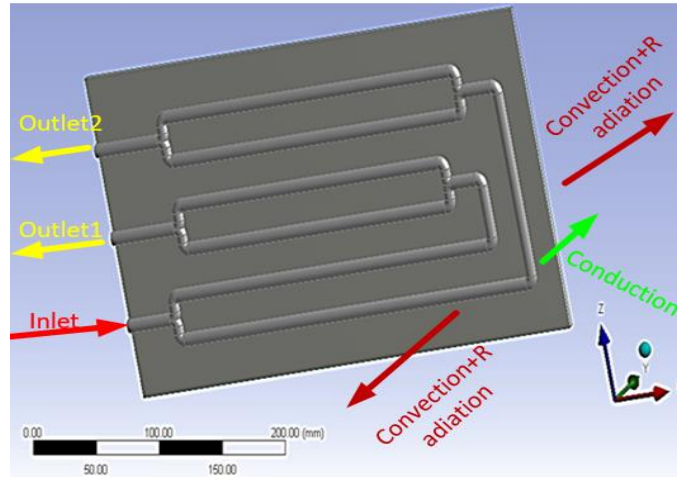


Fig.2.3 Representative 3D simulation model of existing PVT unit condenser

(2) PVT unit condenser model with fins

The model of PVT unit with fins is developed in order to proposed alternative method to further enhance the condensation heat transfer characteristics of existing PVT unit condenser. There are two basic approaches to enhance the efficiency of heat transfer. One is to select preferable materials or change the material properties such heat transfer coefficients, and the other is to optimize the structure's geometry shapes. As a convenient and economic mean, fins or extended surfaces are frequently used to design various shapes to enhance the requirements of high performance heat transfer equipment [148, 149]. With this approach, the heat transfer characteristics of the PVT unit can also be enhanced by adding fins. Therefore, as extra surfaces are added to the already existing model, further reduction is required to avoid both complexity and much time of computation. In this view, a model of 25mm x 150mm in size and with one micro-channel to circulate refrigerant, was taken into consideration. The fins are incorporated at the outer surface of the micro-channel with semi-circular shape (Fig.2.4). Furthermore, to determine fin which best suit for the study, fins of different shapes and various arrangements are incorporated. In fact, four different PVT unit condenser models with fins of straight rectangular fins (Fig.2.4, a), straight triangular fins (Fig.2.4, b), pin fins of rectangular profile (Fig.2.4, c), and pin fins of parabolic profile (Fig.2.4, d); were solved. The reference number, position and dimensions of fins for the simulation, are illustrated in Table 2-3. Fins were chosen due to a big role they play in enhancing the heat transfer characteristics. For instance, the best performance was obtained when incorporating two fins of different shapes (straight rectangular and pin of rectangular) at the heat sink [150]. Also by employing various pin-fin shapes (i.e.

rectangular, circular, square, rhombic, hexagon, trapezoidal and half circle), the efficiency of heat sink improves in the range from 5 to 15%^[151]. Effect of different fin angles on the performance of water/nanofluid based heat sink was experimentally investigated by ^[152] and the system was found to improve up to 84.3% at an angle 22.5°. Overall, in all these mentioned studies, dimension/position of fin parameters (width, height and angle) were selected depending on the both size and type of heat sink, and the amount of heat to be removed. This is to mean that for heat sink length of 50m, the length of straight rectangular/straight triangular fin will be given equals or less than the length of heat sink. Also many fins with both larger width and thickness will be required to fit on a big diameter pipe as compared to the one with small diameter.

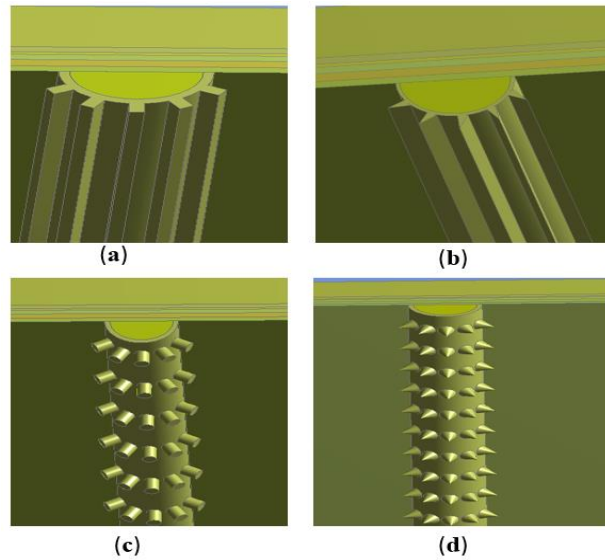


Fig.2.4 Simplified model geometry of PVT unit condenser with fins

Tab.2-3 Details for reference cases of fins

Type of fins	Number	Length (mm)	Width or diameter (mm)	Thickness (mm)	Fin position (°)
Straight rectangular	5	0.5	150	0.3	210,240,270,300,330
	3	0.5	150	0.3	210,270,330
Straight triangular	5	0.5	150	0.3	210,240,270,300,330
	3	0.5	150	0.3	210,270,330
Pin of rectangular profile	65	0.5	0.3	0.3	210,240,270,300,330
	39	0.5	0.3	0.3	210,270,330
Pin of parabolic profile	65	0.5	0.3	0.3	210,240,270,300,330
	39	0.5	0.3	0.3	210,270,330

(3) PVT unit condenser incorporating a novel channel

A model of PVT unit with Hexagon-grid coupled with a serpentine-shape arrangement of fluid channel pattern was considered (Fig.2.5c) to evaluate the effect of channel structure on the condensation heat transfer characteristics and overall performance. The model was drawn and solved based on the already existing one ^[144, 153] Fig.2.5a. The PVT unit incorporates hexagon-grid coupled with a U-shape arrangement of fluid channel pattern and R134a refrigerant is the fluid inside channel, to exchange heat with the environment. The R134a refrigerant is supplied and discharged via two inlets (1) and two outlets (2), respectively. For the sake of simplicity and less computation time, one inlet, one outlet, two rows ((3) and (4)) with 5 hexagon-grids each and 1 hexagon-grid (5) to represent a number of rectangular grids in corner (Fig.2.5b) were considered during model validation. After ensuring validity, the model of Fig.2.5b was further extended to the newly one of our research group, by adding a second U-shape arrangement of fluid channel pattern in order to form a serpentine-shape arrangement of fluid channel pattern (Fig.2.5c). The simplified model of 370mm x 425mm in size is composed by six layers of different materials on top of micro-channels configuration.

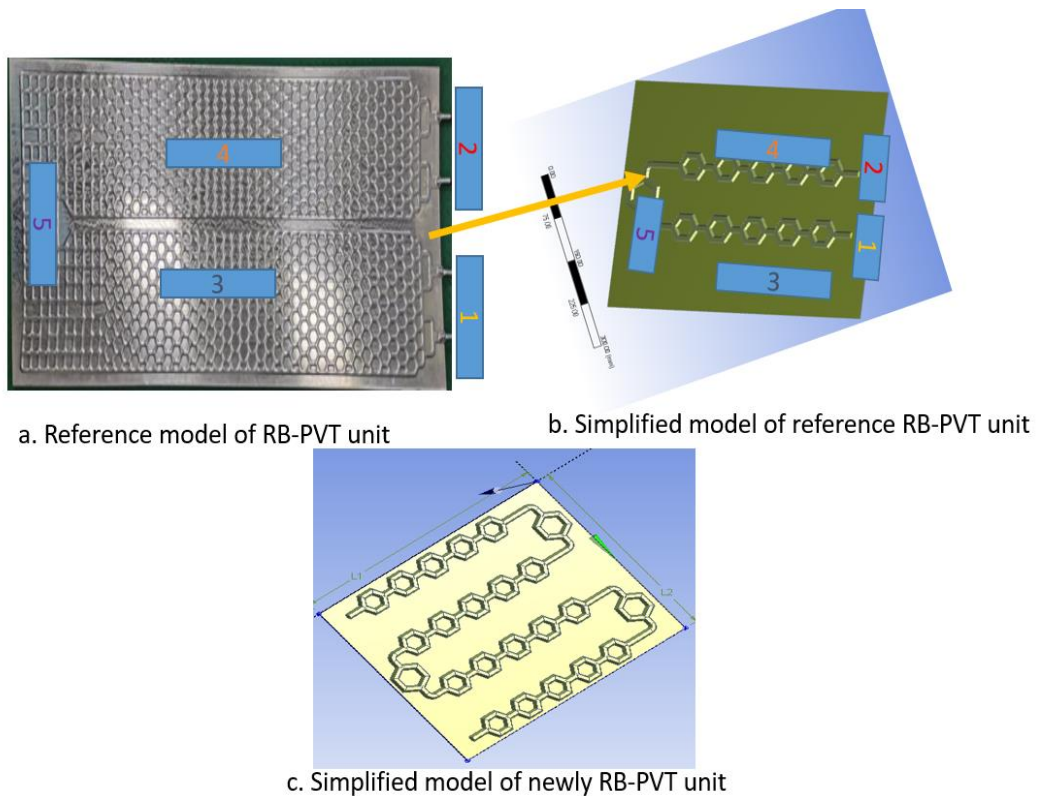


Fig.2.5 Schematic diagram of the existing PVT unit (a), simplified model of existing PVT unit (b) and simplified of newly PVT unit (c)

(4) PVT unit with water- $\text{Al}_3\text{O}_2/\text{Ag}$

In the indirect expansion PVT heat pump system, water and antifreeze are often used as working fluids. Nanofluids can effectively improve the heat transfer performance of water or antifreeze. Therefore, in this section, a 3D model geometry is developed to study the effect of nanofluids on the heat transfer characteristics and performance of PVT unit working under cooling condition, during nighttime. The considered model of PVT unit with 115mm x 230mm in size, is presented in Fig.2.6. The unit is composed by pipe, absorber and 6 layers of different materials. The size of each layer and the related thermo-physical properties are shown in Table.2-2 above. In contrary to the commonly used PVT unit evaporator where the heat input is from solar, the heat of the newly developed unit is released to the ambient environment from fluid inside pipe during summer night. Two nanofluids of Al_3O_2 -water and Ag-water were considered. Upon entering the pipe, a high fluid temperature ($\geq 320\text{K}$) loses heat along the way, by both conduction and convection and reaches the outlet when its temperature is relatively low ($\ll 320\text{K}$).

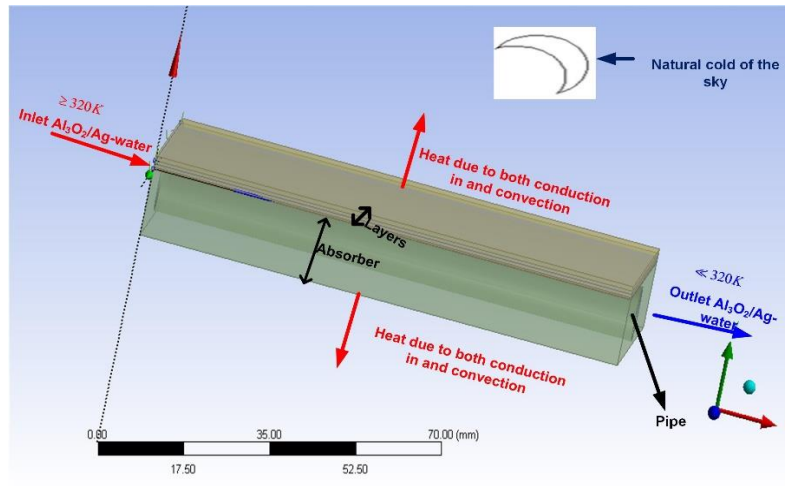


Fig.2.6 Model geometry of the PVT unit with nanofluids

2.2 Analysis of working fluid characteristics in PVT unit under condensation and cooling conditions

In order to establish the numerical models of PVT unit under condensation and cooling conditions, the flow characteristics of refrigerant and nanofluid in PVT unit will be analyzed firstly. With research development of fluid, the properties of liquids can be enhanced and used as fluids medium to improve the heat transfer characteristics and the overall performance of the PVT unit under cooling condition. In contrary to the refrigerants where the flow is always modelled with two phase change, the modelling of nanofluids is done as a single phase. Therefore, the efficiency improvement of the two fluids (refrigerants and nanofluids) will have

different effects on the heat transfer characteristics and performance of the PVT unit under condensation and cooling conditions at night.

2.2.1 Analysis of refrigerant flow characteristics

The refrigerant are fluids with special property to absorb and release heat whenever it is needed and therefore, their incorporation in the channels of PVT unit condenser is of paramount importance in enhancing heat transfer characteristics of this particular unit. In light with this importance, two types of refrigerants R407C and R134a were used in the channels of numerical models of PVT unit condenser. The corresponding thermo-physical properties in both liquid and vapor phase are presented in Table.2-4. R07C was employed in the models of existing PVT unit condenser, PVT unit condenser with fins and while R134a was utilized in the PVT unit condenser incorporating a novel channel. The heat of thermal storage tank is extracted and transported to the PVT unit condenser by the refrigerant (R407C and R134a) inside channels. At the inlet of the channel, the fluid is in vapor phase and undergoes phase change as it exchanges heat with the natural cold of the sky. In addition, due to both the nature of channel and change of phases, the flow experiences some turbulences which would affect the results. In addition, due to both the nature of channel and change of phases, the flow experiences some turbulences which would affect the results.

Tab.2-4 Thermo-physical properties of refrigerants^[154]

Refrigerant	ρ (kg/m ³)	Cp (W/m.K)	μ (kg/m-s)	k (W/m. K)
R407C, liquid	1010.05	1796.5	0.0001076	0.07624
R407C, vapor	93.835	1603	0.00001453	0.019715
R134a, liquid	1002.3	1556	0.0001431	0.0704
R134a, vapor	66.234	1246	0.00001312	0.01672

2.2.2 Analysis of nanofluids characteristics

On the basis of importance of nanofluids (section 1.2.4), two types of nanoparticles (Al₃O₂ and Ag) were dissolved in a base fluid of water to form Al₃O₂/Ag-water nanofluid(s) and used through the channel of the current PVT unit model, under cooling condition. The nanofluids properties were calculated from Equ.(2.5)-Equ. (2.8) based on the properties of nanoparticles (see Table.2-5) and those of water obtained from Equ. (2.1)-Equ. (2.4). Here it should be informed that due to the problem water can cause during winter, it was not used in the results of this thesis instead it was only employed for preparation of nanofluids and validation of a model which can be utilized to model any other kind of fluid. The thermo-physical properties

of water depend on temperature ^[155, 156]. The temperature T from Equ.(2.1)-Equ.(2.4) is obtained by approximation average of inlet and outlet temperature of the fluid ^[157].

Tab.2-5 Thermo-physical properties of nanoparticles

Nanoparticles	ρ (kg/m ³)	Cp (J/kg.K)	k (W/m.K)	μ (kg/m.s)
Al ₃ O ₂ ^[158]	3970	765	40	-
Ag ^[158]	10500	239	429	-

$$\rho_{water} = -4.48 \times 10^{-3} T^3 + 999.9 \quad (2.1)$$

$$C_{pw} = 4.1855 \times 10^3 \left(0.966185 + 0.0002874 + \left(\left(\frac{T+100}{100} \right)^{5.26} \right) \right) + (0.011160 \times 10^{-0.0367T}) \quad (2.2)$$

$$k = -8.01 \times 10^{-6} T^2 + 1.94 \times 10^{-3} T + 0.563 \quad (2.3)$$

$$\mu = \exp \left(-1.6 - \frac{1150}{T} + \left(\frac{690}{T} \right)^2 \right) \quad (2.4)$$

On the other hand, the thermo-physical properties of nanofluid are mathematically illustrated in Equ. (2.5)-Equ. (2.8). The Eqs. for density, viscosity and specific heat capacity are developed following the physical principle of two- phase mixture ^[159, 160] and while Equ.(2.8) of thermal conductivity is written in accordance with theoretical model of ^[161] and considering the temperature coefficient (λ) equals 0.1. At constant density of nanoparticle, the density of the mixture (water and Al₃O₂/Ag) varies depends on both nanoparticle fraction and fluid base density. The specific heat capacity changes proportionally to the sum product of density and specific heat capacity of both water and Al₃O₂/Ag, and inversely proportional to the nanofluid density.

$$\rho_{nf} = (1 - \psi)\rho_f + \psi\rho_s \quad (2.5)$$

$$\psi < 0.05; \mu_{nf} = (1 + 2.5\psi)\mu_f \quad (2.6)$$

$$C_{pnf} = \frac{(1-\psi)\rho_f C_{pf} + \psi\rho_s C_{ps}}{\rho_{nf}} \quad (2.7)$$

$$k_{nf} = k_f - \frac{k_s + 2k_f - 2(1+\lambda)^3(k_s - k_f)\psi}{k_s + 2k_f + (1+\lambda)^3(k_s - k_f)\psi} \quad (2.8)$$

2.3 Mathematical models for PVT unit under condensation and cooling conditions

The characteristics of fluid flow through the channel as well as the mathematical equations for PVT unit materials are developed in this section.

2.3.1 Numerical model of flow and energy of working fluid in PVT unit

The characteristics equations of continuity, momentum, energy and turbulent model are developed in this subsection. In exception to the refrigerants (R407C and R134a) which require volume of fraction (VOF) and turbulent (Equ.2.21 and Equ.2.22) models to respectively handle phase change at different temperatures and flow fluctuations, the rest of characteristic equations (Eqs. (2.9), (2.14) and (2.17)) are applied similar in case when single phase and laminar flow of nanofluids (water-Al₃O₂ and water-Ag) is used as fluid medium in the channel.

(1) Continuity equation

The continuity equation is written as in Equ. (2.9).

$$\nabla \cdot (\rho \vec{u}) = 0 \quad (2.9)$$

In normal case of PVT unit evaporator, the equations for refrigerant flow inside channel are developed based on three principles; $\alpha_v=0$ when the cell is fully occupied by the liquid, $\alpha_l=0$ the cell is fully occupied by vapor and $0 < \alpha_l < 1$ when the cell is at the interface between the liquid and vapor phases^[162]. However, since the PVT unit acts as a condenser in the current research, the equations were developed based on two principles; $\alpha_v=1$ when the cell is fully occupied by the vapor and $0 < \alpha_v < 1$ when the cell is at the interface between the liquid and vapor phase. At the inlet of the channel when one state of fluid is available, continuity equation of vapor can be deduced as shown in (2.10).

$$\nabla \cdot \alpha_v \rho_v \vec{u} = S_m \quad (2.10)$$

At this stage, the cell is fully occupied by the vapor and its representative fraction equation is as shown in Equ. (2.11).

$$\sum_{v=1}^n \alpha_v = 1 \quad (2.11)$$

S_m represents the source term (kJ/s.m³), which is obtained from Equ. 2.12. The terms \dot{m}_{vl} and h_{vl} represent the rate of mass transfer from vapor to liquid (kg/s/m³) and the latent heat (kJ/kg), respectively.

$$S_m = \dot{m}_{vl} h_{vl} \quad (2.12)$$

In the process when the refrigerant exchanging heat with the natural cold of the sky, density and vapor fraction change. As a result, the density of the mixture is obtained by the sum product of pure vapor density and that of fraction of liquid as shown in (2.13).

$$\rho = \alpha_v \rho_v + (1 - \alpha_v) \rho_l \quad (2.13)$$

(2) Momentum equations

In the channel, a number of forces such as gravitational force, pressure force, friction force and surface tension act on the fluid flow. Therefore, their net effect is accounted for in the momentum equation of (2.14).

$$\nabla \cdot (\rho \bar{u}\bar{u}) = \rho \vec{g} - \nabla \cdot p + \nabla \cdot \left[\mu (\nabla u + \nabla \bar{u}^T) - \frac{2}{3} \mu \nabla \cdot u \mathbf{I} \right] + F_{CSF} \quad (2.14)$$

Where u is the flow velocity (m/s); and μ , μ_l and μ_v are average dynamic viscosity, liquid dynamic viscosity and vapor dynamic viscosity (kg/m.s), respectively. The terms ρ , p and g are density (kg/m³), pressure (N/m²) and gravity (m/s²), respectively.

$$\mu = \alpha_v \mu_v + (1 - \alpha_v) \mu_l \quad (2.15)$$

And F_{CSF} which is a force at control surface of liquid (N) is obtained based on the model of [163] as in Equ.(2.16).

$$F_{CSF} = 2\tau_{lv} \frac{\alpha_l \rho_l c_v \nabla \alpha_v + \alpha_v \rho_v c_l \nabla \alpha_l}{\rho_l + \rho_v} \quad (2.16)$$

With τ_{lv} , C_l and C_v the surface tension liquid-vapor (N/m), control surface (m²) for both liquid and vapor, respectively.

The energy equation is written as in Equ. (2.17)

$$\nabla \cdot (\rho e \vec{u}) = \nabla \cdot (k \cdot \nabla T) + \nabla \cdot (p \vec{u}) + S_E \quad (2.17)$$

Where k is the thermal conductivity (W/m.K) and e the average internal energy (J) are determined in Equ. (2.18) and Equ. (2.19).

$$k = \alpha_v k_v (1 - \alpha_v) k_l \quad (2.18)$$

$$e = \frac{\alpha_l \rho_l e_l + \alpha_v \rho_v e_v}{\alpha_l \rho_l + \alpha_v \rho_v} \quad (2.19)$$

The e_l and e_v are internal energies for liquid and vapor (J/kg) and are in turns calculated as in Equ. (2.20) and Equ. (2.21), respectively.

$$e_l = C_{p,l} (T - T_{sat}) \quad (2.20)$$

$$e_v = C_{p,v} (T - T_{sat}) \quad (2.21)$$

Where $C_{p,l}$ and $C_{p,v}$ are specific heat capacities (kJ/kg. K) for liquid and vapor, respectively and T_{sat} represents the saturation temperature(K).

(3) Turbulent models

To account for the effect caused by the mixing of transport quantities, RNG K-Epsilon model is more preferred due to its accuracy, reliability and applicability to a wide range of flows^[164]. Transport models for turbulent kinetic energy and dissipation are respectively shown in Equ.(2.22) and Equ.(2.23) below^[165]:

$$\frac{\partial}{\partial x_i} (\rho k e u_i) = \frac{\partial}{\partial x_j} \left[\frac{u_t}{\sigma_k} + \frac{\partial k}{\partial x_j} \right] + 2u_t E_{ij} E_{ij} - \rho \epsilon \quad (2.22)$$

$$\frac{\partial (\rho k u_i)}{\partial x_i} = \frac{\partial}{\partial x_i} \left[\frac{u_t}{\sigma_\epsilon} + \frac{\partial \epsilon}{\partial x_j} \right] + C_{1\epsilon} \frac{\epsilon}{k} 2u_t E_{ij} E_{ij} - C_{2\epsilon} \rho \frac{\epsilon^2}{k} \quad (2.23)$$

The terms u_i, E_{ij} and u_t represent velocity component in corresponding condition, component of deformation rate and eddy viscosity, respectively. The constants $\sigma_k, \sigma_\epsilon, C_{1\epsilon}$ and $C_{2\epsilon}$ were analytically determined to be 1.00, 1.30, 1.44 and 1.92, respectively^[165].

2.3.2 Thermal modelling of PVT unit under condensation and cooling conditions

The heat of the above described fluids flow (section 2.3.1) inside channel is released to the ambient environment by different means such as; convection and radiation at both top and bottom faces and conduction through layers on top of channel. In addition, convection and conduction at the channel is considered. The effect of different heat transfer modes is accounted for by the overall heat transfer coefficient (U). The mathematical equations of thermal energy for the PVT unit condenser are developed based on the model of ^[166]. The model works on the principle that the overall heat transfer coefficient U(W/m².K) of the entire system is determined by the equivalent heat resistances of the front and back sides of the PVT unit, as shown in Equ. (2.24).

$$U = \frac{1}{R_{front}} + \frac{1}{R_{back}} \quad (2.24)$$

The front and back sides are directly exposed to the ambient where they are experiencing some resistances. The heat resistances are calculated from bottom to top face of the PVT unit condenser (Fig.2.7) and by following the thermal circuit of Fig.2.8. The resistances R_{front} and R_{back} (m².K/W) are calculated from Equ. (2.25)-Equ. (2.35).

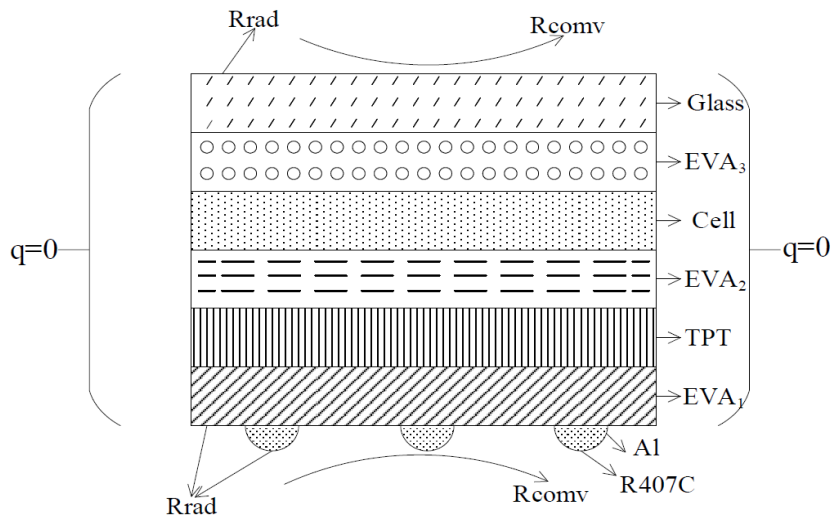


Fig.2.7 Schematic diagram of PVT unit condenser

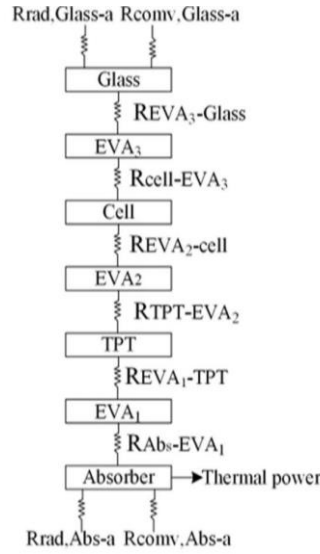


Fig.2.8 Thermal resistance circuit of PVT unit under condensation and cooling conditions

$$R_{front} = \frac{R_{conv,Glass-a}R_{rad,Glass-a}}{R_{conv,Glass-a}+R_{rad,Glass-a}} + R_{cond} + R_{Abs-fluid} \quad (2.25)$$

The convective and radiative resistances between the glass and the ambient are given in Equ. (2.26) and Equ. (2.27).

$$R_{conv,Glass-a} = \frac{1}{2.8+3V} \quad (2.26)$$

$$R_{rad,Glass-a} = \frac{1}{\varepsilon_G \sigma (T_{sky}^2 + T_{mGlass}^2)(T_{sky} + T_{mGlass})} \quad (2.27)$$

The equivalent conduction heat resistance of layer materials (R_{cond}) is given by the Equ. (2.28) and Equ. (2.29).

$$R_{cond} = R_{EVA3-Glass} + R_{cell-EVA3} + R_{EVA2-cell} + R_{TPT-EVA2} + R_{EVA1-TPT} + R_{Abs-EVA1} \quad (2.28)$$

$$R_{cond} = \frac{d_{Glass}}{k_{Glass}} + \frac{d_{EVA3}}{k_{EVA3}} + \frac{d_{cell}}{k_{cell}} + \frac{d_{EVA2}}{k_{EVA2}} + \frac{d_{TPT}}{k_{TPT}} + \frac{d_{EVA1}}{k_{EVA1}} \quad (2.29)$$

The equivalent heat resistance of the back side is given by Equ. (2.30)

$$R_{back} = \frac{R_{conv,Abs-a}R_{rad,Abs-a}}{R_{conv,Abs-a}+R_{rad,Abs-a}} \quad (2.30)$$

The heat resistance due to both radiation and convection at the back side of the PVT unit, are respectively established in Equ.(2.31) and Equ.(2.32) [167].

$$R_{rad,Abs-a} = \frac{T_{mback}-T_a}{\varepsilon_{Abs}\sigma(T_{mback}^4-T_a^4)} \quad (2.31)$$

$$R_{comv,Abs-a} = \frac{1}{1.247[(T_{mback}-T_a)\cos\beta]^{\frac{1}{3}}+2.658V} \quad (2.32)$$

Where β and V are angle of inclination ($^\circ$) of the PVT unit and wind velocity(m/s), respectively. The thermal resistance between fluid and channel wall ($R_{Abs-fluid}$) is determined in Equ. (2.33).

$$R_{Abs-fluid} = \frac{1}{\frac{1}{h_{Abs-fluid}} + \frac{\delta_{micr}}{k_{micr}}} \quad (2.33)$$

The $h_{Abs-fluid}$ in Equ.(2.33) is the convection heat transfer coefficient between channel wall and fluid ($W/m^2.K$), which is calculated by Equ.(2.34) considering the flow in channel as turbulent for; $Re \geq 104$, $0.6 \leq Pr \leq 160$ and $L/d \geq 60$ [167-169].

$$h_{Abs-fluid} = \frac{Nu k_{fluid}}{D_h} \quad (2.34)$$

From Equ.(2.34), Nu is the Nusselt Number (-) which is determined from Equ.235 as a function of Reynold number ($Re(-)$) and Prandtl number ($Pr(-)$) [167-169].

$$Nu = 0.023 Re^{0.8} Pr^t \quad (2.35)$$

Where the exponent $t=0.4$ for heating of fluid and $t=0.3$ if the fluid is being cooled.

2.4 Summary

In this chapter, the physical models of PVT unit under condensation and cooling conditions and the related mathematical equations were established.

First, the experiment set up of existing PVT heat pump system was described in order to lay foundation for the other derived models. On the basis of existing PVT unit condenser, a simplified model was developed to further analyze the heat transfer characteristics.

Second, in order to propose new strategies to enhance the heat transfer characteristics of the PVT unit condenser, three more models were developed based on authors' previous studies. Those include, PVT unit condenser with fin of different shapes at the outer surface of channel, PVT unit condenser incorporating a novel channel of hexagon-grid coupled with a serpentine-shape arrangement of fluid channel pattern and PVT unit with nanofluids (water- Al_3O_2/Ag) as fluid medium through channel.

Third, the mathematical equations related to fluids (R407C, R134a and nanofluids) and thermal energy in PVT unit condenser materials were written down following different approaches.

Last, the establishment of models and the related mathematical equations is an initial and important step towards the solution of a particular problem. Depending on the nature of the problem to be solved, the above four models can be further processed differently. For instance, modelling PVT unit model with refrigerant is more challenging as compared to the one with nanofluid due to the fact that a proper model to handle turbulences needs to be carefully selected. Moreover, the adopted techniques of mesh creation have effect on the mesh quality which in turns impacts the simulation convergence and the quality of the results. Some other selection criteria of a particular model such as solution methods, operating conditions, assumptions and method of evaluating obtained results also affect the research results.

3. Solution strategy for the numerical models of PVT unit and proposal of evaluation indexes

In this chapter, the procedures to solve the four developed physical models of PVT unit condenser (see section 2.1.2) and their related mathematical equations (see section 2.3) are discussed in more details. In addition, the methods to evaluate the solution results as well the models validation are provided. The main procedures and the order in which simulation is performed, are summarized in Fig.3.1. In ANSYS Fluent, a representative model is divided into mesh able to capture the solution of mathematical equations. Moreover, the equations are arranged in a computational domain, discretized into differential equations and solved by iterative methods, under different operating conditions and assumptions. And after, the obtained results are compared with those of previous similar studies in order to validate simulation model. In case of small difference between the results of the two models, validation is realized and otherwise have to revise the whole simulation. The procedures described in this chapter help to build a basic model which can be utilized to further analyze the particular problem under investigation.

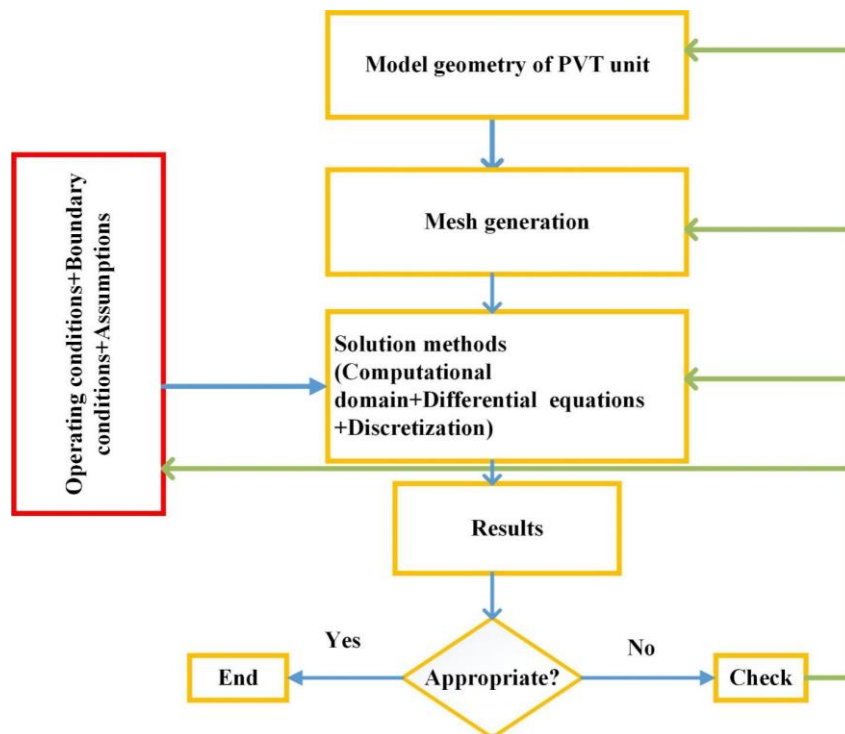


Fig.3.1 Step by step procedure to get solution results from ANSYS Fluent

3.1 The inputs, methods and assumptions to the simulation

This section encompasses the methods, assumptions and operating conditions used to solve the considered models. Depending on the nature of the problem to be solved, different methods as well as operating conditions can be applied to different models. On the other hand, assumptions are set to simply the problem and also reduce calculations.

3.1.1 Operating conditions of weather and flow

Setting up operating boundary conditions is of paramount importance when running simulation. In this section, the basic operating conditions of the PhD study are given. In ANSYS Fluent preprocessor, the first sets of simulation were performed considering the average values of weather conditions (i.e. ambient temperature, sky temperature and wind speed), heat dissipation flux and coefficient of performance (COP) obtained from experimental study conducted for 8 days, from 2018/08/01 to 2018/08/10 during nighttime (0:00 a.m to 5:00 a.m) [138], Fig.3.2. Furthermore, a sensitivity analysis of an optimized model of PVT unit condenser was conducted considering the surface emissivity, weather and flow conditions of Table.3-1. Other operating conditions were decided based on the ranges of values for different measuring devices (Table.3-2) and are described in more details in the next chapters (4,5 and 6).

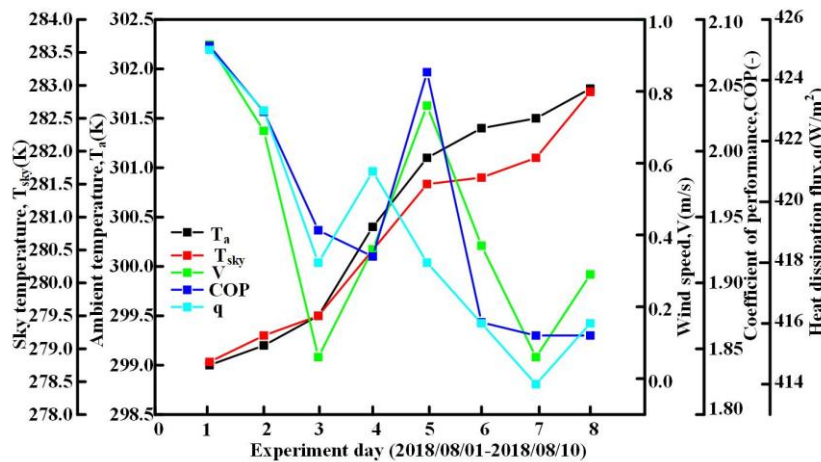


Fig.3.2 Base case of weather conditions, COP and heat dissipation flux

Tab.3-1 Parameter variables for weather, refrigerant flow and surface emissivity

S/N	T_a (K)	T_{sky} (K)	V (m/s)	u (m/s)	T_{flow} (K)	ϵ (-)
1	300	280	0.5	0.09	342.5	0.4
2	302	282	1	0.11	344	0.5
3	304	284	1.5	0.13	345.5	0.6
4	306	286	2	0.15	347	0.7
5	308	288	2.5	0.17	348.5	0.8
6	310	290	3	0.19	350	0.9

Tab.3-2 Testing devices and their corresponding specifications^[138]

Device	Specification	Measuring range	Unit
Mass flow meter	TCD200	0-300	Kg/h
		0-11.322	m/s
Active wattmeter	HDB-P1	0-3.5	kW
		0-2876.4	W/m ²
Temperature sensor	PT100 RTD probes	-40-120	°C
		233-393	K
Pressure transmitter	PCM300	0-4	MPa

3.1.2 Numerical methods and solution assumptions

In ANSYS Fluent 18, except PVT unit condenser models with refrigerant (R407C and R134a) as a fluid medium inside channel which were modeled using Volume of Fluid (VOF) and turbulent models, the rest of models with nanofluids were treated in almost similar manner assuming the fluid is laminar, incompressible and single phase. As the purpose of PVT unit condenser is to release the heat to the ambient environment, a higher fluid temperature was set to enter and leave the channel when its temperature was relatively low. All models related equations were solved at steady state due to the fact that it has less computational cost as compared to transient and also difference between the results of the two methods is small (0.2%)^[170]. In order to get more accurate solution as well as to lower diffusions which may arise, a second order discretization scheme was utilized for continuity and energy. Meanwhile the SIMPLE algorithm was used to enforce a relationship between velocity and pressure corrections and to obtain the pressure field, and while least square was chosen to handle different gradients.

In fact, the models were solved on the basis of 12 assumptions. The first four assumptions were for solving fins^[171, 172]. The assumptions are as follow:

- 1) There are no heat sources in the fin itself;
- 2) The temperature of the surrounding fluid is spatially uniform;
- 3) The heat transfer coefficient is the same over all fin surfaces;
- 4) The temperature of the fin base surface is uniform and equal to the temperature of the tube base surface;
- 5) Thermo-physical properties of all PVT unit materials do not change with temperature;
- 6) Sky temperature is assumed as black body^[173];
- 7) Long wave intensity is assumed to be uniform and absorbed in the first layer of PVT unit condenser (EVA1)^[173, 174];

- 8) The faces (right, left, front and back) of the PVT unit are adiabatic;
- 9) Both top and bottom of the PVT unit are not adiabatic;
- 10) A turbulent model was assumed for refrigerant flow (R407C and R134a);
- 11) To avoid overheating, no heat stored or generated in the PVT unit condenser materials;
- 12) Nanofluid is considered incompressible and single phase materials ^[175, 176]. In all simulation sets, the convergence attained whenever the residuals of velocity, continuity, and energy reached below 10e-4, 10e-3 and 10e-6, respectively.

3.2 Proposal of evaluation indexes of PVT unit

A part from Nusselt number described in Equ. (2.34) above and some other indexes which are directly obtained from ANSYS Fluent, three other evaluation indexes of overall fin efficiency, heat dissipation flux and coefficient of performance have been used in this thesis and their corresponding mathematical equations are derived in this section.

3.2.1 Overall fin efficiency of the PVT unit

The problems on heat transfer particularly in fins continue to be of scientific interest. These problems are modeled by highly nonlinear differential equations which are difficult to solve exactly. A number of authors did their best to get the solution of heat transfer in fins, using different methods ^[177-180]. The mathematical model equations to analyze the performance of fins when incorporated at the channel surface of the PVT unit system, are presented in this section. In fact, the impact of fin on the heat transfer improvement of PVT unit condenser is evaluated in terms of overall array fin efficiency $\eta_{over}(\%)$ ^[181], as shown in Equ.(3.1).

$$\eta_{over} = 1 - \frac{NA_{fin}}{A_{tot}}(1 - \eta_{fin}) \quad (3.1)$$

The terms A_{fin} , A_{tot} and η_{fin} respectively represent the fin area (m²), total pipe-fin area (m²) and efficiency of one fin(%) and are determined according to the profile of fin.

In this study, four different fin profiles of straight rectangular, straight triangular, pin of rectangular, and pin of parabolic, shown in Fig.3.3(a-d) were taken into account and their corresponding fin efficiency formulas are presented in Eqs.(3.1) -(3.5). In all cases, the required parameters to evaluate fin efficiency are; overall heat transfer coefficient (U (W/m².K)), fin length (L(mm)), fin width (w(mm)), fin thickness (δ (mm)), thermal conductivity (k(W/m.K)) and fin diameter (d(mm)).

Fin efficiency for (Fig.3.3, a)

$$\eta_{fin} = \frac{\tanh mL_c}{mL_c} \text{ with; } L_c = L + \delta/2, m = \sqrt{2U/k\delta} \text{ and } A_{fin} = 2wL_c \quad (3.2)$$

Fin efficiency for (Fig.3.3, b)

$$\eta_{fin} = \frac{1I_1(2mL)}{mL_0(2mL)} \text{ with; } m = \sqrt{2U/k\delta} \text{ and } A_{fin} = 2w\sqrt{L^2 + (\delta/2)^2} \quad (3.3)$$

Fin efficiency for (Fig.3.3, c)

$$\eta_{fin} = \frac{\tanh mL_c}{mL_c} \text{ with; } m = \sqrt{2U/kD}, L_c = L + D/4 \text{ and } A_{fin} = \pi DL_c \quad (3.4)$$

Fin efficiency for (Fig.3.3, d)

$$\eta_{fin} = \frac{3I_1(4mL/3)}{2mL I_0(4mL/3)} \text{ with ; } m = \sqrt{4U/kD} \text{ and } A_{fin} = \frac{\pi D^4}{96L^2} \{ [16(L/D)^2 + 1]^{3/2} - 1 \} \quad (3.5)$$

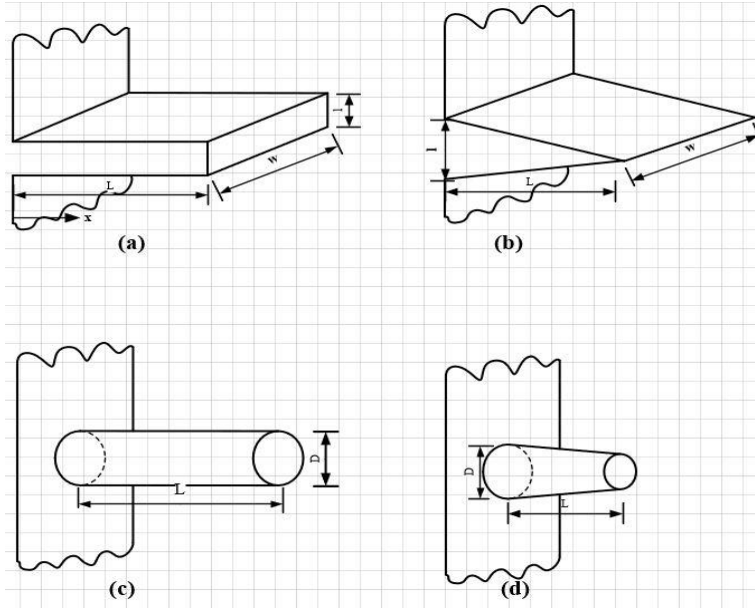


Fig.3.3 Four different types of fins used at the outer surface of PVT unit channel

3.2.2 Heat dissipation flux and percentage discrepancy

In order to determine the validity of simulation models, the heat dissipation flux of experiment was compared with that of simulation using two mathematical correlations. For the first simulation sets, the heat dissipation flux of existing PVT unit was calculated according to Stefan-Boltzmann law ^[168]. On the other hand, an approximation model was created in excel based on the experimental data (see Fig.3.2) and used for the determination of heat dissipation flux of PVT unit with fins. It is to note that, the two models are quite similar as the maximum percentage difference between them is only about 2.6%. In all cases, the comparison was made by use of the average percentage error (MAPE) method ^[182].

$$MAPE\% = \frac{100}{nbr} \sum_n \left| \frac{E_{sim,i} - E_{prev,i}}{E_{prev,i}} \right| \quad (3.6)$$

Where $E_{sim,i}$ and $E_{prev,i}$ are the heat dissipation flux for simulation and previous studies, respectively.

According to Stefan-Boltzmann law, the correlation of heat dissipation flux for the PVT unit is developed as in Equ. (3.7).

$$q = 4\varepsilon\sigma T_a^3 [(T_{mback} - T_{sky}) + (T_{mGlass} - T_{sky})] \quad (3.7)$$

Where the emissivity ε , is taken as 0.9 at both bottom and top surfaces. T_{mback} and T_{mGlass} are the mean temperatures (K) at both bottom and glass, respectively. σ represents Boltzmann constant ($5.67e-8 \text{ W/m}^2\text{K}^4$).

In order to relate the simulation model of PVT unit condenser with fins (see section 2.1.2) with the existing PVT unit condenser without fins, an approximation model to evaluate the heat dissipation flux of PVT unit condenser with fins was developed in excel tool. The model was created based on experimental data of Fig.3.2. The experimental data considered are; ambient temperature (T_a), sky temperature T_{sky} , wind speed (V) and heat dissipation flux (q_{exp}). The model equation (Equ. 3.8) for the total heat dissipation flux(q) was obtained as a function of; wind speed (V), difference between the temperature of PVT surface and ambient ($T_{PVT}-T_a$) and the temperature difference between PVT surface and sky ($T_{PVT}-T_{sky}$).After each simulation set, the T_{PVT} can be replaced in a model of Equ. (3.8) to get the heat dissipation flux (q).

$$q = -3.3(T_{PVT} - T_a)^{-112.3}V^{69.7} + 544.05(T_{PVT} - T_{sky})^{-0.082} \quad (3.8)$$

3.2.3 Ratio of heat dissipation flux to flow resistance of PVT unit

The ratio of heat dissipation flux to flow resistance refers to the ratio of heat dissipation flux per unit area of PVT module to the flow resistance when the fluid flows through the channel of that area.

$$H = \frac{q}{F} \quad (3.9)$$

Where F is the flow resistance through circular channel (kg/s.m^4) and is computed from Equ. (3.10)^[183].

$$F = \frac{8}{\pi}\mu L \frac{1}{r^4} \quad (3.10)$$

At constant channel length (L) and radius (r), the flow resistance will only depend on the viscosity (μ). The μ was obtained as an average after each simulation set.

3.2.4 Refrigeration coefficient of performance of PVT heat pump

PVT heat pump refrigerator works very similar as a refrigerator cycle (Fig.3.4). The evaporator in this case is a thermal storage tank and while a condenser represents the PVT unit. The heat of the refrigerant at saturated vapor is taken to the PVT unit after being scaled to the required conditions of temperature and pressure by the compressor. From PVT unit, the heat of refrigerant is released to the environment and the refrigerant at saturated liquid is sent back to

evaporator through expansion valve. The overall performance is obtained by the ratio between refrigeration capacity (Q_{ref}) and compressor power (Q_{comp}).

$$COP_{ref} = \frac{Q_{ref}}{Q_{comp}} \quad (3.11)$$

Where the (Q_{ref}) and (Q_{comp}) are respectively calculated from (3.10) and (3.11)^[184] :

$$Q_{ref} = \frac{\dot{m} \cdot c_{pfluid} \cdot (T_{in} - T_{out})}{1000} \quad (3.12)$$

$$Q_{comp} = m_r \frac{p_{in} v_{in}}{\eta_{comp}} \frac{\gamma}{\gamma - 1} \left[\left(\frac{p_{in}}{p_{out}} \right)^{\frac{\gamma - 1}{\gamma}} - 1 \right] \quad (3.13)$$

The term(s) p_{in} (Pa) is the constant inlet pressure and while p_{out} (Pa) represents outlet pressure of the refrigerant which is obtained from ANSYS Fluent, after each simulation set. The constant vapor inlet specific volume v_{in} of $0.0971 \text{ m}^3/\text{kg}$ and $0.0841 \text{ m}^3/\text{kg}$ were respectively considered for R407C and R134a^[154] and while a polytropic exponent (γ) of 1.088923 ^[185] was used in both cases. Meanwhile, the compressor efficiency η_{comp} was selected based on the low size compressor as 0.75% .

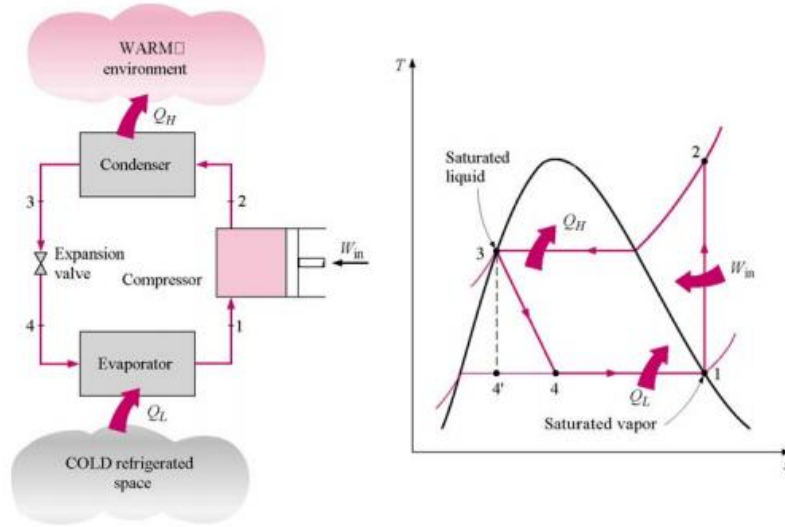


Fig.3.4 Schematic diagram of Vapor-Compression refrigeration cycle

Unlike the case of condensation in the channel of PVT unit condenser where a compressor is used to bring the refrigerant flow to the required conditions, a single phase nanofluid only requires pump to circulate the flow in the loop. Therefore, the evaluation method of coefficient of performance for PVT unit condenser with nanofluids is different from that used when a refrigerant is used, as shown in Equ.3.14.

$$COP_{nano} = \frac{Q_{nano}}{Q_{pump}} \quad (3.14)$$

In fact, a high temperature nanofluid is set at the inlet of the PVT unit condenser and comes out with low temperature. This means that H_{in} (kJ/kg) and H_{out} (kJ/kg) will respectively take + and – sign. Therefore, thermal energy produced by the nanofluid is determined in Equ. 3.15.

$$Q_{nano} = \dot{m}(H_{in} - H_{out}) \quad (3.15)$$

The pump power (Q_{pump} (kW)) on the other hand is determined from (Equ. 3.16)^[186].

$$Q_{pump} = \dot{Q} \times (p_{in} - p_{out}) \quad (3.16)$$

The term $\dot{Q}(m^3/s)$ is the volumetric flow rate obtained by the ratio between mass flow rate $\dot{m}(\text{kg/s})$ and density ($\rho(\text{kg/m}^3)$), Equ. (3.17). Meanwhile, p_{in} (kPa) is the inlet flow pressure which was taken to be 2000kPa and p_{out} (kPa) is the outlet pressure obtained from ANSYS Fluent, after each round of simulation.

$$\dot{Q} = \frac{\dot{m}}{\rho} \quad (3.17)$$

3.3 Mesh creation and model validation of numerical simulation

Model preparation includes creation of mesh able to capture solution and validation of simulation model with the previous studies. The quality mesh is selected after performing a grid independent test. This method helps determine the mesh which is too fine and too coarse to affect the results. In addition, depending on the nature of the problem to be solved, different mesh methods are used for different model geometries. In this section, the determination of quality mesh and validation of the considered models is carried out.

3.3.1 Preparation for existing PVT unit condenser model

The mesh of the model of Fig.2.3, is shown in (Fig.3.5). As can be observed, fifteen layers' inflation were incorporated at the glass top face to properly capture the natural cold of the sky. In order to determine the best mesh number for the simulation, a sensitivity was carried out at constant flow conditions and weather of 0.011m/s, 350K, 1, 300.4K, 280.5K and 0.36 m/s for inlet flow velocity, inlet temperature, volume vapor fraction, ambient temperature, sky temperature and wind speed respectively. Five types of mesh was created by changing both minimum and maximum face size. The minimum size was changed from $1.20 \times 10^{-4}\text{m}$ with an increment step of $0.10 \times 10^{-4}\text{m}$ up to $1.80 \times 10^{-4}\text{m}$, while the maximum face size was from $1.20 \times 10^{-3}\text{m}$ with an increment of $0.15 \times 10^{-3}\text{m}$ up to $1.80 \times 10^{-3}\text{m}$. The change in face size resulted in obtaining the mesh of the following order respectively; 6443025, 5471580, 4749835, 4158652, and 3753276. Moreover, grid independent was performed in terms of both Nusselt and Stanton numbers at the bottom face of the PVT unit and constant values of these two numbers started to be observed from a mesh of 5471580 (Fig.3.6). In the interest of computational time; $1.35 \times 10^{-4}\text{m}$ minimum face size, $1.35 \times 10^{-3}\text{m}$ maximum face size and 5471580 were utilized for the rest of the study.

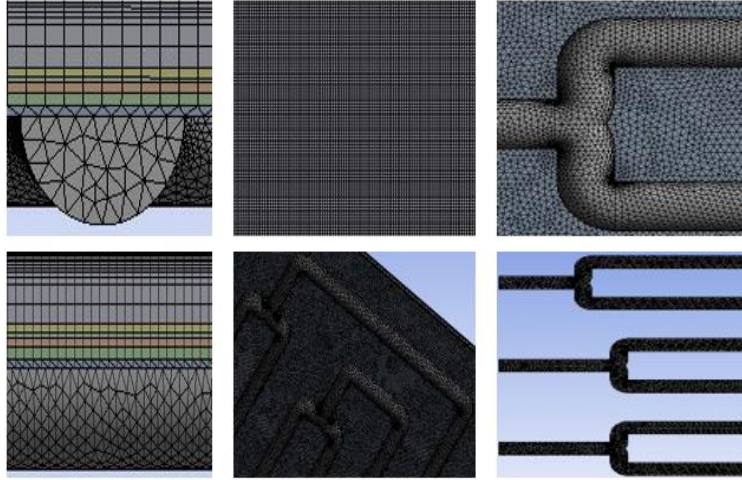


Fig.3.5 Local views of mesh for the CFD model of PVT unit without fins

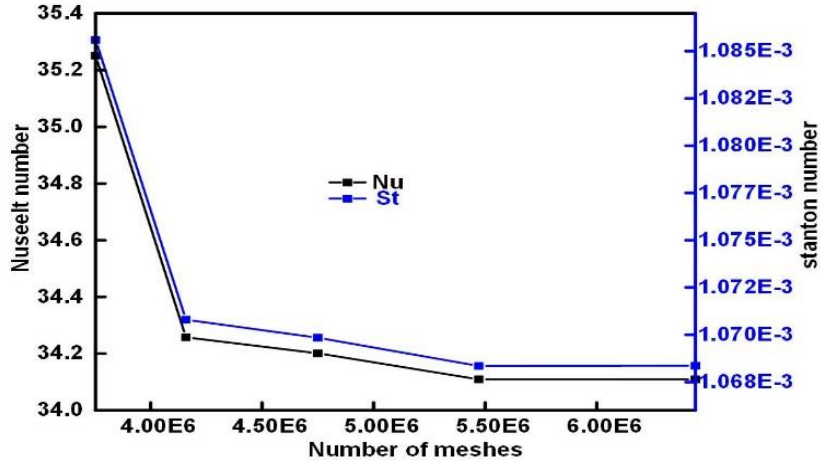


Fig.3.6 Grid independent study for PVT unit without fins

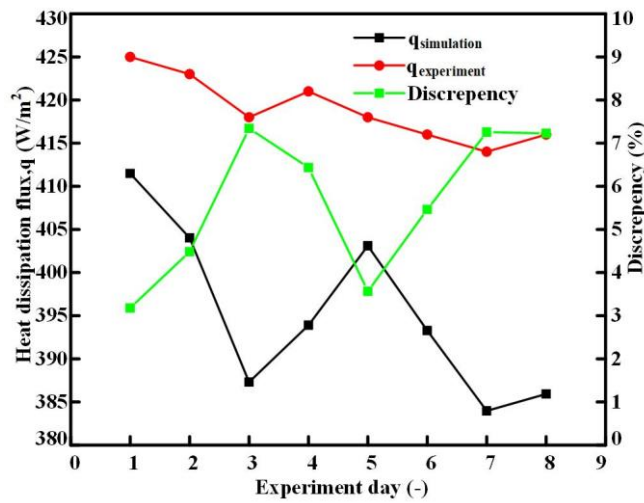


Fig.3.7 Comparison between simulation and experimental results

The accuracy of the model was checked on the basis of heat dissipation flux and by comparison between the current simulation model and experimental model of ^[138]. The model (Fig.2.3) was solved at constant flow conditions of 0.011m/s, 350K and 1 for inlet flow velocity, inlet temperature and volume vapor fraction, respectively and under the average weather conditions of each day of experiment (Fig.3.2). As can be observed from Fig.3.7, the maximum percentage discrepancy between simulated and experimental results is around 7.25 %, while the minimum is 3.18 %. With these bounds, the results of two models are in a good agreement and hence validated.

3.3.2 Preparation for PVT unit condenser with fins

Mesh creation, grid independent test and validation was carried out on basis of model of Fig.2.4. Grid independence test was conducted at constant flow conditions and weather of 0.011m/s, 350K, 1, 300.4K, 280.5K and 0.36 m/s for inlet flow velocity, inlet temperature, volume vapor fraction, ambient temperature, sky temperature and wind speed respectively and on the basis of three different temperatures (top, bottom and finned area). During mesh creation, a MultiZone method with Hexa type was used and fifteen layer inflations were incorporated at the top glass to properly capture weather conditions (Fig.3.8). Six set of meshes in order of 864875, 1053011, 1324050, 1656108, 2376957 and 3313233; were created by changing both Max Face Size and Max Tet Size in order of 0.37mm, 0.34mm, 0.31mm, 0.28mm, 0.25mm and 0.22mm, respectively. To determine the mesh best suit for the simulation, the evaluation of the temperature at top, bottom and finned surface was carried out and plotted as shown in Fig.3.9. In all six cases, the temperature remained constant at a mesh greater than 2376957. To avoid too fine mesh which can lead to time consuming or too coarse mesh which can lead to inaccurate solution, the same mesh was taken as reference for the rest of simulation sets.

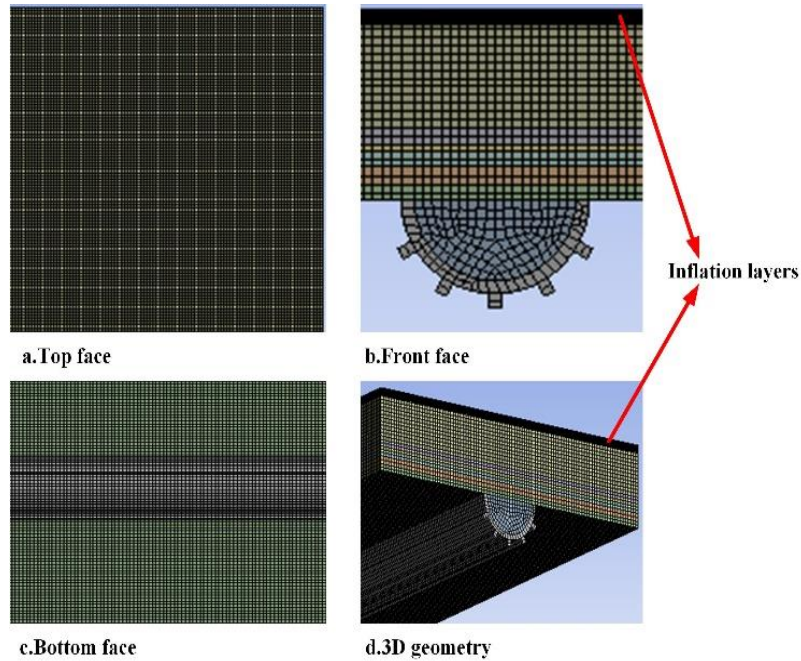


Fig.3.8 Local views of mesh for RB-PVT unit model with fins

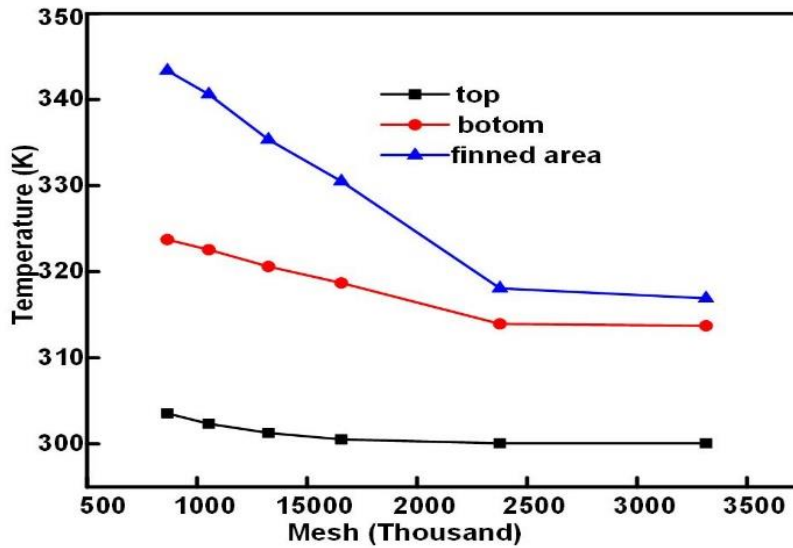


Fig.3.9 Grid independent study for PVT unit with fins

The simulation was performed at constant inlet flow vapor conditions of 0.011m/s for velocity, 350K for temperature and 1 for fraction volume vapor, under the average weather conditions obtained at each day of experiment (Fig.3.2). The accuracy of the current model was checked in two steps, comparing the average heat dissipation flux and COP from experiment ^[138] with those achieved from simulation. The simulation heat dissipation flux was calculated from Equ. (3.8), as a function of surface PVT temperature, ambient temperature and wind speed.

As can be seen from Fig.3.10, the heat dissipation flux of simulation is lower in magnitude than of experimental at all conditions but with only percentage discrepancy in a range of 2.304 to 3.25%. Meanwhile, the experimental and simulation COP is presented in Fig.3.11. The COP experienced an abrupt change mainly due to a big difference in average weather conditions used. In these circumstances, simulation COP was obtained to be 3.4% lower than that of experiment at the conditions of day 1 and while at the conditions of day 7, the simulation COP is 1.75% higher than that of experiment. On the basis of these results, the simulation model of PVT unit without fins has a very good accuracy and reliability for further simulations.

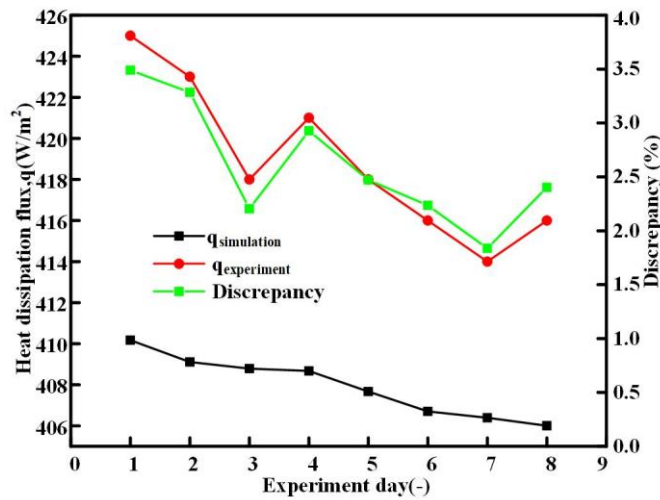


Fig.3.10 Comparison of two models (experimental and simulation) in terms of heat dissipation flux

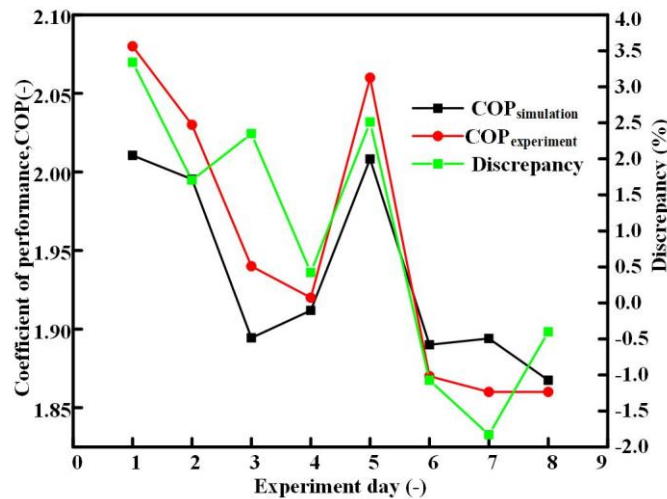


Fig.3.11 Comparison of two models (experimental and simulation) in terms of COP

3.3.3 Preparation for PVT unit condenser incorporating a novel channel

In the process of determining quality mesh, the models of Fig. 2.5, b, c were simulated at the constant operating conditions of 100W/m^2 for radiation/long-wave intensity, 298K for ambient temperature, 1 for inlet vapor volume fraction, 0.72kg/h for inlet mass flow rate and 288K for inlet flow temperature. A special attention was paid to the fluid domain and top surface of glass due to the fact a number of heat transfer mechanisms (conduction, convection and radiation) take place in these two areas. Therefore, they were meshed differently from the PVT unit layers where heat transfer is only due to conduction mode. In fact, except the fluid domain which was meshed by sweet method, the rest were meshed using multi-zone method. In addition, 10 inflation layers were incorporated at the glass top surface to properly capture both solar radiation intensities in the case of PVT unit evaporator and natural cold of the sky when PVT unit acts as a condenser during nighttime. Due to the fact that the surface of fluid domain works as an intermediate between fluid and the rest of parts, grid independent test was conducted in terms of Nusselt number at that particular surface. Typically, for turbulent flow inside pipe, the Nusselt number is in the range of 100-1000 and the higher the number, the more the active convection^[187]. As can be observed from Fig.3.12, six mesh were created for PVT condenser. The convection at the surface of fluid domain for PVT condenser is more active at a mesh 1268566. In addition, from a mesh of the 1331345, the Nusselt experiences a small change and therefore, the same mesh number was selected for the rest of simulation sets.

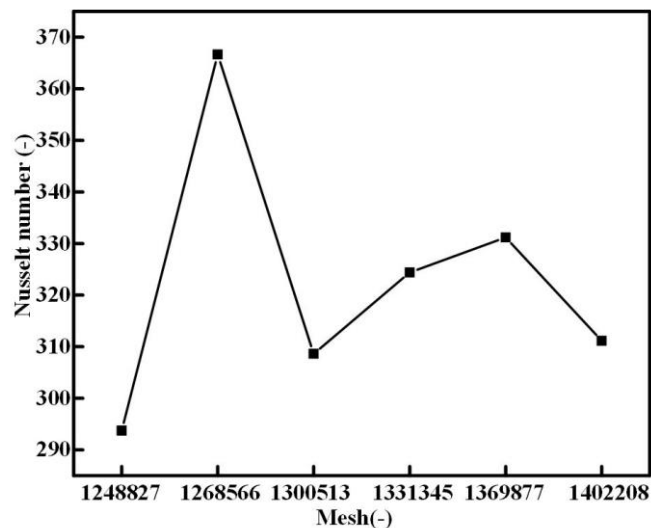


Fig.3.12 Nusselt number at different meshes of PVT unit condenser

During model validation, the same boundary and operating conditions as for^[144] were used. Moreover, the contours of; top temperature, velocity and vapor volume fraction of the current study were compared with those produced in the study of^[144]. As can be seen from Fig.3.13,

the maximum and minimum temperature attained in the top surface of the current model (Fig.3.13a) is respectively 1.1°C and 2.9°C higher than that of [144] (Fig.3.13b). Moreover, the temperature distribution is less uniform in the current study as compared to that of [144]. The fact is that the representative channels cover a small surface of the PVT unit and the heat of the area away from the channels is less exchanged with the fluid inside micro-channel. Meanwhile, the velocity distribution in the flow channels of the two models ([144] and current study) is presented in Fig.3.14. From Fig.3.14, the distribution patterns of the two studies ([144] and current study) looks quite similar according to the ranges of velocity achieved. The velocity range is a little bit different in the two considered models (i.e. 0-1.3m/s for [144] and 0.000043-1.246m/s for current study). This is due to the temperature difference of the absorbed fluid, which may affect some fluid properties and therefore as a results, the velocity can increase or lower. On the other hand, the contours for vapor fraction are shown in Fig.3.15. Like in velocity contours, the same distribution patterns in vapor volume fraction is obtained by the two studies. At the same inlet vapor volume fraction of 0.84, the maximum vapor volume fraction achieved by the current study is 0.1 less than that of [144]. This is because the heat of unoccupied area for the current study was not able to be absorbed by the fluid inside channel and further increase the temperature of the refrigerant to that of [144]. In fact, on the basis of the achieved results (Table.3-3), the current model has good accuracy and reliability for further simulations.

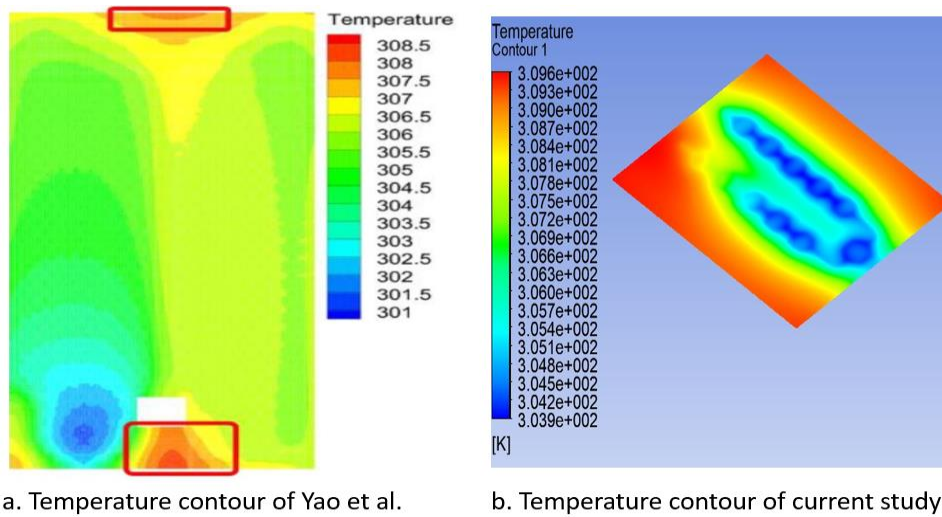


Fig.3.13 Comparison between temperature contours of [144] and current study

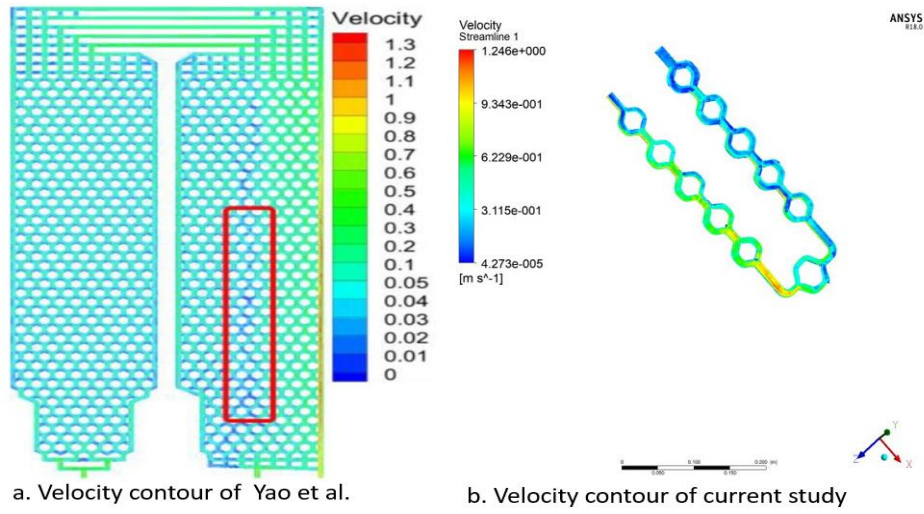


Fig.3.14 Comparison between velocity contours of ^[144] and current study

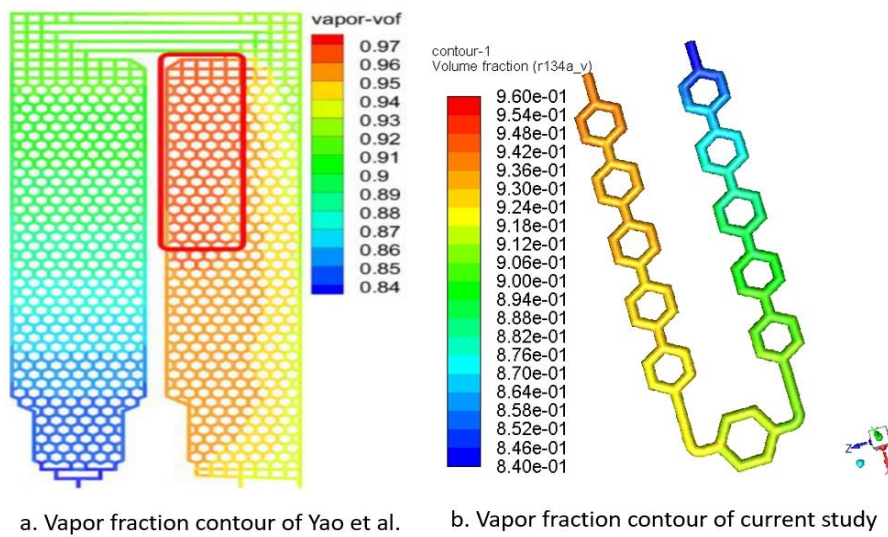


Fig.3.15 Comparison between vapor fraction contours of ^[144] and current study

Tab.3-3 Summary results of Yao et al.^[144] and current study

Parameters	Yao et al. ^[144]	Current study	Difference
Average temperature (K)	304.75	306.75	2
Average velocity (m/s)	0.65	0.623	0.027
Average vapor fraction (-)	0.905	0.9	0.05

3.3.4 Preparation for PVT unit with nanofluids

To determine the best mesh number for simulation model of Fig.2.6, a grid independent study was performed based on both top face heat transfer coefficient and temperature. The distribution of mesh patterns for various components of PVT unit condenser is presented in Fig.3.16, a-c. During mesh creation, a special attention was paid to the fluid (Fig.3.16, a) and pipe (Fig.3.16, b) domains due to the fact that the heat is released to the ambient from these two areas.

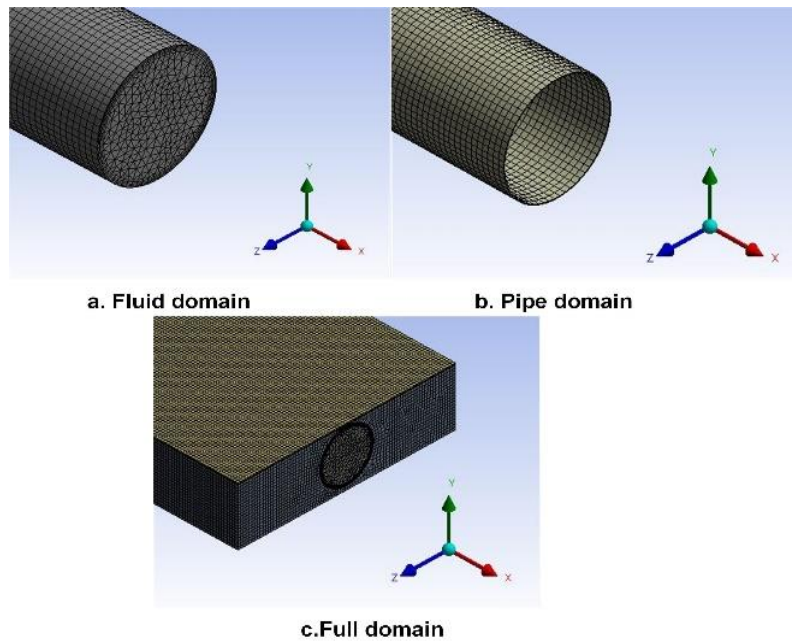


Fig.3.16 Mesh patterns of different components of water/nanofluids based PVT unit

In this circumstance, a tetrahedral and sweep methods were respectively applied to the fluid and pipe domains and with outer wall surface of fluid domain inflated by 8 layers. The rest of components were meshed in a similar way, by MultiZone method (Fig.3.16, c). In total, five mesh in order of 449374, 545357, 683015, 863719 and 1136152 were created (Fig.3.17). To select mesh which is not too fine or too coarse to affect the results, a sensitivity was performed in terms of pipe wall temperature of both Al_3O_2 -water/PVT unit and Ag-water/PVT unit condenser (Fig.3.17), under constant operating conditions of 14kg/h, 320K, 0m/s, 298K and 100W/m^2 for inlet mass flow rate, inlet flow temperature, wind speed, ambient temperature and long-wave radiation intensity respectively. As can be seen from Fig.3.13, the pipe wall temperature for Ag-water/PVT is higher than that of Al_3O_2 -water/PVT at all considered mesh, due to a higher thermal conductivity of Ag as compared to Al_3O_2 . At the first meshes, the pipe wall temperature experienced fluctuations but it became stable from a mesh of 863719. Therefore, the same mesh was chosen for the rest of simulation sets.

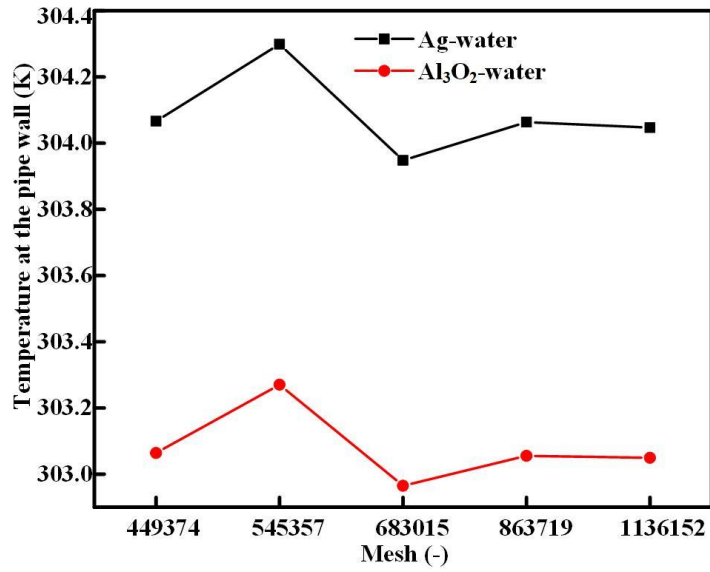


Fig.3.17 Wall pipe temperature at five mesh of Ag-water/ PVT unit and Al₃O₂-water/PVT unit

The model validation of the current study was ensured in three steps, after comparing both water outlet and absorber temperature of the current study with the corresponding results from the previous studies about water/PVT unit and nanofluids/PVT unit . As it has already been mentioned in section 2.2.2, water was used in this thesis only to prepare nanofluids and validate a model which can be utilized to model any kind of liquid. During validation, similar geometries and same boundary conditions as for those used by the authors in the two mentioned models, were considered. To better characterize the differences between the current results and those of previous studies, the average percentage error (MAPE) of Equ.2.42 method was utilized.

To validate the model of water-based-PVT system, the results from the work of Selmi et al.^[188] have been the reference. The same model geometry and boundary conditions as Selmi et al.^[188] were considered in the current study. The results of Fig.3.18 were obtained at inlet mass flow rate of 0.000136kg/s, inlet temperature range of 32-46°C and solar radiation range of 470-542W/m². As can be observed the inlet and out temperature increases from 9:35 to 11: 45 and after then, a slight decrease occurs. The obtained current results are in the range of 5.34-11.13% lower than those of Selmi et al. when the whole pipe is used, while an outlet temperature in the range of 1.025-5.63% and higher than that of Selmi et al.^[188] is achieved for semi-circle pipe. This implies that the use of semi-circle pipe increases the contact surface and as a results, the heat transfer enhances. On the basis of these results, the two models are in good agreement.

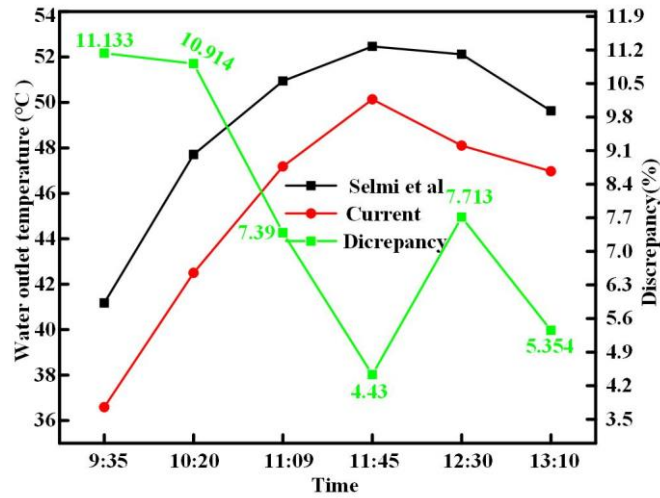


Fig.3.18 Comparison between of the outlet water temperature of the current study and that of Selmi et al.^[188]

The accuracy of the current simulation of nanofluids/PVT unit was determined considering two types of nanofluids; Al_3O_2 -water (5% fraction nanoparticles) and Ag-water (5% fraction nanoparticles) as fluids medium inside pipe. The attained absorber temperature when the inlet flow velocity of each of the two mentioned nanofluids was varied in the range of 0.04-0.23m/s was compared with that of Khanjari et al.^[157], taking into account 35° of model inclination and constant operating conditions of $800\text{W}/\text{m}^2$ and 298.15K for solar radiation intensity and inlet flow temperature, respectively. The results of Ag-water/PVT unit and Al_3O_2 -water/PVT unit were respectively presented in Fig.3.19 and Fig.3.20. Like in the case of water/PVT unit, the absorber temperature of the current study is higher than that of Khanjari et al. ^[157] at all considered inlet flow velocities, possibly due to the thermal resistance between absorber and pipe, which is a little bit higher than that in Khanjari's model. Also, the percentage discrepancy increases in a parabolic manner as the flow velocity increases (Fig.3.19 and Fig.3.20). Overall, the maximum percentage discrepancies of 5.913 % and 5.885% were respectively obtained at Ag-water/PVT unit and Al_3O_2 -water/PVT unit and hence implying a good agreement between the two models.

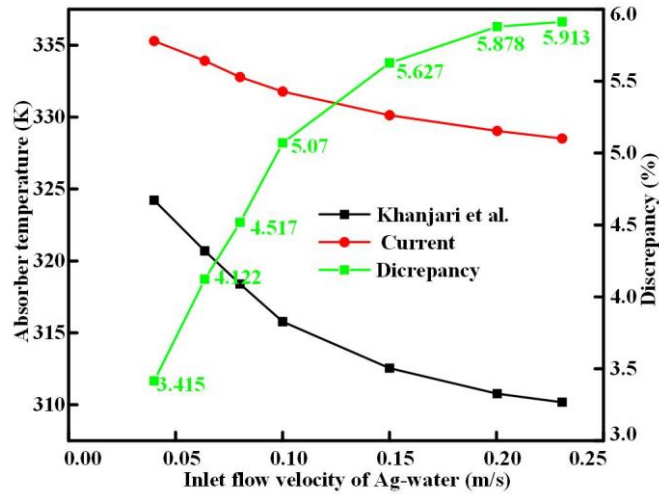


Fig.3.19 Comparison between the absorber temperature of the Ag-water/PVT unit for current study and that of Khanjari et al. [157]

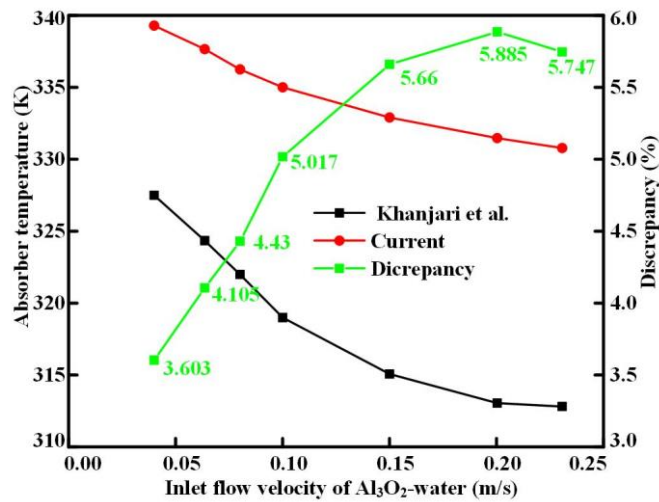


Fig.3.20 Comparison between the absorber temperature of the Al₃O₂-water/PVT unit for current study and that of Khanjari et al. [157]

3.2 Summary

This chapter sets up proper methods, operating conditions, assumptions and creation of mesh quality leading to the accuracy of the 4 considered models in this PhD thesis. As summarized in Table.3-4, the 4 models with different purposes are divided into small elements able to capture the solution of mathematical equations, solved and validated against the models from previous studies. In all the 4 cases, the validation is ensured based on the attained range of percentage discrepancy.

Tab.3-4 Summary information of the validated PVT unit models under consideration

Considered model	Purpose	Mesh selection number	Reference model	Validation discrepancy range
Existing PVT unit condenser	Further analysis the heat transfer characteristics	5471580	The model of Lu et al [138]	3.18%-7.25%
PVT unit condenser with fins	Investigate the effect of fins	2376957	The model of Lu et al [138]	1.75%-3.4%
PVT unit condenser with novel channel	Study the impact of new channel structure	1331345	The model of Yao et al. [144]	0.55%-4.15%
PVT unit with nanofluids	Introduction of nanofluids in the research of PVT unit for cooling at night	863719	The models of Selmi et al. [188] and Khanjari et al. [157]	3.415%-11.133%

The tasks performed in this chapter are of great importance in obtaining and analyzing the results of the particular case study, as given here below:

Firstly, the determination of model accuracy is the most important step as it can allow implementing knowledge from different fields of study to the real problem. Due to this, the step requires to pay much attention which in turns leads to time consuming. In fact, the main objective is to build a basic model which can be utilized to further get results and deeply analyze the problem under investigation. This is to mean that the same model of each of validated models can be employed to obtain the results of a particular case study.

Secondly, the 4 validated models will be used to study different problems. In this circumstances, the first validated model of existing PVT unit condenser has been useful to design and optimize the heat transfer characteristics of PVT unit condenser. The effect of fins on the heat transfer characteristics and overall coefficient of performance of PVT unit condenser has been determined on basis of the validated model of PVT unit condenser with fins. In order to further seek alternative ways to improve the night cooling performance of PVT unit condenser, a validated model of PVT unit condenser incorporating a novel channel of hexagon-grid coupled with a serpentine-shape arrangement of fluid channel pattern has been investigated both in terms of heat transfer characteristics and overall coefficient of performance. The impact of applying new fluid of nanofluid has been studied considering a validated model of PVT unit with nanofluids.

Thirdly, as a specialty of ANSYS Fluent, the contours of thermal behaviors for each of the above mentioned case studies will be presented first and then followed by other results. The contours of thermal behaviors provide a better understanding on how heat is being transferred in both fluid channel and materials of PVT unit.

4. Numerical analysis of existing PVT unit condenser

In this chapter, a numerical simulation was carried out to further study the existing PVT unit condenser (model 1, section 2.2.1). In contrary to the previous research where much focus was to investigate the heat dissipation flux and overall coefficient of performance under Dalian weather conditions (Fig.3.2), the key issue for the current study is to determine the optimum parameters (internal and external diameter, distance between two channels, longitudinal and lateral distance) of the PVT unit condenser and to use an optimized model in analysis of heat transfer characteristics at different external and internal factors of Table.3-1. To achieve the objective, a validated model of existing PVT unit condenser (section 3.3.1), was considered. At first, a detailed explanation of the parameters for the design as well as the method to determine optimum dimensions was provided. Next, the model (section 3.3.1) was solved and the obtained results were discussed in three perspectives. Initial set of results were to analyze the velocity and temperature distribution in flow channel and PVT unit condenser materials. The heat transfer characteristics of the PVT unit condenser is affected depending on the distribution uniformity of the two stated parameters of temperature and velocity. Having the knowledge of the distribution patterns, the two heat transfer characteristics of heat dissipation flux and average Nusselt number were discussed at different parameters change in order to propose new dimensions of PVT unit condenser. On the basis of optimum dimensions, a new model of PVT unit condenser was built and further solved to evaluate the effect of different internal and external on the heat transfer of PVT unit condenser. Last, the heat dissipation flux of optimized model was determined and discussed in comparison with that of existing model.

4.1 Design of PVT unit condenser

In this section, optimum dimensions of existing PVT unit condenser (section 3.3.1) were numerically determined at constant flow and weather conditions of 300.4K, 350K, 1, 0.011m/s and 0.36m/s for ambient temperature, inlet flow temperature, vapor fraction, inlet flow velocity and wind speed, respectively. Fig.4.1 and Fig.4.2 respectively show the parameters considered for the design of full model of existing PVT unit condenser and the representative simulation model of section 2.1.2. Those parameters include the distance between two channels, internal diameter, outer diameter, lateral and longitudinal distance. As pointed out in section 2.1.2, for the sake of simplicity and less computational, the existing model PVT unit condenser (Fig.4.1) with one inlet and two outlets was reduced by 1/4 before being solved in ANSYS Fluent. This means the number of channels, longitudinal and lateral distance were reduced by 4 (Fig.4.2). But the dimensions of channels such thickness, internal diameter and the distance between two channels were taken the same for both two models (Fig.4.1 and 4.2). During simulation in

ANSYS Fluent, the Volume of Flow (VOF) was used to model two phase change refrigerant and while turbulent models of Equ. 2.21 and Equ.2.22 were employed to account for the fluctuations caused by the fluid transport inside channel. The impact of parameter dimensions was discussed in terms of two heat transfer characteristics of outlet average fluid Nusselt number and heat dissipation flux with the objective to select the optimum dimensions which can minimize the area of PVT unit condenser. As the channels are embedded at the bottom face, the change in channels area has less effect on the actual area occupied by the PVT unit as compared to the lateral and longitudinal distance. Therefore, the optimum dimensions were determined by the intersection points between the maximum values in both outlet average fluid Nusselt number and heat dissipation flux considering the internal and external diameters to increase in the range of 0-1.5mm, and the distance between two channels and longitudinal distance to decrease in range of 0-10mm. Here it should be notified that the lateral distance was obtained based on the attained distance between two channels. Moreover, the two heat transfer characteristics of outlet average fluid Nusselt number (Equ.2.35) and heat dissipation flux (Equ.3.7) were adopted due to the fact that they vary inversely proportional to each other. Nusselt number is a dimensionless number which measures the ratio between the heat transfer by convection and the heat transfer by conduction. In PVT unit condenser, the heat dissipation flux at the outer surfaces highly depends on the amount of heat conduction through the materials. This means that higher amount of heat transfer by conduction incurs higher heat dissipation flux and while the outlet average fluid Nusselt number lowers, and vice versa.

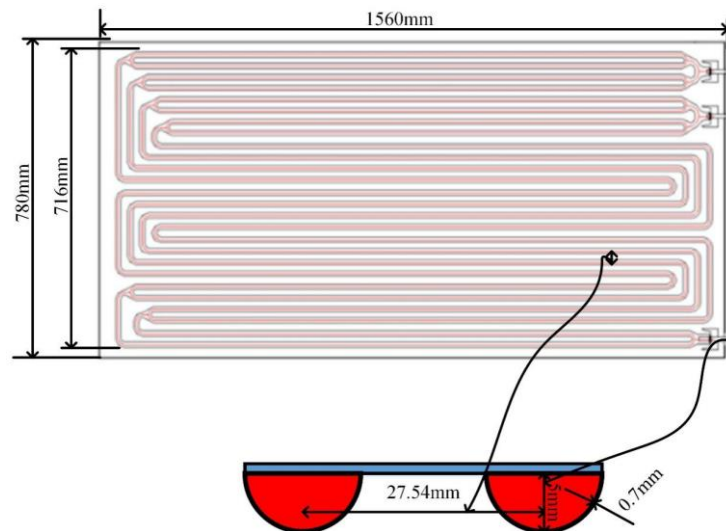


Fig.4.1 Design parameters of existing physical model of PVT unit condenser

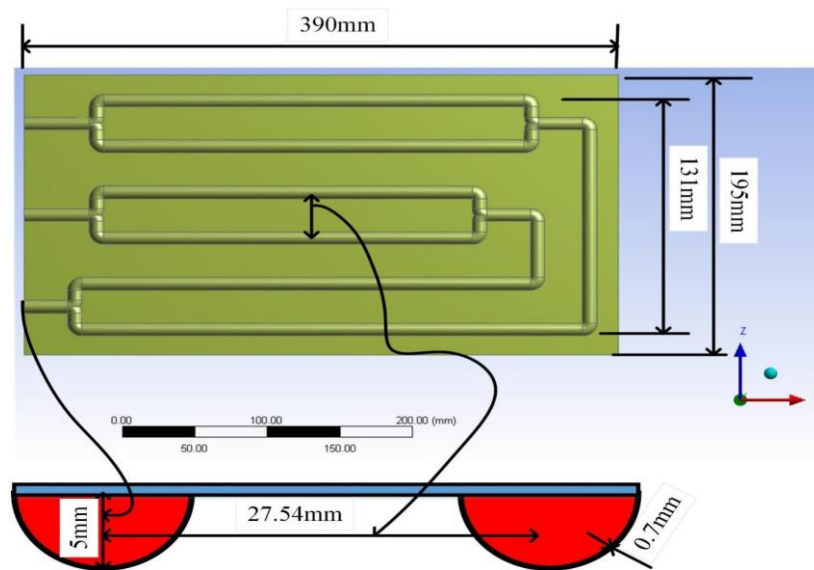


Fig.4.2 Design parameters of existing simulation model of PVT unit condenser

4.1.1 Temperature and velocity distribution in both PVT unit layers and channels

The extent of heat transfer is determined based on the distribution patterns of flow quantities in both fluid flow and PVT unit materials. The temperature distribution in PVT unit layer materials is shown in Fig.4.3. As can be observed, the highest temperature of about 341.9K is attained inside channels and decreases as the layer thickness increases, mainly due to an increase in thermal resistance and close proximity of the layers to the cold environment. Meanwhile, the temperature of refrigerant raises in channels bends and when the flows of different branches are mixed (Fig.4.4). The fact is that the slow flow rate caused by the joints and bends increases friction and as a result the temperature in both coolant and channel material increases at those particular positions. Due to this, the corresponding temperature of the top surface of the PVT unit becomes higher as compared to the rest of positions (Fig.4.5). Like in the case of temperature distribution in channels (Fig.4.4), a higher velocity of flow is attained at the channel bends and joints (Fig.4.6). In fact, the distribution patterns of the two flow quantities (temperature and velocity) as well as the heat transfer characteristics are in turns affected at different dimensions of the PVT unit condenser materials.

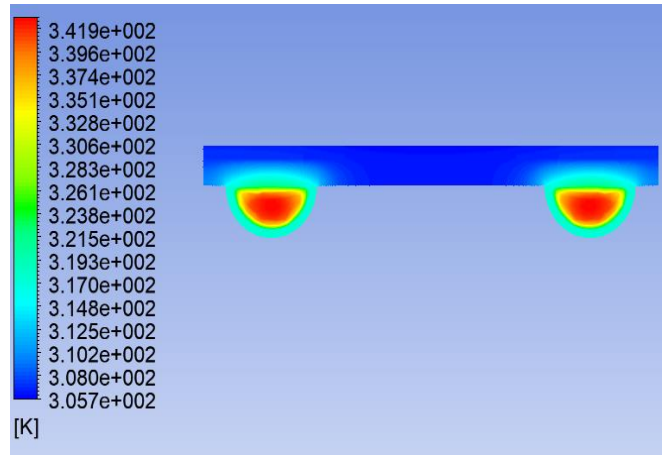


Fig.4.3 Temperature distribution in PVT unit material at distance $x=250\text{mm}$ and considering the first 2 channels

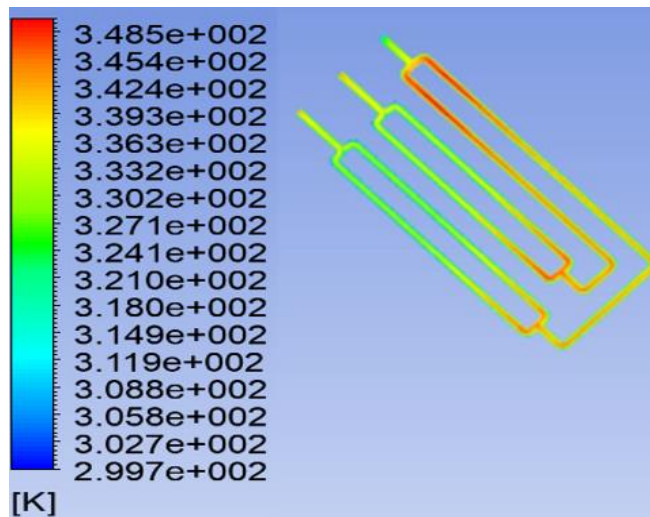


Fig.4.4 Temperature distribution inside 3D channels

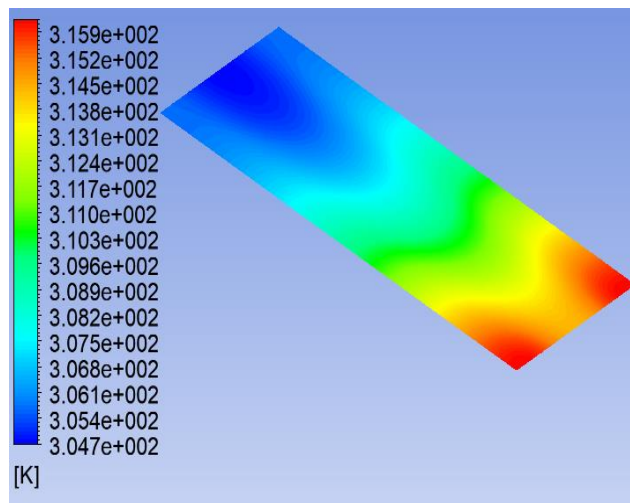


Fig.4.5 Temperature distribution at the top surface of the PVT unit condenser

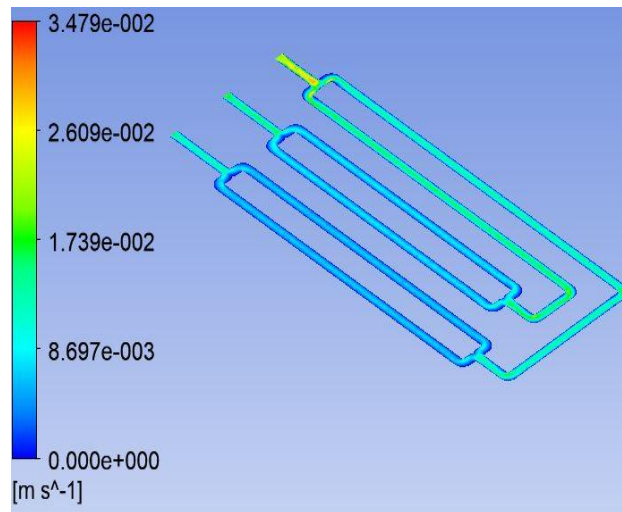


Fig.4.6 Velocity distribution in channel of the PVT unit condenser

4.1.2 Effect of lateral and longitudinal distance on heat transfer characteristics

As shown in Fig.4.7, two intersection points (one at a distance of 5.3mm and another at 9.65mm) are obtained when the distance between two channels is reduced from 0 to 10mm. The reduction in the distance by 5.3mm is selected due to the fact that the highest values in heat dissipation flux and Nusselt number of 392.8W/m^2 and 62.7 are obtained, respectively. The existing PVT unit system incorporates 26channels at its lateral distance of 716mm and with 27.54mm distance between two channels. With optimized system of the PVT unit, the distance between two channels is reduced to 22.24mm. Based on this distance, two conclusions can be made; either to fit 26channels on a lateral distance of 578.24mm or to increase the number of channels on the original lateral distance up to 32. On the other hand, two intersections points (one at a distance of 6.3mm and another at 9.4mm) are obtained when reducing the longitudinal distance by 10mm. The point at a distance of 6.3mm presents highest values in both heat dissipation flux and Nusselt number (391.2W/m^2 and 62.2), and therefore selected as an optimum reduction in longitudinal distance. By decreasing the length (1560mm) of the existing

PVT unit by 6.3mm, the new dimension becomes 1553.7mm. This not only can reduce the space occupied by the unit but also can lower the per meter square price of the PVT unit.

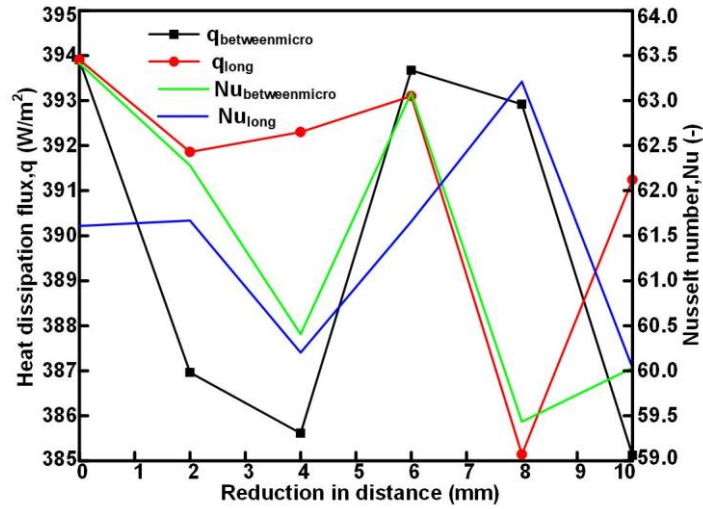


Fig.4.7 Effect of PVT unit parameter distance on heat transfer characteristics

4.1.3 Effect of channel parameters on heat transfer characteristics

Increases in both inner and outer diameter of the channel, from 0mm to 1.5mm affects the heat transfer characteristics, Fig.4.8. Increases in inner diameter increases heat dissipation flux and while Nusselt number reduces. Meanwhile, a similar trend is observed when outer diameter increases. The optimum values are obtained at 0.35mm and 0.76mm for outer and inner diameter, respectively. This implies, the new dimensions for internal and external diameter are respectively 5.06mm and 5.35mm. In comparison to the manufacturer dimensions (i.e. ID:4.3mm and OD:5mm), an increase in two channel parameters is observed. The channels are embedded to the bottom face and which means increasing their dimensions will not affect the area normally occupied by the PVT unit. Instead, it will have impact on two heat transfer characteristics; reduces the slowness of the flow rate which may cause a larger increase in temperature of both channel material and fluid, and also a uniform pressure may be achieved as result of increasing Reynold number.

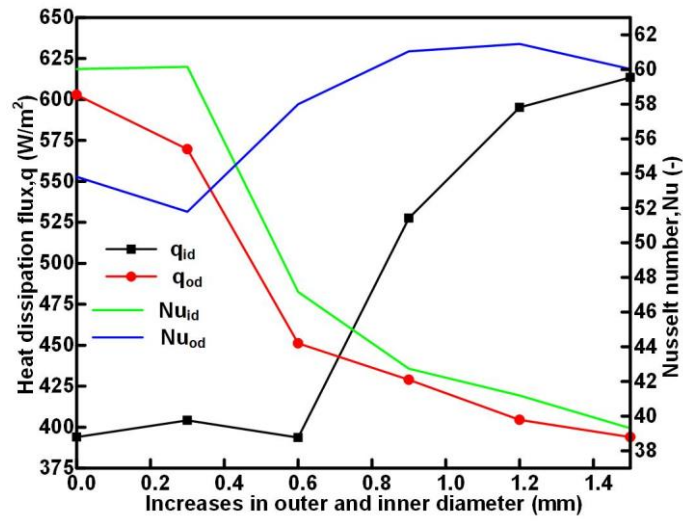


Fig.4.8 Effect of channel parameters on heat transfer characteristics

In fact, from the above results and discussions, the main findings as well as their implications in practical situation are illustrated in Table.4-1. The new design model can be further studied to compare it with the existing one and also to explore its heat transfer characteristics at different internal and external factors.

Tab.4-1 Summary optimum dimensions of the PVT unit condenser for experiment and simulation models

Parameter	Experiment PVT unit condenser model	Simulation PVT unit condenser model	Implication
Distance between two channels (mm)	22.24	22.24	Reduction in lateral distance
Lateral distance occupied by channels (mm)	642.24	160.56	Number of PVT units can be increased or reduced
Longitudinal distance (mm)	1553.7	388.425	Reduce the actual area and price per meter square
Internal diameter (mm)	5.06	5.06	Improve uniformity of both temperature and pressure distribution
External diameter (mm)	5.35	5.35	

4.2 Investigation of optimized model of PVT unit condenser

This section is devoted to discuss the impact of internal and external factors (Table 3-1) on the operating condition of an optimized model of PVT unit condenser (Table.4-1). In addition, the heat dissipation flux of optimized PVT unit condenser is discussed in comparison with that of existing model.

4.2.1 Distribution of internal flow properties

In this section, the distribution patterns of internal flow properties (molecular viscosity and Prandtl number) are presented at two inlet flow velocities in order to have an idea on how flow properties and the heat transfer characteristics of the PVT unit condenser can be influenced at different magnitudes of external and external factors. At constant values of 300.4K, 350K, 1 and 0.36m/s for ambient temperature, inlet flow temperature, vapor fraction and wind speed respectively, the two inlet flow velocities of 0.12m/s and 0.14m/s result in different distribution patterns of molecular viscosity and Prandtl number inside fluid as shown in Fig. 4.9, Fig.4.10, Fig.4.11 and Fig.4.12. The heat transfer characteristics of PVT unit condenser especially the heat dissipation flux to flow resistance and overall heat transfer coefficient change as a results of increase or decrease in molecular viscosity and Prandtl number. The distribution patterns of molecular viscosity of the fluid inside channel indicate the extent of flow resistance and the higher the molecular viscosity, the more the flow resists movement. On the other hand, Prandtl number determines the relationship between the thermal boundary layer and the thickness of hydrodynamic layer inside fluid. The difference in distribution patterns of molecular viscosity and Prandtl number at two inlet flow velocities of 0.12m/s and 0.14m/s would be a very helpful tool to better understand the effect of different internal and external factors on the other fluid flow properties and heat transfer characteristics of the PVT unit condenser.

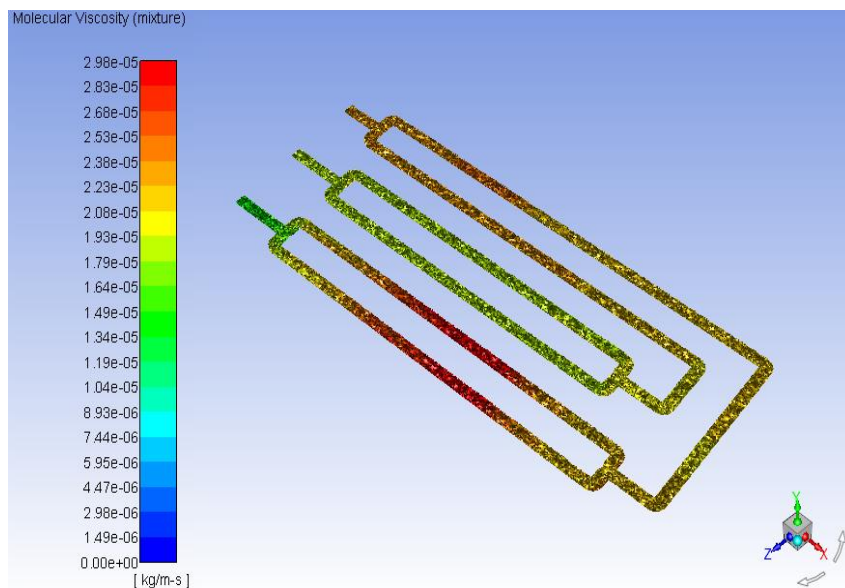


Fig.4.9 Distribution patterns of molecular viscosity at 0.12m/s

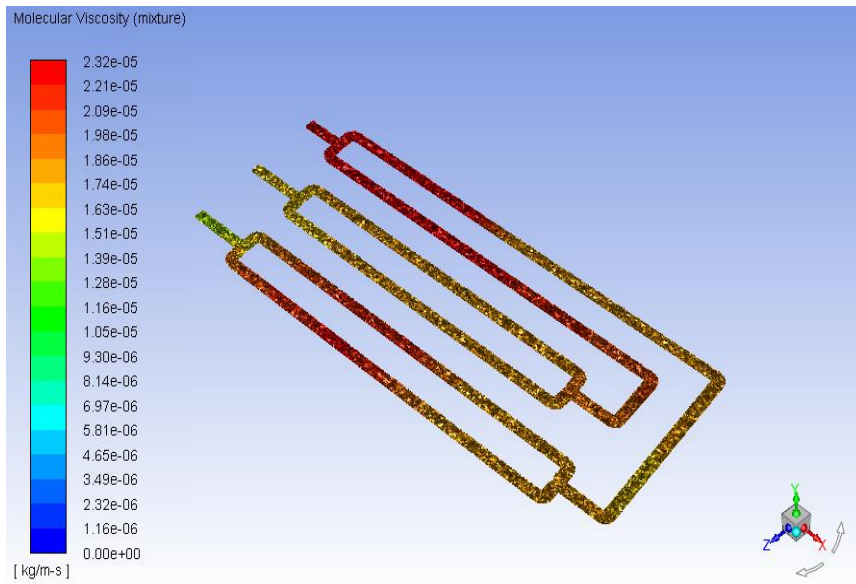


Fig.4.10 Distribution patterns of molecular viscosity at 0.14m/s

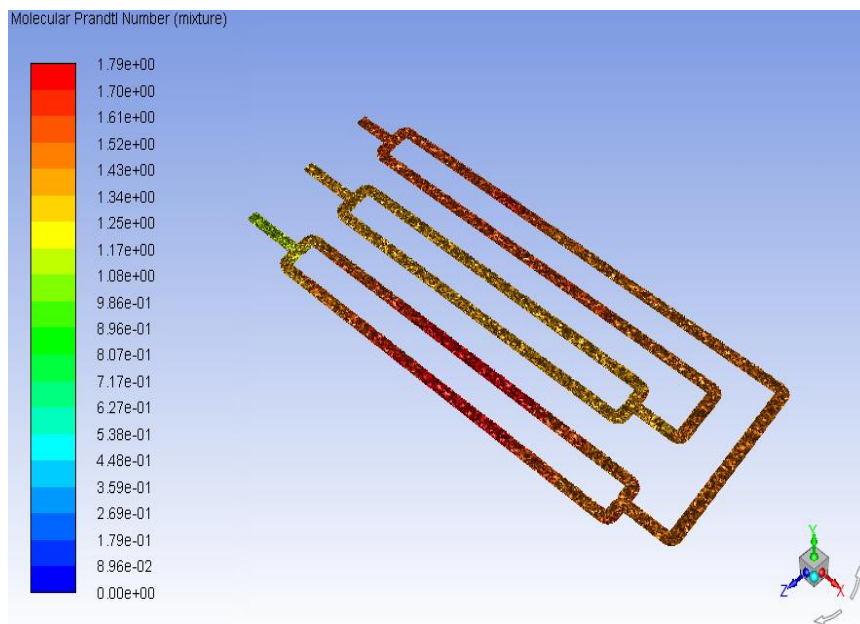


Fig.4.11 Distribution patterns of Prandtl number at 0.12m/s

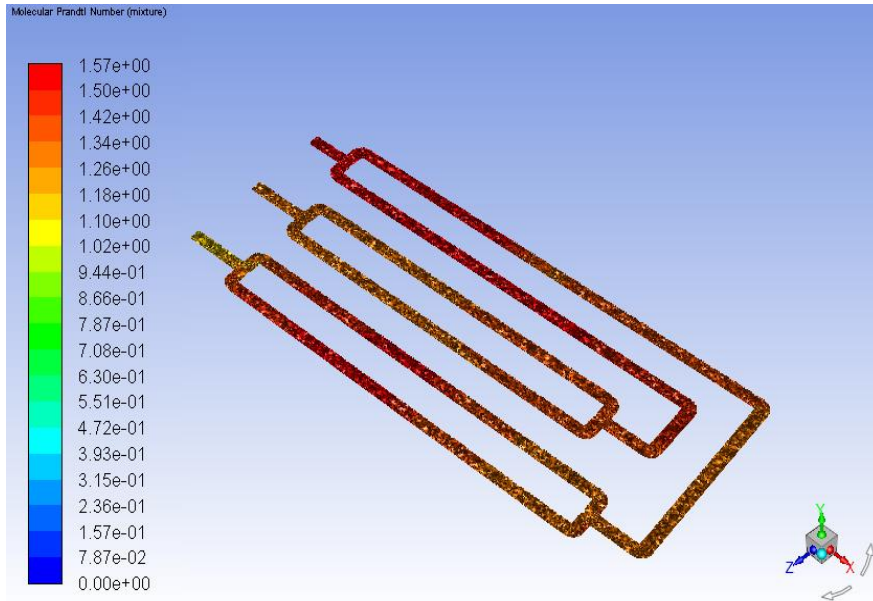


Fig.4.12 Distribution patterns of Prandtl number at 0.14m/s

4.2.2 Effect of internal factors on the heat characteristic of optimized PVT unit condenser

The internal factors discussed in this section are ; inlet flow temperature, inlet flow velocity and inlet flow fraction. In ANSYS Fluent, an optimized model of PVT unit condenser (Table.4-1) was simulated under constant weather conditions of 299K, 278.8K and 0.93m/s for ambient temperature, sky temperature and wind speed respectively. In the PVT unit condenser, refrigerant inside channel acts as a heat source. Depending on the insolation of the day, the heat absorbed by the refrigerant may increase its temperature and attains a vapor fraction of 1 or less. In addition, various flow inlet velocities can be set to meet the flow conditions in the channels. Therefore, it is of utmost importance to study the heat transfer characteristics of the PVT unit condenser at different values of the three mentioned internal factors. The inlet flow temperature was varied from 342.5K with an increment step size of 1.5K up to 350K (Fig.4.13), and at constant inlet velocity and flow fraction of 0.011m/s and 1, respectively. Meanwhile, at constant inlet flow temperature of 350K, the effect of inlet flow velocity and inlet flow vapor fraction was discussed considering the flow velocity in the range of 0.09m/s to 0.19m/s (Fig.4.14) and vapor fraction in the range of 0.85-1 (Fig.4.15). Initially, a higher vapor fraction of refrigerant is considered at the inlet channel of the PVT unit condenser. In the process of heat exchange between the refrigerant inside channel and the cold ambient environment, the fraction vapor as well the density change. This in turns has an impact on the flow velocity, overall heat transfer coefficient (U) and heat dissipation flux to flow resistance (H). At the same operating conditions of the PVT unit condenser, increase in the inlet flow temperature increases U and H, and while

density and velocity reduce. From thermo-physical properties of R407C (Table.2-4), the density and viscosity of vapor are much lower than those of liquid.

Therefore, increase in inlet flow temperature (Fig.4.13) further increases the vapor fraction and as a results, the density and flow resistance are reduced. However, due to an increase in temperature difference between flow inside channel and cold ambient, H and U improve. On the other hand, increasing inlet flow velocity (Fig.4.14) linearly increases the outlet velocity. This affects the density to decrease inversely proportional to the velocity. The fact is that a higher velocity reduces the residence time of the flow inside channel and consequently, a higher vapor fraction which is directly proportional to the density reaches the outlet. At two ranges of inlet flow velocity; 0.09m/s-0.13m/s and 0.17m/s-0.19m/s, U and H change inversely proportional to each other and while in the flow velocity range of 0.13m/s-0.17m/s, they present similar variation patterns with higher value of both two obtained at inlet flow velocity of 0.15m/s. In PVT unit condenser, the increase in U and H at a particular condition indicates an excellent heat transfer and therefore, for a considered inlet flow velocity range, 0.15m/s would be taken as an optimum inlet flow velocity. Meanwhile, as can be observed from Fig.4.15, increasing the inlet flow fraction in the range of 0.85-0.95 slightly varies the outlet flow velocity and outlet flow density but has no effect on the two heat transfer characteristics of U and H. However, as in the case of inlet flow temperature (Fig.4.13), U and H highly improve when the flow is supplied with vapor fraction of 1. This implies that a better performance of the PVT unit condenser is achieved at higher value of inlet flow temperature and inlet fraction of 1.

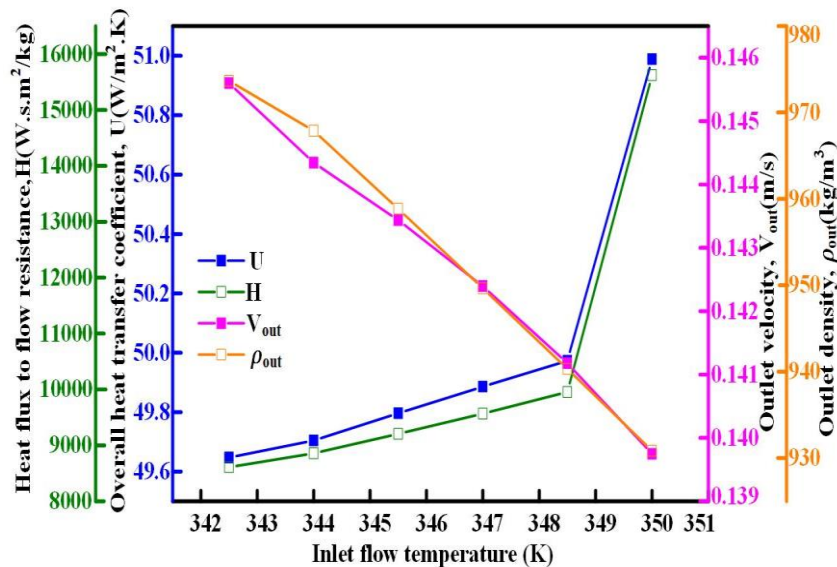


Fig.4.13 Influence of inlet flow temperature on heat characteristics

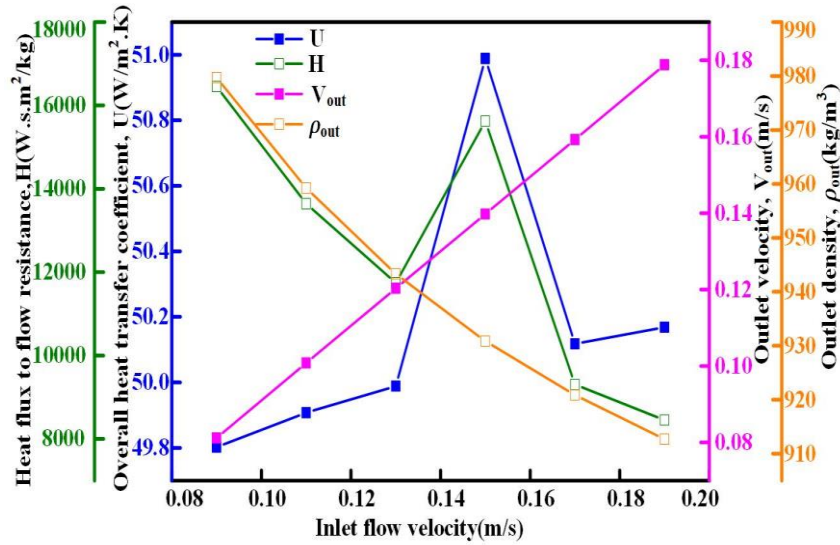


Fig.4.14 Influence of inlet flow velocity on heat characteristics

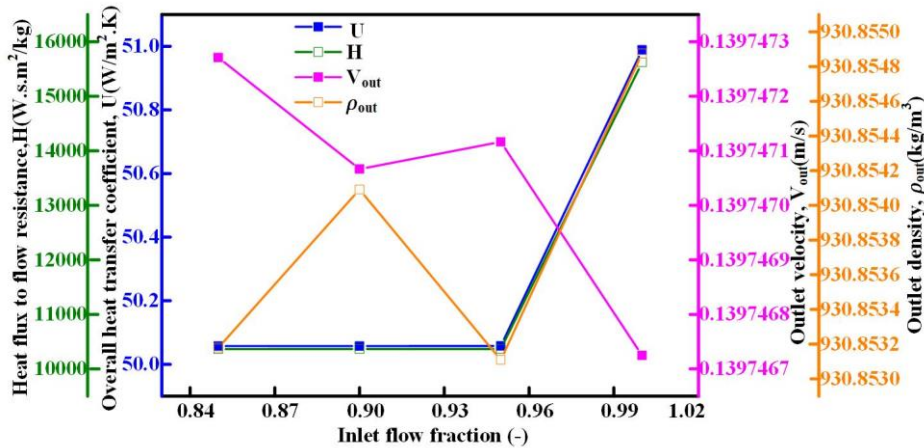


Fig.4.15 Influence of inlet flow fraction on heat characteristics

4.2.3 Effect of external factors on the heat characteristic of optimized PVT unit condenser

In this section, a simulation was performed at constant inlet flow parameters of; velocity of 0.011m/s, temperature of 350K, and vapor fraction of 1 to study the effect of external factors. The results were discussed in terms of outlet flow velocity, outlet density, overall heat coefficient (U) and heat dissipation flux to flow resistance (H), considering emissivity of the two exposed surfaces of PVT unit condenser, ambient temperature and wind speed. The outlet velocity and density were directly obtained from ANSYS Fluent and while U and H were respectively computed from Equ.2.23 and Equ.3.9. An emissivity of PVT unit materials especially for the exposed surfaces influences the heat transfer characteristics of the PVT unit condenser due to its ability to allow outgoing of heat of the refrigerant. With this perspective,

the effect of various values of emissivity (0.4 to 0.9) was investigated at a constant; sky temperature of 280.5K, ambient temperature of 300.4K and wind speed of 0.36m/s(Fig.4.16). The impact of ambient temperature change was studied at constant sky temperature of 280.5K and wind speed of 0.36m/s (Fig.4.17). On the other hand, simulation was carried out at constant ambient temperature of 300.4K and sky temperature of 280.5K to analyze the effect of wind speed on the heat transfer characteristics of PVT unit condenser, Fig.4.18.

By incrementing the surface emissivity from 0.4 by 0.1 step size up to 0.9 (Fig.4.16), increases the outlet flow density and while outlet flow velocity reduces. The reason behind this change is that extra heat removed as a result of increasing surface emissivity affects more liquid to form in the mixture of vapor-liquid and consequently both flow viscosity and density linearly rise closer to those of liquid refrigerant (Table.2-4). Increase in flow resistances in turns causes the reduction of outlet flow velocity. At emissive less than 0.8 U and H are not affected and while a sharp increase is observed at emissivity of 0.9. Also, as the weather changes time to time, the knowledge about the effect of various weather conditions on the heat transfer characteristics would be very helpful in predicting the performance of the PVT unit condenser at particular weather conditions of the day, week, month or year. The increase in ambient temperature (Fig.4.17) enhances the radiation heat transfer and the U . However, due to the reduction in temperature difference between ambient and fluid inside channel, the actual amount of vapor fraction reaching the outlet increases a little bit and causes the outlet flow velocity and outlet density to increase and decrease, respectively. For this case, the heat dissipation flux to flow resistance (H) is only impacted at higher ambient temperature (310K). Meanwhile, increase in wind speed (Fig.4.18) causes a parabolic increase of U and outlet density, and while decreasing trends are observed for H and outlet velocity. This can be explained in a way that, increasing the wind speed slightly enhances the convection heat transfer at the outer surfaces of the PVT unit condenser and the U . But as more liquid is formed inside channel, the density and viscosity increase closer to those of liquid. From Equ.3.9, increase in flow viscosity reduces the heat dissipation flux to flow resistance (H).

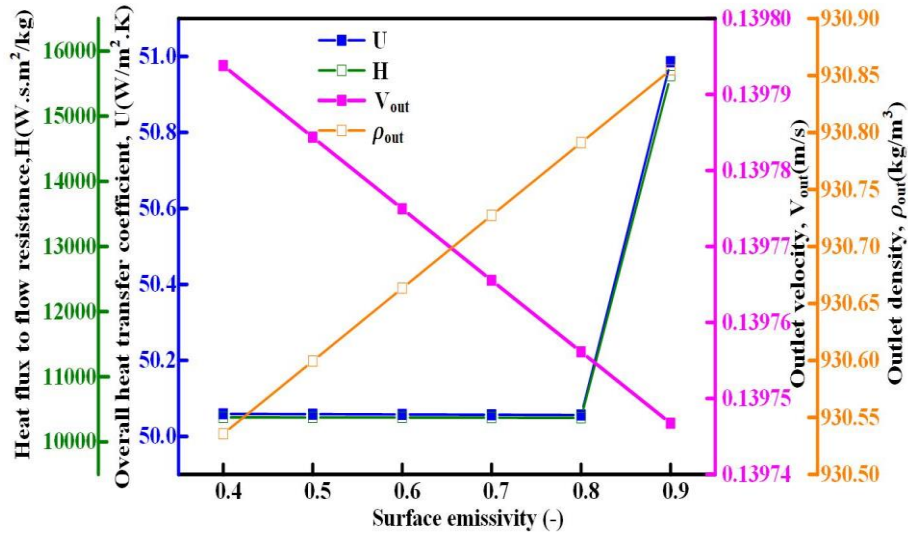


Fig.4.16 Effect of emissivity change on the heat characteristics of the PVT unit

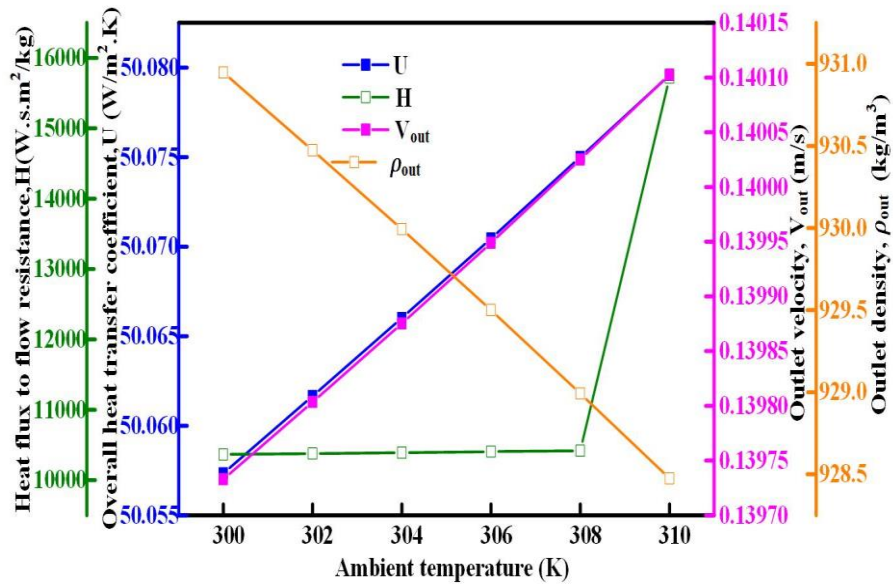


Fig.4.17 Effect of ambient temperature on the heat characteristics of the PVT unit

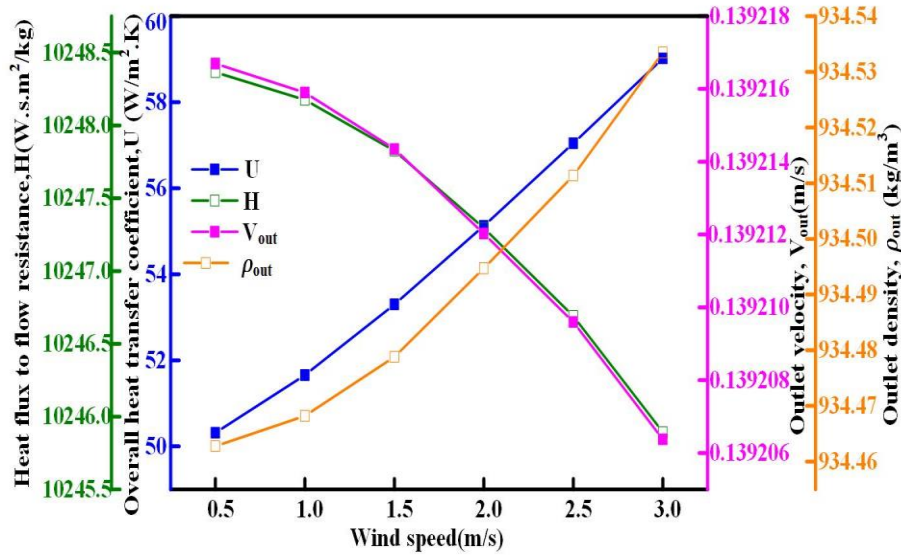


Fig.4.18 Effect of wind speed on the performance of the PVT unit

To sum up from the sections 4.2.2 and 4.2.3, the heat dissipation flux to flow resistance might be obtained highest at some factors and lowest at others. This happens mainly due to two reasons; 1) a higher heat dissipation flux might be achieved at lowest molecular viscosity and 2) a smaller heat dissipation flux might be obtained at highest molecular viscosity. Therefore, it is also important to determine the magnitude of heat dissipation flux alone.

4.2.4 Heat dissipation flux of optimized PVT unit condenser

In consideration to the optimum model of PVT unit condenser developed from the previous section (Table.4-1) and knowledge about the effect of internal and external factors, a numerical simulation was performed under the same operating conditions (Fig.3.2) as for experimental work. At the inlet of the channel, a refrigerant flow (R407C) with vapor fraction of 1 and a temperature of 350K were set. The flow turbulences were modelled using Eqs. 2.22 and 2.23 at steady state condition (section 3.1.2). The obtained heat dissipation flux (Equ.3.7) of an optimized PVT unit condenser was compared with that of experiment (Fig.3.2) in terms of percentage improvement (Equ. 3.6).

The obtained heat dissipation flux of an optimized model of PVT unit condenser is shown in Fig.4.19. As can be seen from Fig.4.19, the heat dissipation flux of an optimized model improved at all considered conditions. The highest and lowest percentage improvement of 12.5% and 8% were respectively achieved at the conditions of day 3 and day 8 where the ambient and wind speed are (299.5K,0.06m/s) and (301.8K,0.29m/s). The performance of PVT unit condenser improves proportional to the amount of heat dissipation flux. In comparison to the average experimental coefficient of performance (1.86)^[138], the corresponding value at 12.5%

improvement in heat dissipation flux is 2.1. The enhancement in both heat dissipation flux and COP of an optimized model of PVT unit condenser is due to the reduction in distance of both lateral and longitudinal, which in turns increases the thermal concentration on a small area of the unit. With this case, the temperature difference between the PVT unit condenser and night natural cold of the sky will rise and consequently boost the heat transfer mechanisms. This has some implications in perspectives of customers and, time and amount of cooling load production. Instead of ordering the already designed PVT systems, customers can also advise the manufacturers about the proper size of the unit based on their preliminary studies. Besides, the operation of PVT unit condenser can speed up the cooling process and produce cooling load demand within a short time.

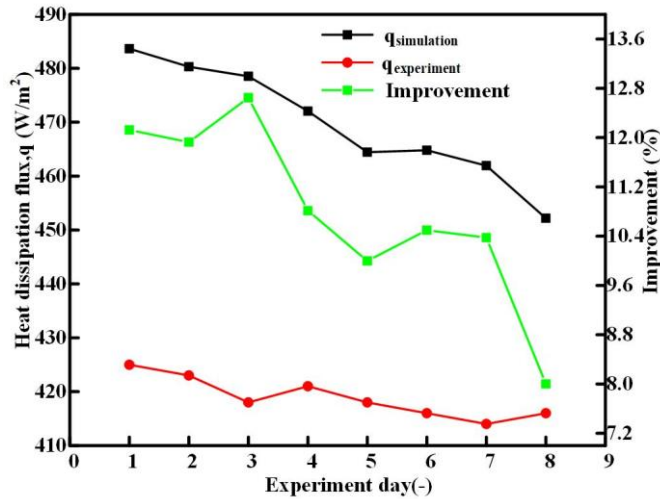


Fig.4.19 Comparison of heat dissipation flux between optimized and experiment

4.3 Summary

In this chapter, a numerical simulation was performed to further analyze the heat transfer characteristics of existing PVT unit condenser. The main conclusions are summarized here below:

Firstly, the optimum dimensions for different parameters (lateral and longitudinal distance, distance between two channels and internal and external diameter) of the PVT unit condenser were determined. Apart from internal and external diameter which increased in dimensions, the rest of PVT unit parameters present a reduction in dimensions, Table.4-1. Reducing the size of PVT unit while fulfilling the same need is profitable in different perspectives; either it lowers the cost or it increases the number of PVT units on the same area.

Secondly, the effect of internal and external factors on the operation the PVT unit condenser was discussed mainly to study the relationship between overall heat transfer characteristics and internal fluid flow, which is taken as a heat source of the unit. Knowledge about effect of internal and external factors would be very helpful tool in predicting the

performance of PVT unit condenser at particular flow condition and weather condition of the day, week, month and year.

Thirdly, under weather conditions of Fig.3.2, the heat dissipation flux of optimized model was computed and compared with that of existing PVT unit condenser. The maximum improvement in heat dissipation flux of about 12.5% was achieved. This can speed up the cooling process and result in obtaining cooling load within a short time.

5. Numerical study of PVT unit condenser with fins and novel channel

In addition to the design and optimization of the PVT unit condenser (Chapter 4), incorporation of both fins to the outer surface of the channel and new channel structure are other options. Fins are extra surfaces added to the surface of heat source (channel) to remove excess heat and maintain a good operation of the equipment. The use of fins has been shown to significantly raise the efficiency of heat sink (see section 2.2.1). On the other hand, new channel structures are being developed and tested with the objective to both optimize the flow uniformity and maximize the flow residence time inside. Achieving flow uniformity reduces the pressure drop and the related compressor power and while increases of residence time increases the heat removal. Therefore, in this chapter, the two models of PVT unit condenser with fins (see section 3.3.2) and PVT unit condenser incorporating a novel channel of a hexagon-grid coupled with fluid channel pattern with the serpentine arrangement (see section 3.3.3) were numerically solved to further propose the methods for condensation heat transfer characteristics enhancement.

5.1 Numerical study of PVT unit condenser with fins

To study the effect of fins on the heat transfer characteristics of PVT unit condenser, four different models of PVT unit condenser with fins of straight rectangular, straight triangular, pin of rectangular and pin of parabolic were considered. The reference case of fin number, dimensions and position are shown in Tab.2-3. First, the temperature distribution in the materials of PVT unit condenser with 3 fins of straight rectangular shape was compared with that of PVT unit condenser without fins. Second, the heat dissipation flux of the PVT unit condenser with fins of four different shapes was discussed to determine the best fin shape. On the basis of the fins-PVT unit condenser with high percentage in heat dissipation flux, the heat dissipation flux of the model was further discussed to determine the number of fins best suit for the current study. At last, the impact of fin size (length and width) and position on the performance of PVT unit with 3 fins of rectangular shape as the best option, was presented and discussed in reference to the other related works. .

5.1.1 Comparative study of PVT unit condenser with and without fins

The comparison between PVT unit condenser with and without fins is carried out considering the model of PVT unit condenser with 3 fins of straight rectangular and in terms of temperature distribution in of materials for each of two PVT unit condenser models with and without fins, shown in Fig.5.1 and Fig.5.2. The contours were produced at constant weather

conditions of 299K, 278.8K and 0.93m/s for ambient temperature, sky temperature and wind speed respectively and constant flow conditions of 350K, 1 and 40.485kg/h for inlet flow temperature, vapor fraction and mass flow rate, respectively. The figures are presented in a such way that the left (a) and right (b) sub-figures illustrate the temperature distribution in PVT unit condenser with 3 fins of straight rectangular shape and PVT unit condenser without fins, respectively. The comparison of temperature distribution at the top surface of the PVT unit condenser with and without fins, is shown in Fig.5.1. As can be observed, the temperature decreases as the distance increases. Due to an exchange of heat between refrigerant inside channel and natural cold of the sky, the amount of heat reaching the top surface will gradually reduce as the flow moves towards the outlet. The maximum attained temperature of the top surface of PVT unit condenser with fins is 9.6K lower than that without fins due to the fact that additional heat is lost through fins by both convection and radiation. The temperature distribution in PVT unit materials is given in Fig.5.2. At the same cross-section area, the temperature gets reduced as the thickness of PVT unit layers' increase. However, in contrary to the previous case, temperature distribution in the PVT unit with fins is a bit higher as compared to that without fins. In fact, the reason behind is that at that particular position, the heat wasn't yet exchanged with the cold of the sky and some amount was still retained in the fins materials. In terms of uniformity, the temperature distribution in the materials of PVT unit condenser with fins is more uniform as compared to the one without fins. The extent at which temperature is distributed in PVT unit condenser materials will determine how excellent heat is transferred. In addition, the heat transfer of the unit will depend on the fin shape, number of fins and fins position.

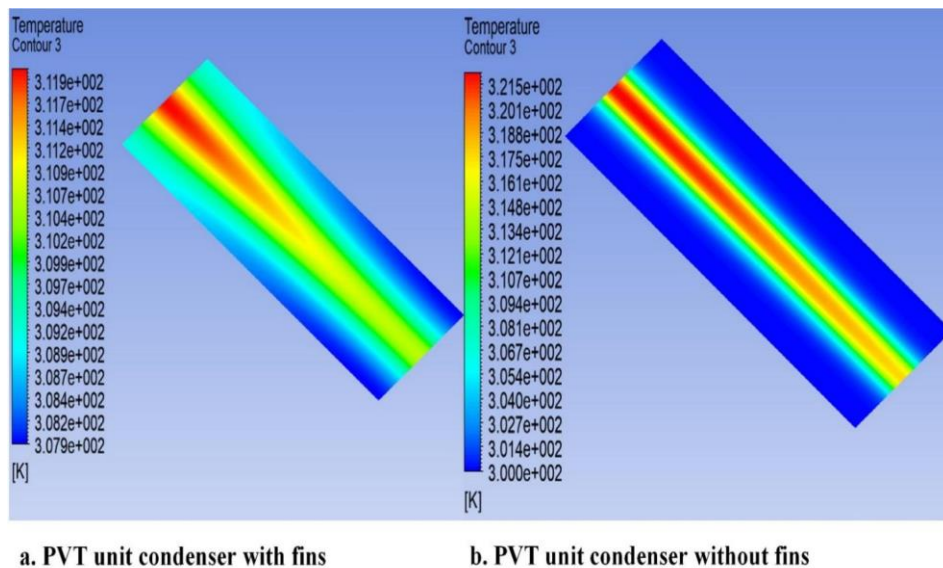


Fig.5.1 Temperature distribution at the top face of PVT unit condenser

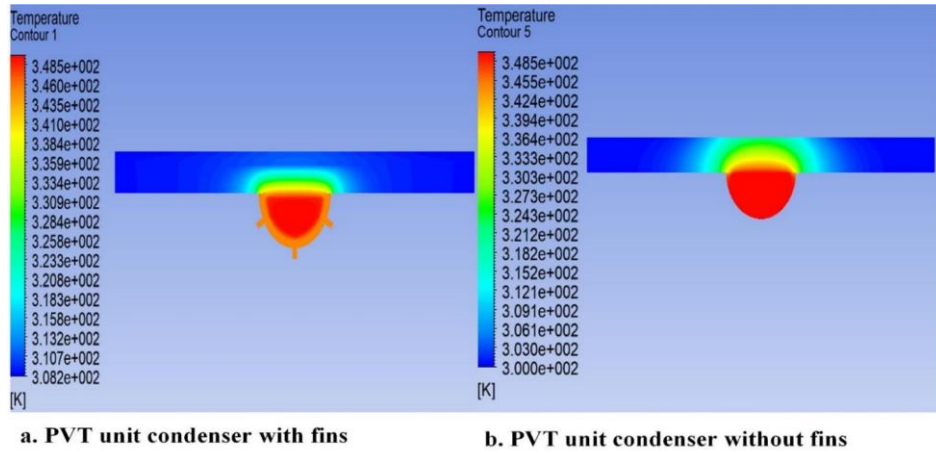


Fig.5.2 Temperature distribution in PVT unit materials at the lateral cross-section (X=50mm)

5.1.2 Heat transfer characteristics of PVT unit condenser with fins of different shapes

The presentation of temperature distribution in fins and PVT unit condenser materials is an important step that helps to understand how heat transfer characteristics are affected at different types of fins. Therefore, in this section, the temperature distribution in 5 fins of straight rectangular shape and its effect on the lateral and longitudinal cross-sections of the PVT unit condenser are respectively shown in Fig. 5.3, Fig.5.4 and Fig.5.5. The contours were obtained at constant weather conditions of 299K, 278.8K and 0.93m/s for ambient temperature, sky temperature and wind speed respectively and constant flow conditions of 350K, 1 and 40.485kg/h for inlet flow temperature, vapor fraction and mass flow rate, respectively. As can be observed from Fig. 5.3, the fins on the bottom of channel dissipate more heat as compared to those on extreme positions. This is mainly due to gravity effect which makes the flow to concentrate on the bottom and as a result, more heat escapes at that particular area. This will in turn affect the temperature in other cross-sections of the PVT unit condenser (Fig.5.4 and Fig.5.5). The fin shape, fin number and fin position will affect the temperature distribution as well as other characteristics of PVT unit condenser like heat dissipation flux and the overall performance of coefficient. Therefore, different fin shapes on the outer surface of the channel will result in different values of heat dissipation flux of the PVT unit condenser.

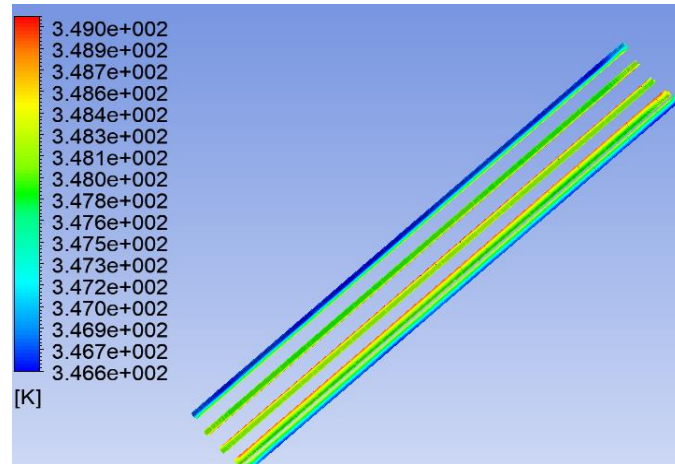


Fig.5.3 Temperature distribution in 5 fins of straight rectangular shape

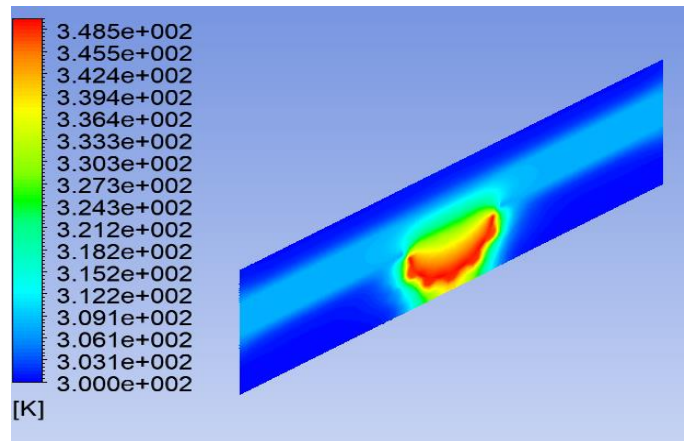


Fig.5.4 Temperature distribution in lateral cross-section materials of PVT unit condenser, at X=135mm

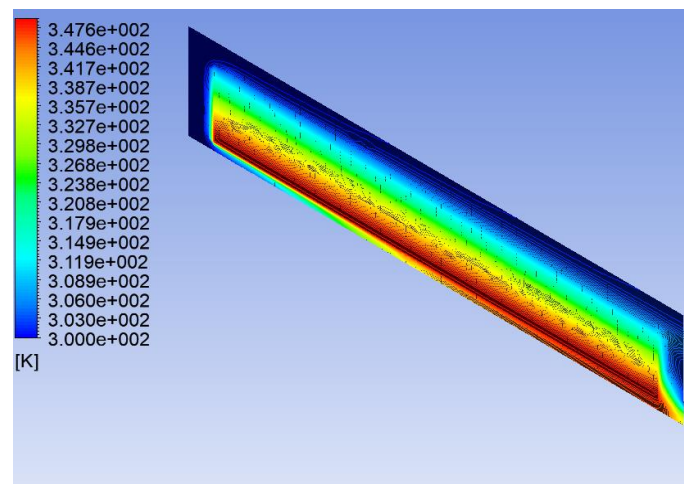


Fig.5.5 Temperature distribution in longitudinal cross-section materials of PVT unit condenser, at Z=16mm

The comparative study of heat dissipation flux of PVT unit condenser with 5 fins of both straight rectangular and triangular shape, and 65 fins of both pin rectangular and parabolic at the outer surface of channel was performed at constant values of 40.485kg/h for inlet mass flow rate, 350K for inlet flow temperature and 1 for vapor fraction, under weather conditions of Fig.3.2 with the objective to select fin shape best dissipates heat. The heat dissipation flux (Equ. 3.8) of PVT unit condenser with fin of different shapes was obtained and compared with that of experiment as presented in Fig.5.6. As can be observed from Fig.5.6, the maximum improvement in heat dissipation flux was obtained at the conditions of day 1 where the values of ambient and sky temperature are the lowest. This can be explained in a way that, in principles, the heat moves from the area with high temperature to the area with low temperature and the bigger the difference in temperature between the two areas, the more the heat transfer enhances. In the current study, the heat is released to ambient environment from the refrigerant inside channel. Increasing/decreasing the ambient and sky temperature, will reduce/rise the temperature difference between the two areas (i.e. inside channel and ambient environment) and as a results, the heat dissipation flux will be lowered/increased. The heat dissipation flux of PVT unit with fins of straight rectangular shape at the surface of channel, presents a highest amount of heat dissipation flux at all conditions as compared to the rest cases of fins.

Even though the same number and position, a constant area of the straight rectangular fin from the channel base to the tip end makes it a better conductor of heat. This result is in accordance with the study of ^[141] whereby among three periodically expanded grooves used to cool PVT unit evaporator, rectangular column-type groove was determined to be the strongest in both flow distribution and heat transfer. Meanwhile the PVT unit system incorporating fins of triangular shape, can be a second option to dissipate heat. The rest of two PVT units; with fins of pin parabolic and pin of rectangular shapes dissipate almost the same amount of heat and become inefficient after day 4. The more densely of fins on the channel will increase the velocity of flow and cause a large amount of fluid to flow out of channel without exchanging heat with the natural cold of the sky. This will in turns impact the temperature distribution as well as decrease the heat transfer efficiency. Besides, the contact surface between outer surface of channel and fins is another possible fact which would alter flow behavior in some positions and cause a big pressure to drop in inside channel.

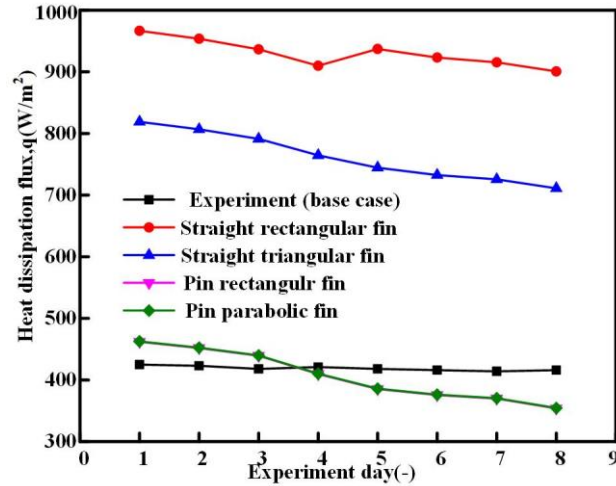


Fig.5.6 Comparison in terms of heat dissipation flux of PVT unit condenser with and without fins

5.2 Characteristics analysis at different fins number and fin parameters

5.2.1 Impact of fins number on heat transfer characteristics of PVT unit condenser

To determine the number of fins best suit for the study, models of PVT unit condenser with fins of both straight rectangular and triangular shape were solved at constant inlet mass flow rate of 40.485kg/h, inlet flow temperature of 350K and vapor fraction of 1, under weather conditions of Fig.3.2. In order not to overfit or underfit fins on the either side of a fixed one (270°), 5 and 3 fins were used in each case considering two fins on either side and one fin on each side, respectively. The position of fins is illustrated in Tab.2-3. The results were obtained and discussed in terms of heat dissipation flux (Equ. 3.8) and overall fin efficiency (Equ.3.1). As can be observed from Fig.5.7 and Fig.5.8, the heat dissipation flux slightly decreases from day 1 to day 8 with PVT unit with 3 fins always dissipates more heat than the system with 5 fins. The reason behind was that attaching 5 fins to the outer surface made the heat to be trapped inside pipe-fin system and there was no enough space for it to escape. This confined heat would increase the refrigerant vapors inside channel, which in turns increases the pressure drop. A higher pressure drop will significantly affect both the temperature distribution and the overall heat transfer in PVT unit condenser. An exception was notified to day 5 where a sudden increase in heat dissipation flux occurred, possibly because of high average wind speed. Meanwhile, the maximum overall fin efficiency was obtained at the conditions of day 1 for PVT unit with fins of straight rectangular (Fig.5.7) and at conditions of days 3 for PVT unit with fins of straight triangular profile (Fig.5.8). The trending curves of overall fin efficiency for PVT unit with both 3 and 5 fins show an abrupt variation at conditions of all the days and this possibly caused by

non-uniform area of the triangular fin, from the base of micro-channel to its tip end. Overall, comparing the results of the two figures, the PVT unit condenser with 3 fins of straight rectangular shape presents an excellent performance and needs to be investigated further in the next section.

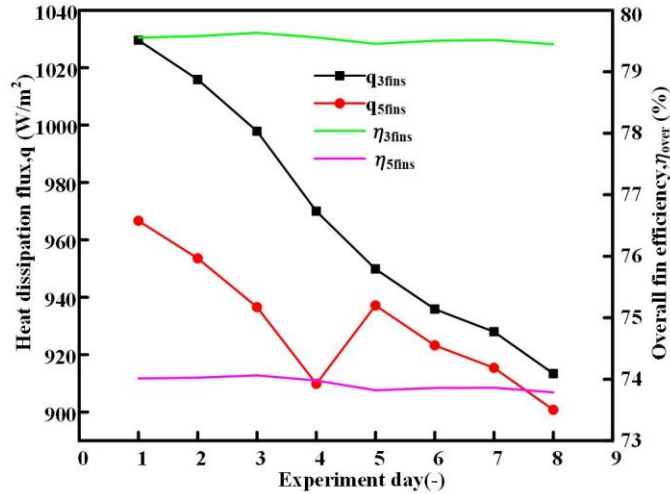


Fig.5.7 PVT unit condenser with 3 and 5 fins of straight rectangular profile

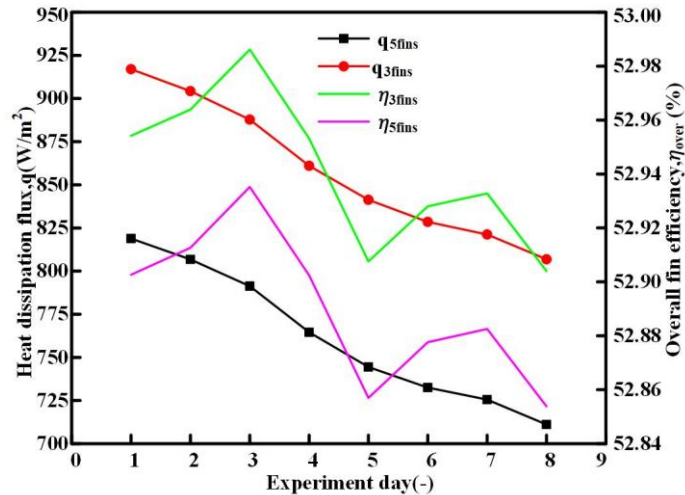


Fig.5.8 PVT unit condenser with 3 and 5 fins of straight triangular profile

5.2.2 Effect of fin size and position on the operation of PVT unit condenser

The PVT unit condenser with 3 fins of straight rectangular shape was studied in perspective of heat dissipation flux (q), overall fin efficiency (η_{over}), coefficient of performance (COP) and pressure drop (Δp) under the constant weather conditions of day 1, at ambient temperature of 299K, sky temperature of 278.8K and wind speed of 0.93m/s. Furthermore, the simulation was performed considering different ranges of fin parameters. Width and length of fin were varied from 0.2mm to 0.7mm, and while the position of the two fins was changed from 195° to 255° and 345° to 285° for fin at the left side and at the right side of the fixed one (at

270°), respectively. The position of the two fins was increased/decreased by an equal step size of 10°. The results obtained as a function of changing fin length, fin width and fin position are presented in Fig.5.9, Fig.5.10 and Fig.5.11, respectively. Increasing fin length results in a parabolic reduction of COP and heat dissipation flux, and while the overall fin efficiency decreases (Fig.5.9). This can be explained in way that reducing the heat removal from the refrigerant inside channel due to an increase in fin length delays the process of cooling load formation and consequently the system refrigeration coefficient of performance (COP) is lowered. Further the overall fin efficiency depends on the amount of heat conduction through the material of fin. That is to mean that high heat would alter some properties of fin material and causes reduction of its overall efficiency. The system COP is inversely proportional to the compressor power and the higher the compressor power, the lower the COP. The higher compressor power is required to overcome a big pressure drop in micro-channel. As can be observed from Fig.5.9, pressure drop increases with increase in fin length. However, increase in length by more than 0.6mm would result in reducing pressure drop.

Meanwhile, increasing fin width will increase the overall fin efficiency and while a decreasing trend is observed in both COP and heat dissipation flux (Fig.5.10). In contrary to the previous case of length change (Fig.5.9), the lowest overall fin and highest COP and heat dissipation flux are achieved when increase fin width by 0.3mm (Fig.5.10). The highest pressure drop of 60kPa was reached when increased fin width by 0.7mm. On other hand, placing fins at different positions angle affect the performance of PVT unit condenser, as shown in Fig.5.11. Increasing and decreasing the position angle of first and third fin towards a fixed one (270°), lowers the overall fin efficiency and while the rest of results (COP, heat dissipation flux and pressure drop) increase. Due to gravity effect, the refrigerant flow in channel will be more concentrated at the bottom and therefore, positioning the first and third fin 15° on either side of a fixed one (270°) will result in more heat removal and COP. This will in turns increase the turbulences in micro-channel, which would incur a high pressure drop. The high pressure drop on the other hand will require a high compressor power. From Fig.5.11, the optimum angle of the two fins (first and third) would be found at (201° and 339°), with heat dissipation flux, COP, overall fin efficiency and pressure drop are respectively 1010W/m², 4.96, 79.613%, 85.2kPa.

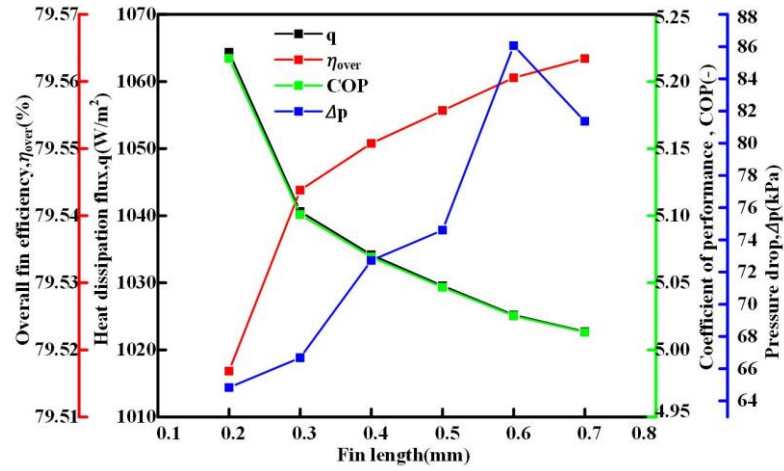


Fig.5.9 Effect of fin length on heat dissipation, overall fins efficiency, pressure drop and performance

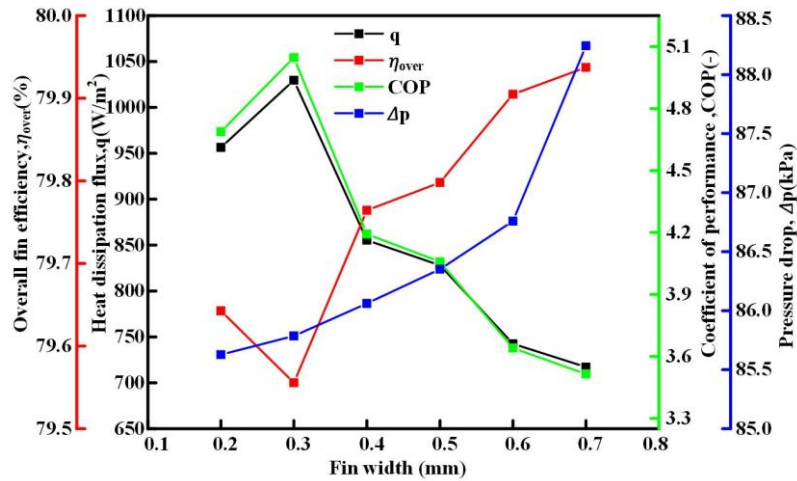


Fig.5.10 Effect of fin width on heat dissipation, overall fins efficiency, pressure drop and performance

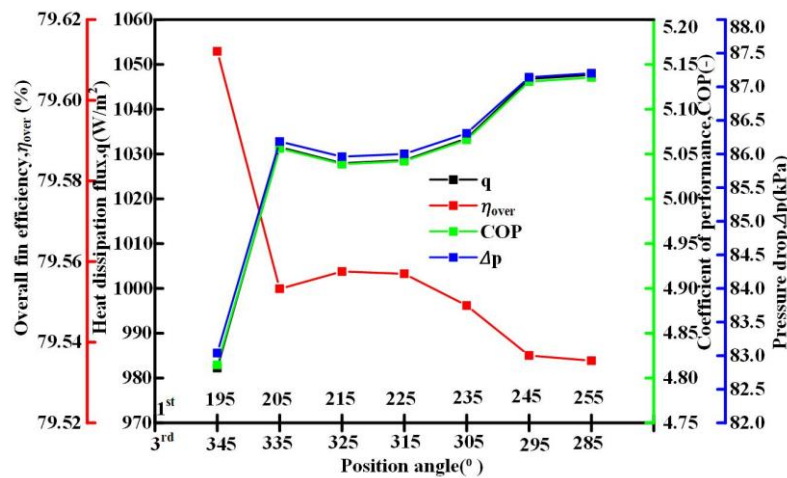


Fig.5.11 Effect of fins positions on heat dissipation flux (q), overall fins efficiency, pressure drop and performance

5.2.3 Optimization process of PVT unit condenser with fins

In this section, the step by step procedure (see sections 5.1.1 to 5.1.4) to arrive at the optimized model of PVT unit condenser with fins as well as the summary of obtained results, are provided. Initially, the comparison between PVT unit condenser with 3 fins of straight rectangular shape and PVT unit condenser without was made in terms of temperature distribution in a top surface and in cross-sections area at $X=50\text{mm}$ (see section 5.1.1). It was found that the temperature of top surface of PVT unit condenser with fins is 9.6K less than that of PVT unit condenser without fins. In addition, a good temperature uniformity was achieved in the PVT unit condenser with fins, which confirms a better heat transfer. Next, four models PVT unit condenser with fins of 5 straight rectangular, 5 straight triangular, 65 pin of rectangular profile and 65 pin of parabolic profile were solved to determine fin shape with higher improvement in heat dissipation flux. The selection was made in reference to the heat dissipation flux obtained from experimental study about existing PVT unit condenser. The results revealed that a higher heat dissipation flux achieved in PVT unit condenser with 5 fins of straight rectangular shape followed by PVT unit condenser with 5 fins of straight triangular shape and while the two last models of PVT unit condenser with 65 fins of both 65 pin of rectangular profile and 65 pin of parabolic profile dissipated the same amount of heat. On the basis of PVT unit condenser with fins of both rectangular and triangular shape, the two models were solved considering 3 and 5 fins in order to select fin number best suit for the study. The selection was performed based on the overall fin efficient and heat dissipation flux attained in each case. The maximum values of 79.57% and $1036\text{W}/\text{m}^2$ were achieved from PVT unit condenser with 3 of straight rectangular shape and while 52.98% and $924\text{W}/\text{m}^2$ were obtained from PVT unit condenser with 3 of straight triangular shape.

Last, the impact of fin parameters (length and width) and position on the PVT unit condenser with 3 fins of straight rectangular shape was investigated in terms of heat dissipation flux (q), coefficient of performance (COP), pressure drop (Δp) and overall fin efficient (η). PVT unit condenser with 3 fins of straight rectangular shape and with 2 fins placed 15° on the left and right side of a fixed one at 270° was selected as a best option to enhance the condensation heat transfer characteristics of PVT unit condenser. In addition, for the considered range of both fin length and width (0.2mm - 0.7mm), the optimum fin length and fin width were respectively obtained at 0.2mm and 0.3mm . Overall, as can be observed from Table.5-1, the achieved COP as a result of changing fin length, fin width and fin position is proportional to the heat dissipation flux and inversely proportional to both pressure drop and overall fin efficient. In this regards, a maximum COP of 5.079 was obtained at a maximum heat dissipation flux of

1036.107W/m² and lowest values of 79.548% and 74.376kPa for overall fin efficient and pressure drop, respectively.

Tab.5-1 Maximum obtained results from PVT unit condenser with 3 fins of straight rectangular shape, at different fin parameters change

Items	Angle	width	length
q (W/m ²)	1028.325	854.834	1036.107
COP(-)	5.041	4.190	5.079
Δp (kPa)	85.977	86.471	74.376
η(%)	79.557	79.767	79.548

5.3 PVT unit condenser incorporating a novel channel

The aim of this section is to propose alternative channel structure which can be used in PVT unit condenser and replace the already existing one of Fig.4.1 (see section 4.1). To achieve the objective, a model of PVT unit condenser incorporating a novel channel of hexagon-grid coupled with fluid channel pattern with the serpentine arrangement was numerically solved in ANSYS Fluent, considering a validated model developed from section 3.3.3. A Volume of Fraction (VOF) and k-ε models were respectively used to model two phase refrigerant of R134a and to handle turbulences occurred during phase change at different temperatures. At first, the contours of vapor fraction in the channels were discussed at constant operating conditions of weather and flow. Next, the results of heat dissipation flux, coefficient of performance and average vapor fraction were obtained and discussed at different operating conditions of flow and weather.

5.3.1 Distribution of vapor fraction in novel channel

The contour of vapor volume fraction (Fig.5.12) was obtained at constant values of 100W/m² for long-wave radiation intensity, 298K for ambient temperature, 0m/s for wind speed, 320K for inlet flow temperature and 1 for inlet vapor fraction. A refrigerant (R134a) condensates along the way as it releases heat to the ambient environment. In the process, the amount of R13a liquid increases slightly at each position of the channel. As can be observed from Fig.5.12, the vapor volume fraction leaving the outlet of channel is nearly 0.18 lower than that at the inlet. The distribution patterns as well as difference in vapor volume fraction between the inlet and the outlet of the PVT unit condenser incorporating a hexagon-grid coupled with fluid channel pattern with the serpentine arrangement will vary depending on the operating conditions of weather and flow. In addition, it will have effect on the heat characteristics and the overall performance.

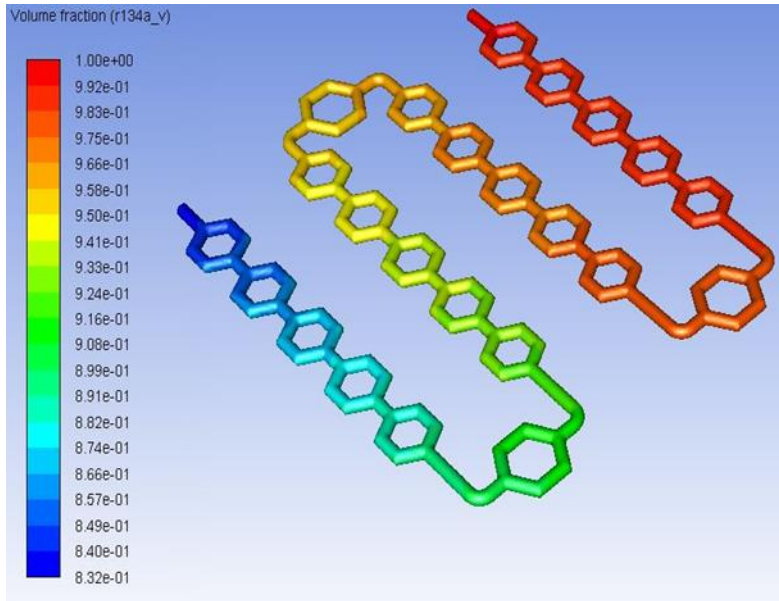


Fig.5.12 Variation of vapor volume fraction in the channel

5.3.2 Impact of change in flow conditions

The effect of inlet mass flow rate and inlet flow temperature on the fluid average vapor fraction, heat dissipation flux and coefficient of performance of the PVT unit condenser was determined and respectively presented in Fig.5.13 and Fig.5.14, considering constant radiation intensity of 100W/m^2 , vapor fraction of 1, ambient temperature of 298K and wind velocity of 0m/s . As can be observed from Fig.5.13, increasing the inlet mass flow by a constant step size of 0.18kg/h , affects the heat dissipation flux to change inversely proportional to the COP. This can happen due to 2 reasons; 1) at a given inlet mass flow rate, a large amount of heat can be released but COP becomes low due to a big pressure drop in channel and 2) alternatively, COP can be increased due to low resistance of flow offered by the mass flow rate but with less heat emitted to the ambient environment, possibly because of complexity of channels structure. On the other hand, the effect of inlet flow temperature is illustrated in Fig.5.14. During daytime, the thermal energy produced from PVT unit evaporator might be at higher or lower temperature depending on the available solar intensity. This has an effect on the operation of the PVT unit condenser whereby the refrigerant flow might enter the channel with higher/lower value of temperature and vapor fraction. From Fig.5.14, the trending lines of heat dissipation flux, average vapor fraction and COP obtained when changing the inlet flow temperature from $320\text{-}330\text{K}$ are quite similar. At given inlet flow temperature, the heat dissipation flux, average vapor fraction and COP may drop or rise because the value of inlet temperature is far away, closer and matches to the inlet vapor fraction of 1. Unlike the case of change in mass flow rate where

highest values in both heat dissipation flux (400W/m^2) and COP (4.67) were respectively achieved at 0.72kg/h and 1.26kg/h , the maximum values in both heat dissipation flux of 550W/m^2 and COP of 4.65 were respectively determined at inlet flow temperature of 330K and 322K , Fig.5.14.

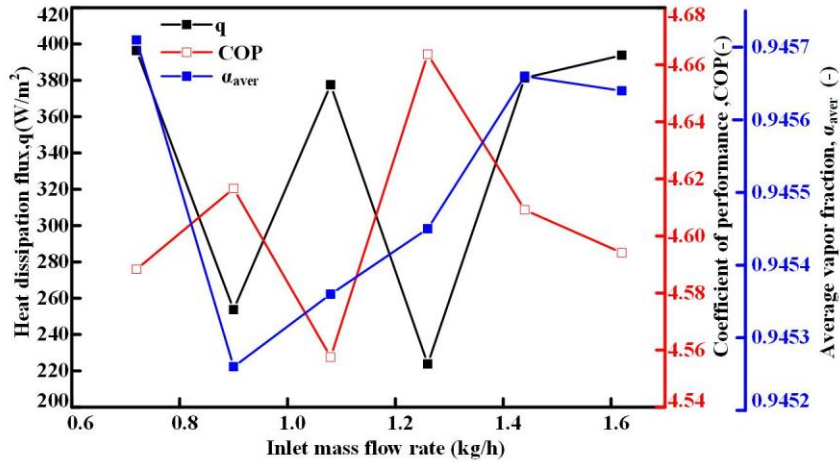


Fig.5.13 Impact of mass flow rate on the heat dissipation flux (q), average vapor fraction (α_{aver}) and refrigeration coefficient of performance (COP) of PVT condenser

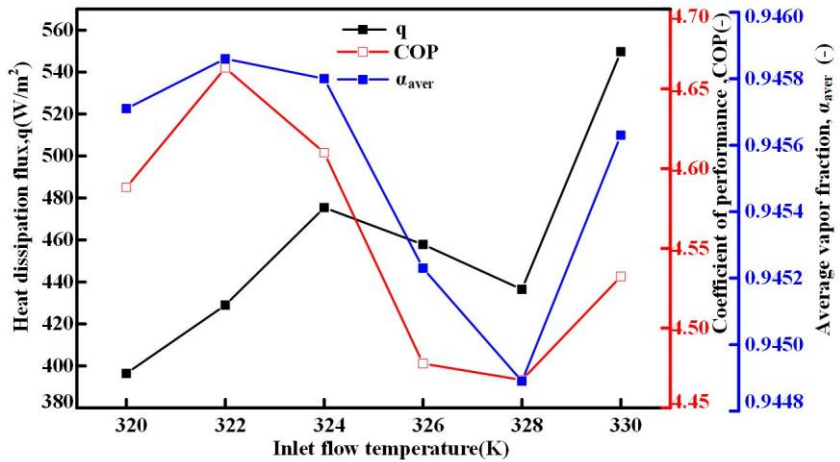


Fig.5.14 Impact of flow temperature on the heat dissipation flux (q), average vapor fraction (α_{aver}) and refrigeration coefficient of performance (COP) of PVT condenser

5.3.3 Impact of change in weather conditions

In the meantime, the impact of change in both ambient temperature and long-wave radiation on the fluid average vapor fraction, heat dissipation flux and coefficient of performance of PVT unit condenser was evaluated at constant inlet conditions of 320K for temperature, 1 for vapor fraction and 0.72kg/h for mass flow rate and the obtained results are respectively presented in Fig.5.15 and Fig.5.16. As can be seen from Fig.5.15 and Fig.5.16, incrementing ambient temperature in the range 298K - 313K and long-wave radiation in

100W/m²-600 W/m² has the same effect on the operation of PVT unit condenser. The coefficient of performance decreases and while average vapor fraction and heat dissipation flux increase. The fact is that the two weather conditions (ambient temperature and long-wave radiation), boost radiation heat transfer at the outer surfaces of the PVT unit condenser and as a result, the heat dissipation flux increases. However, due to the reduction in temperature difference between the flow inside channels and ambient environment, the amount of heat released from fluid decreases and consequently increases the average vapor volume fraction. For the considered ranges of ambient temperature and long-wave radiation, the maximum COP of 4.7 and 4.558 were respectively obtained at the lowest values of 298K for ambient and 100W/m² for long-wave radiation.

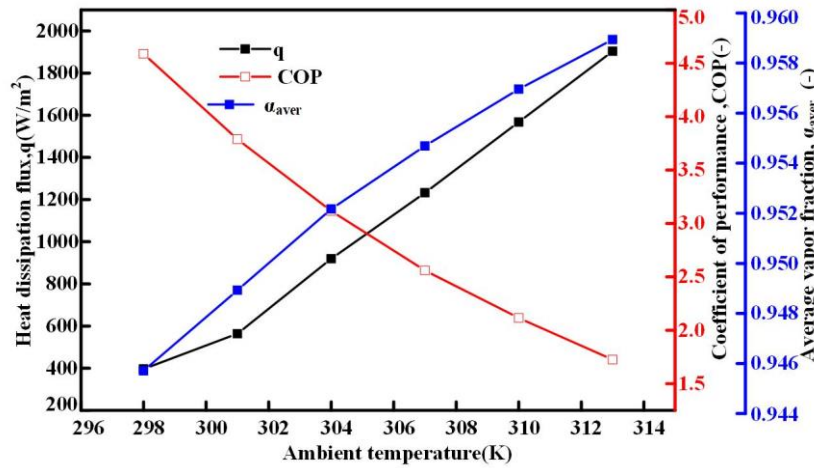


Fig.5.15 Impact of ambient temperature on the heat dissipation flux (q), average vapor fraction (α_{aver}) and refrigeration coefficient of performance (COP) of PVT condenser

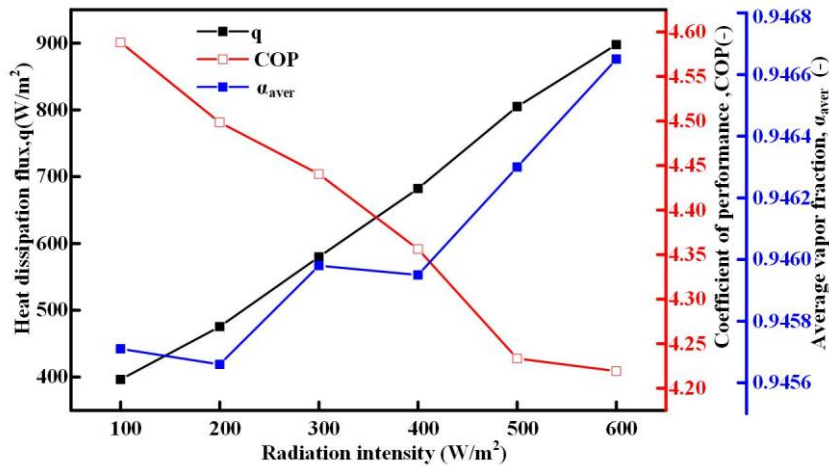


Fig.5.16 Impact of radiation intensity on the heat dissipation flux(q), average vapor fraction (α_{aver}) and refrigeration coefficient of performance (COP) of PVT condenser

5.4 Summary

The models of PVT unit condenser with fins at the outer surface of channel and PVT unit condenser incorporating a novel channel were solved in order to propose new methods for condensation heat transfer characteristics enhancement.

First, the results were analyzed in terms of temperature distribution and heat dissipation flux considering 4 fins of different shapes. The main purpose was to determine the improvement in those two aforementioned heat transfer characteristics as compared to the corresponding results of PVT unit condenser without fins.

Second, on the basis of PVT unit condenser model with fins of both straight rectangular and triangular, the heat dissipation flux and overall fin efficiency were discussed at different fins number to select number of fins best suit for the study.

Third, the effect of fin size and fin position on the coefficient of performance, heat dissipation flux, overall fin efficient and pressure drop was discussed based on the best case model of PVT unit condenser with 3 fins of straight rectangular shape. Overall, attaching fins to the outer surface of channel improved both heat dissipation flux and performance of the PVT unit condenser up to 5.079. With this improvement, the cooling process can be speeded up and results in obtaining the cooling load demand within a short time.

Fourth, incorporation of novel channel of hexagon-grid coupled with fluid channel pattern with the serpentine arrangement in the absorber of PVT unit condenser resulted in a maximum average COP of about 4.66, which is 2.58 and 0.474 higher than that achieved from existing PVT unit condenser and less than that obtained from PVT unit condenser with fins, respectively. This implies that in addition to the above mentioned strategies, incorporation of hexagon-grid coupled with fluid channel pattern with the serpentine arrangement has also a great potential in enhancing the overall COP of PVT unit condenser.

6. Numerical simulation of nanofluid-based PVT unit for cooling

With research development of fluids, the thermo-physical properties of water can be enhanced and used in the channel of PVT unit to further improve its heat transfer mechanisms (see sections 1.2.4). This is realized by adding solid nanoparticles to the base fluid of water (see section 2.2.2). In this chapter, the effect of nanofluids on the heat transfer characteristics and overall performance of the PVT unit operating under night natural cold of the sky to produce cooling load demand is analyzed. Unlike the PVT unit condenser models of Chapter 4 and Chapter 5 where refrigerants (R407C and R134a) were used in the channel, two nano-fluids of water- Al_3O_2 and water-Ag are proposed as fluids medium in the channel of PVT unit model with nano-fluid (see section 3.3.4). Moreover, this kind of unit works in a reverse manner with the conventional one (Fig.1.2) with pump being employed to keep the nanofluid flow in the circulation loop. By changing the direction, the of flow control and bypass valves, the heat of thermal energy of tank stored at daytime becomes the heat source and while flat plate collector/PVT unit becomes a heat sink (Fig.1.1). During simulation in ANSYS Fluent software, the heat exchange takes place similar to that of Fig.1.12 for cooling process by natural night cold (see section 1.3). The heat of nano-fluids (water- Al_3O_2 and water-Ag) in channels of flat plate collector/PVT unit represents the heat storage capacity and while different layers' materials on top of the channel (Fig.1.3) represent internal partitions, walls and upper part.

6.1 Description and contours inside of nanofluid-based-PVT unit

The details description of obtaining solution of nano-fluid based PVT unit model as well as the obtained results are presented in this section. The current model of PVT unit was solved assuming that the flow of nano-fluid inside pipe is laminar, incompressible and single phase. In addition, the unit was considered to operate in a clear sky of the night, under constant operating conditions of 14kg/h, 320K, 0m/s and 298K for, inlet mass flow rate, inlet flow temperature, wind speed and ambient temperature, respectively. A very low long-wave radiation intensity of $100\text{W}/\text{m}^2$ was taken into account to reflect the natural cold of the sky and applied at the glass top to exchange heat with the flowing fluid inside pipe, by conduction through absorber and different layers' materials on top. To solve the related model mathematical equations, steady state was selected over transient.

At the same boundary and operating conditions, the contours of temperature and velocity at the pipe outlet is respectively shown in Fig.6.1 and Fig.6.2. Two subfigures are presented in

each Figure to show the contours of the two stated flow quantities when two fluids medium of a. Al_3O_2 -water and b. Ag-water are employed inside pipe, to release heat to the ambient environment. In addition, 5% nanoparticles were used to form the two nanofluids (Al_3O_2 -water and Ag-water). In contrary to the outlet temperature contour of ^[157] where the temperature of the outer pipe is higher than that of flow inside, the inside pipe flow temperature for the current model of PVT unit is higher than that of pipe outer surface. As previously mentioned, the heat of solar intensity is absorbed by the fluid inside pipe in case the PVT unit is operated as during daytime and while during nighttime, the heat is released to the ambient from fluid flow inside pipe. Meanwhile, the outlet velocity distribution is also influenced similar to that of temperature distribution. For better performance of the PVT unit, the difference in temperature between inlet and outlet should be as higher as possible.

Depending on the type of fluid medium used, various fluids can result in different outlets temperature. As can be observed from Fig.6.1, the outlet temperature of water- Al_3O_2 /PVT unit is a little bit higher as compared to the outlet temperature of Ag-water/PVT unit. The fact is that the thermal conductivity of these fluids differ and the higher the thermal conductivity, the lower the outlet temperature. In fact, upon entering the pipe, fluid with higher thermal conductivity will release a huge amount of heat along the way and leaves when the temperature is relatively low. On the other hand, the same distribution patterns as of outlet temperature will be observed for outlet velocity, Fig.6.2. At the same inlet flow velocity, a low outlet velocity will be attained in case of Ag-water as compared to the velocity of Al_3O_2 -water. This occurs due to the fact that fluid with higher thermal conductivity will exchange a huge amount of heat and cause a big pressure to drop inside pipe.

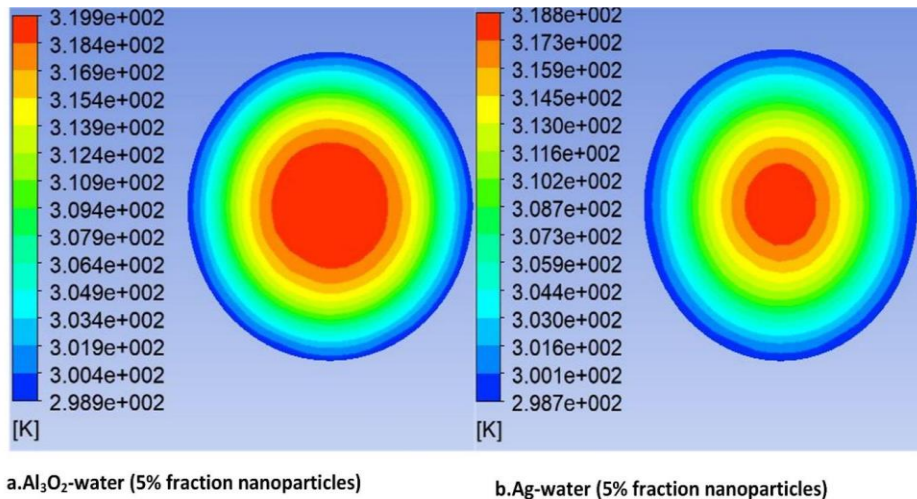


Fig.6.1 Temperature distribution at the pipe outlet of the PVT unit with a. Al_3O_2 -water and b. Ag-water used as fluids medium

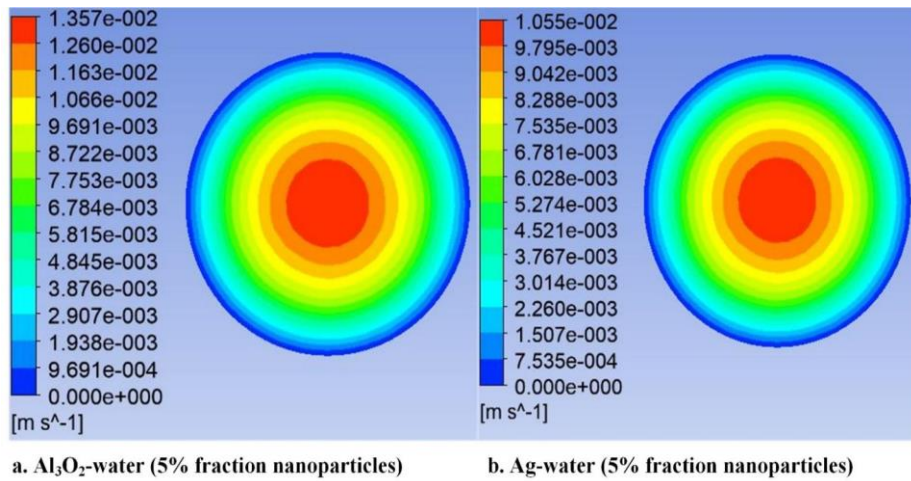


Fig.6.2 Velocity distribution at the pipe outlet of the PVT unit with a. Al_3O_2 -water and b. Ag-water used as fluids medium

The temperature and velocity distributions are effected due to some other reasons. Among them, there are convection heat transfer between fluid domain and pipe wall, and the disorders of fluid inside pipe. The Nusselt is a dimensionless number which determines the extent of convection heat transfer mode inside fluid and it is the ratio of convective to conductive heat transfer across the fluid boundary wall. This implies that the more the Nusselt number, the more heat transfer is due to convection and vice versa. Meanwhile, the fluid disorders inside pipe is measured in terms of entropy generation. These two; Nusselt number and entropy will adversary affect the outlet temperature and the overall performance. In addition, the variation of Nusselt number, entropy, outlet temperature and performance in turns depend on some other factors such as nanoparticle fractions, inlet flow and weather conditions. The three Nusselt number (Nu), entropy generation (ΔS) and outlet temperature (T_{out}) were directly obtained from ANSYS Fluent after simulation round and coefficient of performance (COP) was determined from Equ. 3.14.

6.2 Effect of nanoparticles fraction on the PVT unit cooling

In addition to the type of nanofluid, the % fraction of nanoparticles added to the base fluid of water will affect the performance characteristics of the PVT unit. In Fig.6.3 and Fig.6.4, increment of nanoparticles fraction of Al_3O_2 and Ag from 0 to 5% reduces Nusselt number, entropy and outlet temperature and while the COP increases. Increasing the amount of nanoparticles in water, will enhance the thermal conductivity of nanofluid and as a result, a big part of heat will be transferred to the ambient environment by conduction mode, through PVT unit materials. However, the more densely of nanoparticles in water will somehow stabilize the flow movement and consequently reduces the entropy generation. The low entropy will reduce

pressure drop and its related power. On the other hand, continuous removal of heat from fluid, will cause the flow to reach the outlet of the pipe with low temperature.

The role of operating PVT unit under cooling condition is to produce cooling load from unused solar thermal energy. The performance of the unit is enhanced when a huge amount of heat is removed at low pump power. In this regards, the maximum COP of 2.72 and 2.98 were respectively achieved when 5% of nanoparticles for Al_3O_2 (Fig.6.3) and Ag (Fig.6.4) are immersed in water. The use of Ag-water produces COP which is 0.26 higher than that of Al_3O_2 -water due to its thermal conductivity which is a little bit higher than that of Al_3O_2 -water. Except the COP of Ag-water which is higher than that of Al_3O_2 -water at all nanoparticle fractions, the values of the rests of parameters (Nu, ΔS and T_{out}) are obtained a little bit lower. Even though the study of other flow parameters is required to analyze the behaviors of fluid inside pipe, overall COP of the PVT unit is the most desired result. In this case of nanoparticles addition, a better COP was obtained at higher nanoparticles fraction. However, this may cause deposition which would after some time block the pipe if no regular cleaning is done. Considering extra costs which would incur in cleaning, it will be up to the operator to judge whether using a higher fraction nanoparticle will be more beneficial than using lower fraction nanoparticles and vice versa.

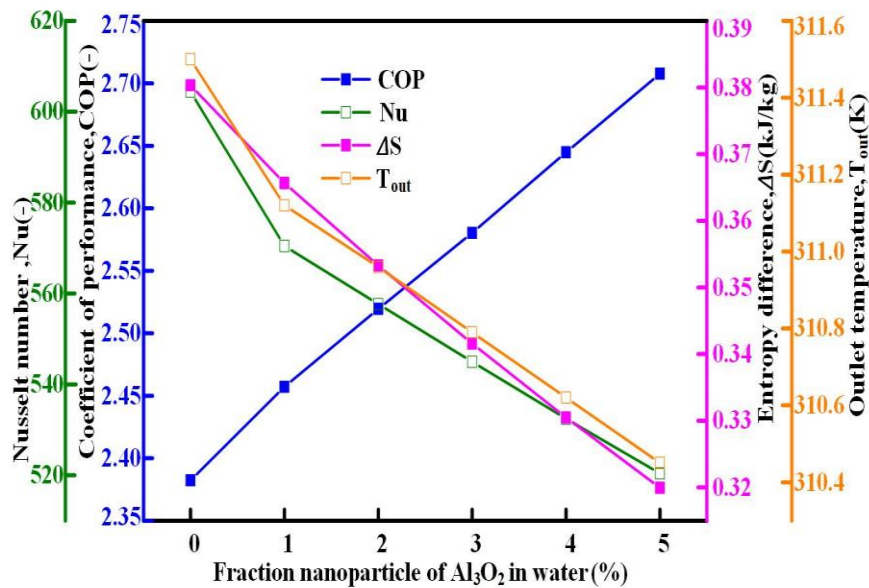


Fig.6.3 Effect of incrementing nanoparticles fraction of Al_3O_2 in the Al_3O_2 -water through the pipe of the PVT unit

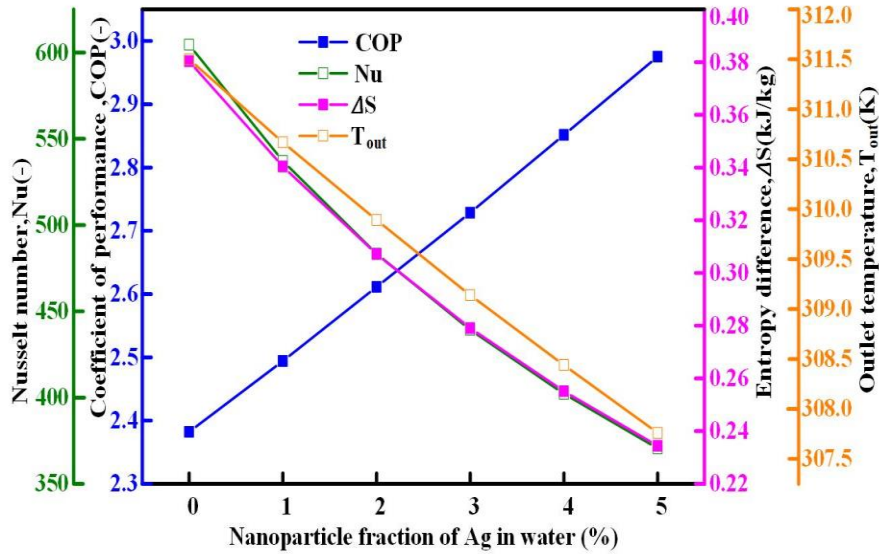


Fig.6.4 Effect of incrementing nanoparticles fraction of Ag in the Ag-water through the pipe of the PVT unit

6.3 Effect of flow conditions on the PVT unit cooling

The flow conditions considered in this section are inlet mass flow and inlet flow temperature. The effect of different mass flow rates on the flow behaviors and overall COP of Al_3O_2 -water/Ag-water-PVT unit is presented in Fig.6.5 and Fig.6.6. For both nanofluids (Al_3O_2 -water and Ag-water) the mass flow rate was increased from 8.4kg/h to 14.4kg/h. Increment of mass flow rate by 1kg/h, will increase all flow parameters (Nu, ΔS and T_{out}) and overall COP. Higher mass flow rate will enhance convection heat transfers inside fluid as well the entropy generation. The higher entropy generation will in turns increase the pressure drop in pipe, which is an indicator of bad temperature uniformity in the PVT unit materials. Due to this, fluid inside pipe will not be fully exchange its heat with the natural cold of the sky and consequently a high flow temperature will reach the pipe outlet.

In normal cases, a higher COP is achieved at both low outlet temperature and entropy generation. However, it is not the case when increasing the mass flow rate of nanofluids (Al_3O_2 -water (Fig.6.5) and Ag-water (Fig.6.6)) at the inlet of pipe of the PVT unit, where COP increases with increase in the two flow parameters (T_{out} and ΔS). This proportionality occurs possibly because the amount of heat transfer due to convection inside fluid is big enough to recover all the losses. Meanwhile, by utilizing two nanofluids (Al_3O_2 -water and Ag-water) with different thermal conductivities, low values in flow parameters (T_{out} , ΔS and Nu) and higher COP will be achieved at nanofluid with higher thermal conductivity. In this circumstance, Ag-water/PVT unit resulted in higher COP and low values in flow parameters (T_{out} , ΔS and Nu)

at all considered mass flow rates, as compared to the Al_3O_2 -water/PVT unit. Using a higher mass flow rate nanofluid not only can increase the overall performance but it can also alleviate deposition problem, by forcing most of nanoparticles to flow out of pipe.

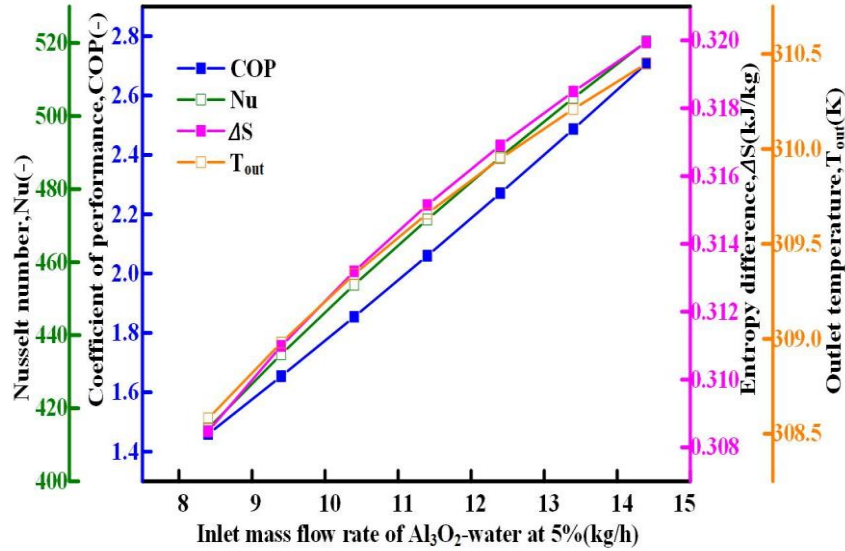


Fig.6.5 Effect of applying different mass flow rates of Al_3O_2 -water at the pipe inlet of the PVT unit

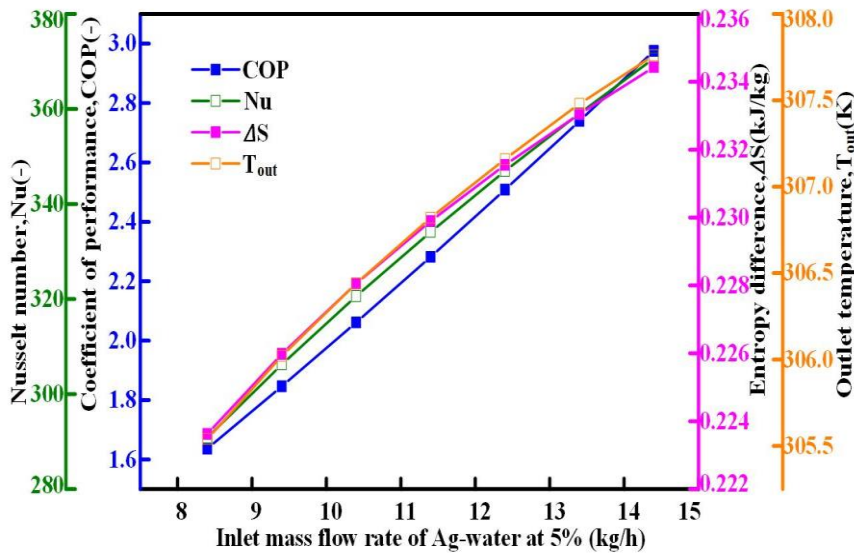


Fig.6.6 Effect of applying different mass flow rates of Ag-water at the pipe inlet of the PVT unit

The impact of inlet flow temperature is discussed considering Al_3O_2 -water and Ag-water to act as fluids medium inside pipe of the PVT unit and on the basis of the results presented in Fig.6.7 and Fig.6.8, respectively. In contrary to the previous cases of nanoparticles fraction and mass flow rate change, increasing inlet flow temperature will increase Nu, ΔS and T_{out} and while COP reduce. At the same operating conditions, increasing the inlet flow temperature will

rise both the actual entropy generation and the outlet temperature. As extra heat is being supplied, the amount of heat which would be occurred due to convection inside fluid will also increase. In addition, as the main role of the PVT unit is to convert unused thermal energy into cooling load by releasing heat of the fluid to the ambient environment, the extra heat will be kept in circulation loop and cause the COP to drop. By comparing the two PVT units with Al_3O_2 -water and Ag-water based PVT unit, the obtained values of Nu, ΔS and T_{out} are higher in Al_3O_2 -water based PVT than those achieved in Ag-water based PVT unit. Due to low thermal conductivity of Al_3O_2 -water as compared to Ag-water, the flow velocity will increase and consequently increases and reduces the convection inside fluid and the time for heat to exchange between fluid and natural cold of the sky, respectively. The fast movement of flow inside pipe will in turns result in less heat removal and thereby affecting the flow to reach the outlet with higher temperature. For optimum operation of the PVT unit, it would be more advisable to supply a flow with a temperature in the range of 324K -326K, where all flow parameters cross the line curve of COP. Assuming an inlet flow temperature of 325K, the optimum COPs of 2.22 and 2.36 will be attained from PVT unit with Al_3O_2 -water and Ag-water, respectively.

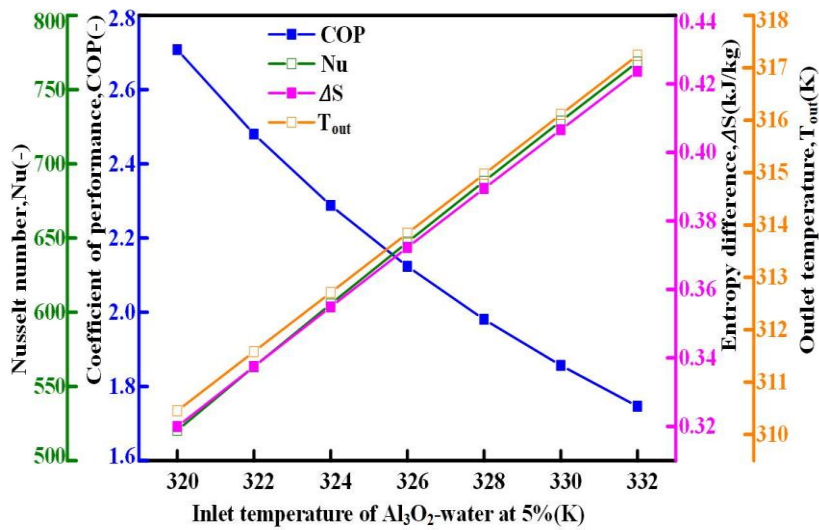


Fig.6.7 Effect of applying different temperatures of Al_3O_2 -water at the pipe inlet of the PVT unit

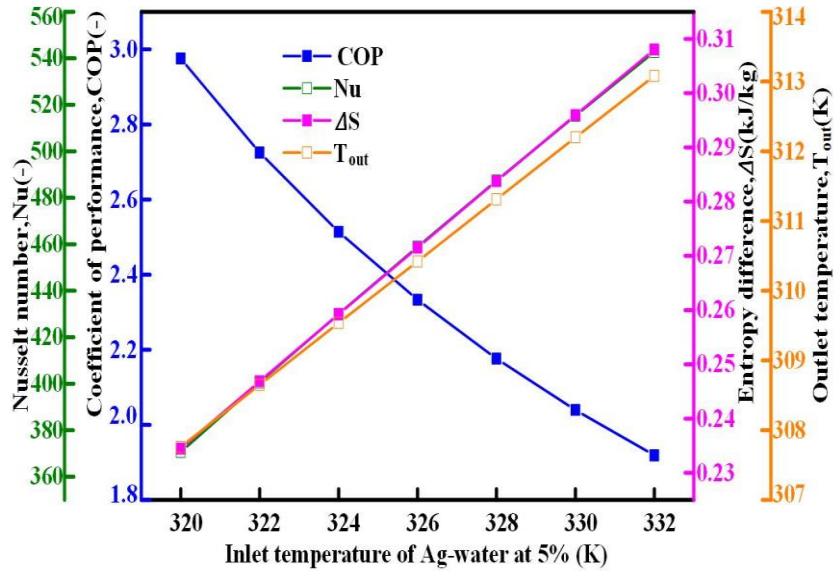


Fig.6.8 Effect of applying different temperatures of Ag-water at the pipe inlet of the PVT unit

6.4 Effect of weather conditions on the PVT unit cooling

The effect of various ambient temperatures on the operation of Ag-water/PVT unit and Al_3O_2 -water/PVT unit is presented in Fig.6.9 and Fig.6.10, respectively in terms of flow parameters (Nu, ΔS and T_{out}) and COP. As can be observed from Fig.6.9 and Fig.6.10, incrementing ambient temperature will decrease both Nu and COP and while ΔS and T_{out} increase. In principle, the heat transfer enhances when the difference in temperature between two areas exchanging heat is high. In the case of PVT unit, the main two areas exchanging heat are inside pipe (hot) and the ambient environment (cold). Increasing the ambient temperature will reduce the temperature difference between the two stated areas and hence lowers heat transfer. The amount of heat trapped inside fluid pipe will effect both ΔS and T_{out} to increase linearly and while a parabolic reduction in Nu will be observed. The higher ΔS will incur much resistances of flow inside pipe, which would require a higher pump power to overcome them. In addition, the low refrigeration effect will be obtained due to a very low temperature/enthalpy difference between the inlet and outlet of pipe. Therefore, these two facts will linearly reduce the overall COP of the PVT unit. Comparing the two PVT units, the maximum achieved COP of Al_3O_2 -water/PVT unit is 0.15 lower than that of Ag-water/PVT unit. In addition, a higher COP in both two cases was attained at low ambient temperature of 298K.

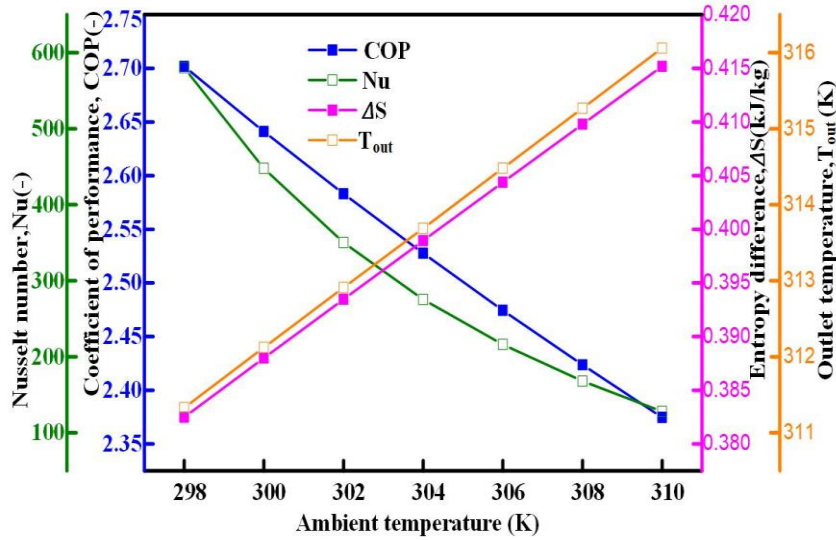


Fig.6.9 Impact of operating Al₃O₂-water/PVT unit at various ambient temperatures

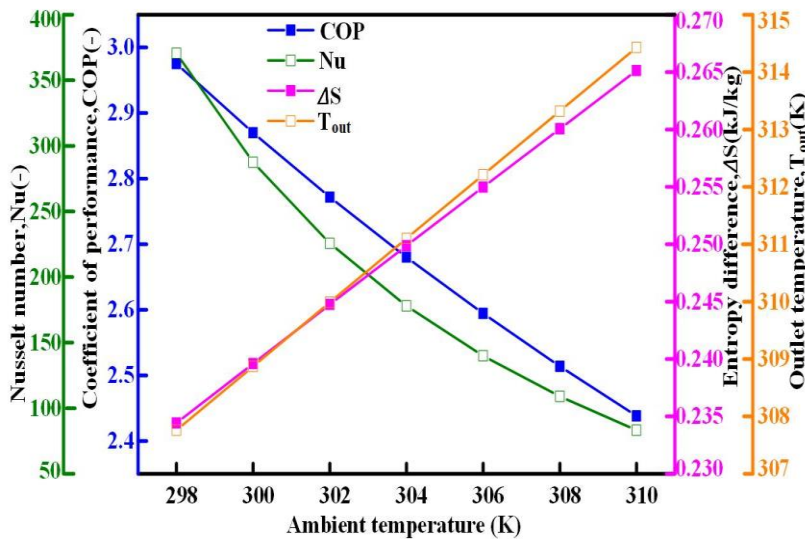


Fig.6.10 Impact of operating Ag-water/PVT unit at various ambient temperatures

6.5 Summary

In this chapter, the new strategies to further boost the heat transfer characteristics and the refrigeration coefficient of performance of PVT unit were investigated. More specifically, a model of PVT unit with nano-fluids was solved and the corresponding results were determined and discussed.

First, the internal fluid phenomena (Nusselt number and entropy generation) to influence the performance of coefficient (COP) for PVT unit with nano-fluids were discussed under

different operating parameters/conditions of nanoparticles, mass flow rate, inlet flow temperature and ambient temperature.

Second, operating PVT unit with nano-fluids resulted in maximum COP of about 3 when Ag-water was used through the pipe to exchange heat with the natural cold of the sky. The current COP is 0.9 and 0.5 lower than that obtained from the experimental studies of ^[16] and ^[137] respectively when refrigerant was used as a fluid medium in the pipe of the PVT unit condenser. Moreover, the current average maximum COP is 0.92 higher than that of attained in the study of existing PVT unit condenser^[138]. Further, in comparison to the attained COP from Chapter 5, the current maximum COP is 2.079 and 1.66 less than that obtained from PVT unit condenser with fins and PVT unit condenser with novel channel structure, respectively.

Third, on the basis of the results, the use of nano-fluids especially Ag-water would be another option of fluid medium to be used in the channel of PVT unit under cooling condition in case refrigerant is not available or its cost is higher than that of nano-fluid.

7. Conclusions and Outlook

7.1 Conclusions

The solar assisted heat pump is a technology being developed at the rapid pace to solve energy demand for cooling in hot climatic zones and at the same time reducing the detrimental impacts caused by CO₂ emissions. More specifically, during daytime, PVT unit is operated as an evaporator to convert solar energy into useful energy of heat, electricity and hot water and while during nighttime, the same PVT unit is used as a condenser to turn unused thermal energy into cooling load demand, especially by taking advantages of night natural cold (NNC) of the sky. In particular, to the recent developed component of PVT unit condenser, the refrigerant vapor flows into the inflatable heat exchanger plate, cools down, condenses and releases condensation heat in its serpentine channel, and then flows out. In the process, the condensation heat of the PVT heat pump continuously releases to the ambient and the sky by different modes until the required temperature of cooling load is reached. The condensation and heat release characteristics of PVT unit are closely related to the shape of channel structure, the shape of surface structure, the flow and heat transfer state of refrigerant in channel, the thermal conductivity between the plate and PV unit, and the sky effective temperature. Therefore, in order to further improve the night cooling performance of PVT heat pump system, it is necessary to deeply study the heat transfer characteristics and enhance heat transfer methods of PVT unit operating at night in summer. In this PhD thesis, a numerical simulation with ANSYS Fluent 18 was performed to propose the methods for further enhancement of the heat transfer characteristics of PVT unit under condensation and cooling conditions, at nighttime. The first sets of simulation were to determine the optimum dimensions of PVT unit condenser (i.e. width, length, and internal/ external diameters of microchannel). Based on the optimized model, the heat transfer improvement and the impact of different external and internal factors on the heat transfer characteristics were determined. Second, the heat transfer characteristics of PVT unit condenser were enhanced by both attaching fins of different shapes at the outer surface of channel and incorporation of new channel structure. Last, the use of nanofluids as fluids medium in the channel of PVT unit for cooling at night, was investigated. The detailed sequence of activities, achieved results and the main implications are given here below:

(1) Four models of existing PVT unit condenser, PVT unit condenser with fins, PVT unit condenser incorporating a novel channel of hexagonal-grids coupled with fluid channel of serpentine arrangement and PVT unit with nanofluids were developed. In addition, the mathematical equation for fluid flow inside channel and thermal energy in PVT unit materials were established. The main objective was to build physical model geometries and mathematical

models to be solved in ANSYS Fluent and further get results of a particular case studies. The establishment of models and mathematical equations is an initial and important step towards the solution of a problem under investigation. These models were developed based on author's previous studies and different approaches from various disciplines of engineering. Therefore, they need to be further processed in order to fit into the real problems.

(2) The above four developed physical models were prepared for better solution of the mathematical model equations. The preparation included determination of methods, assumptions and operating conditions, creation of quality mesh able to capture the solution of mathematical equations and proposal of evaluation indexes. The tasks of this section were performed with the aim to determine the accuracy of the models. The step helps to build a basic model which can be utilized to get the results of a particular case study. Depending on the nature of the problem to be solved, the above four models can be further processed differently. For instance, modelling PVT unit model with refrigerant is more challenging as compared to the one with nanofluid due to the fact that a proper model to handle turbulences needs to be carefully selected. In addition, a volume of fluid (VOF) is required to model phase change of refrigerant at different temperatures. In this circumstance, three rounds of simulation sets were conducted to propose the methods for further performance improvement of the PVT unit under condensation and cooling conditions.

(3) A first round of simulation sets was carried out on the basis of validated model of existing PVT unit condenser to determine optimum dimensions of the PVT unit condenser and also to analyze heat transfer characteristics of the optimized model, at different external and internal factors. Apart from internal and external diameter which increased in dimensions, the rest of PVT unit parameters presented a reduction in dimensions. Reducing the size of PVT unit while fulfilling the same needs is profitable in different perspectives, depending on the decision of operator. Either the costs can be minimized as a result of reducing the number of PVT units or the number of PVT units can be increased on the same area for more production of cooling load demand. Meanwhile, a sensitivity analysis of an optimized model was performed to determine the effect of emissivity and different conditions of flow and weather on the heat transfer characteristics of PVT unit condenser. The knowledge of the effect of different internal and external factors is a very helpful tool in predicting the heat transfer characteristics and overall performance of the PVT unit condenser at particular surface emissivity and conditions of the day, month and year. Furthermore, the heat dissipation flux of an optimized model of PVT unit condenser was determined and compared with that of existing model. The maximum heat flux improvement of 12.5% was determined at ambient temperature of 299.5K, sky temperature of 279.5K and wind speed of 0.06m/s. In comparison to the average COP for existing model^[138] at the same operating conditions, the 12.5% improvement in heat dissipation flux would increase the COP from 1.86 to 2.1. This implies that instead of ordering the already

designed PVT units, customers can also advise the manufacturers about the proper size of the units based on their preliminary studies.

(4) The main objective of the second round of simulation sets was to put forward strategies to enhance the condensation heat transfer characteristics of PVT unit condenser. In addition to the design and optimization of the unit, incorporation of both fins to the outer surface of the channel and new channel structure were other options. At first, a validated model of PVT unit condenser with fins of different shapes was solved to determine optimum fin shape, fin number and fin position. PVT unit condenser with 3 fins of straight rectangular shape and with 2 fins placed 15° on the left and right side of a fixed one at 270° was selected as a best option to enhance the condensation heat transfer characteristics of PVT unit condenser. In addition, for the considered range of both fin length and width (0.2mm-0.7mm), the optimum fin length and fin width were respectively obtained at 0.2mm and 0.3mm. Overall, extending fins to the outer surface of channel improved coefficient of performance up to 5.079. Second, a validated model of PVT unit condenser incorporating a novel channel of hexagonal-grids coupled with fluid channel of serpentine arrangement was solved to investigate the condensations, heat dissipation flux and the overall performance of coefficient. The results revealed an average maximum COP of 4.66, which is 0.474 and 2.58 less than that of PVT unit with fins and higher than that of existing PVT unit condenser, respectively. Increasing the performance while operating the same number of PVT units condenser has benefits. It can speed up the cooling process and results in obtaining the cooling load demand within a short time.

(5) The third round of simulation sets was to integrate new fluid medium of nanofluids in the research of PVT unit under cooling condition. A validated model of PVT unit with water- Al_3O_2 and water-Ag as fluids medium through the pipe was solved in ANSYS Fluent software and the related results were presented and discussed. Due to higher thermal conductivity of Ag as compared to Al_3O_2 , the maximum COP of 3 was achieved from PVT unit with Ag-water, which is 0.3 higher than that of PVT unit with water- Al_3O_2 . In addition, by comparing to conducted studies about PVT unit condenser, the obtained maximum COP of PVT unit with Ag-water is 0.9 and 0.5 lower than that obtained from the experimental studies of ^[16] and ^[137] respectively when refrigerant was used as a fluid medium in the pipe of the PVT unit. Moreover, the current average COP is 0.92 higher than that of attained in the study of ^[138]. Operating PVT unit with Ag-water would be another option to be used in the channel of PVT unit under cooling condition in case refrigerant is not available or its cost is higher than that of nanofluid.

7.2 Innovative points

The system of PVT heat pump is composed by many components interconnected together to fulfil energy need. In the latest technology of PVT heat pump system, PVT unit component has a dual function to act both as an evaporator during daytime and as a condenser in nighttime. Especially for the recent incorporated component of PVT unit condenser and the main focus of this PhD thesis, the existing research studies are mainly to prove its practical feasibility under different climatic zones. Moreover, most of those studies were conducted experimentally. Therefore, a numerical strategy with ANSYS Fluent was employed to test and propose new ideas which can be introduced in the research of PVT unit and further improve both its heat transfer characteristics and overall performance. As a recently developed unit, the methods utilized in this PhD thesis seem all to be innovative points/ideas as detailed here below:

(1) The research establishes the mathematical models for fluid flow and heat transfer in PVT unit materials with new structures of channels with fins of straight rectangular, straight triangular, pin of rectangular profile, pin of parabolic profile, and evaluation index of flow and heat transfer performance of PVT unit condenser, highlights the simulation model of phase change process and proposes alternative flow channel of hexagonal-grids coupled with fluid channel with serpentine arrangement.

The use of fins had been entirely the method to remove excess heat from electronic equipment and ensure its good operating condition, by maintaining its temperature to or below that of manufacturer's. With time, the method has been adopted in other fields of engineering, including PVT unit. Meanwhile, the development and utilization of new channel structures has been found to have a vital role in improving the heat transfer characteristics and performance of the PVT unit. However, those two methods have been applied considering PVT unit working during daytime to produce heat and electricity and it is rarely to find research on PVT unit operating at night to produce cooling load demand. The simulation results reveal that straight rectangular fin is a fin shape with highest heat transfer performance, which enhances the heat transfer mechanisms between the back side of the PVT unit and ambient environment.

(2) A CFD simulation calculation method to simultaneously consider multiphase fluid phase change heat and heat transfer in PVT unit materials is proposed to solve the problem that conventional CFD simulation methods do not consider. It also provides a feasible numerical simulation method for solving the heat-fluid-structure coupling heat transfer problem of phase change.

The study takes into account the PVT unit working at night to exchange heat with the night natural cold (NNC) of the sky. In contrary to the conventional unit where solar energy is absorbed at the top surface of the panel collector, the heat source for the current PVT unit is provided from the fluid carrier inside pipe. In principle, the heat moves from the area with higher temperature to the area with low temperature. Therefore, unlike in the case of former

unit whereby a top-bottom approach is used to solve the mathematical equations for heat transfer in fluid and materials, a bottom-top approach is employed to solve the present PVT unit and analyze its heat transfer characteristics.

(3) The practical feasibility of using nano-fluids as fluids medium in the channel of PVT unit with natural cold of the sky under cooling condition at night is proven in this research, and it is found that the maximum coefficient of performance can be obtained when the fluids of Ag-water is used as the working fluid of nano-fluids.

The available studies about use of nano-fluids are mostly focused on maximizing the heat removal from PV cells materials and enhance both electrical and thermal efficiencies of PVT unit working during daytime and it is rare to find research on the use of nanofluid in the channel of PVT unit for cooling load production, at night. By comparing the two PVT units for cooling load production, the proposed one with Ag-water as fluid medium in the channel resulted in a maximum coefficient of performance of 3, which is 0.92 higher than that of existing PVT unit with R407C as fluid medium in channel.

7.3 Future Outlook

The current research used the methods of design and optimization, addition of fins to the outer surface of the channel, new channel structure and nano-fluids as fluids medium through the channel in order to enhance the heat transfer characteristics of PVT unit under condensation and cooling conditions. The research presented in this thesis seems to have raised more questions which need to be addressed for future researchers. In addition, many others strategies previously used to enhance the heat transfer characteristics of the most popular system of PVT heat pump system with PVT unit acting as an evaporator, can also be applied to the new system by future researchers. The following are some ideas which need to be further investigated:

(1) The current research has been conducted taking into account different operating conditions of weather. Future researchers especially those in the aforementioned climatic zones should take advantages and implement the system. If a big number is adopted to operate PVT units under natural cold of the sky at night, the energy sustainability will be achieved as result of using clean energy source to produce cooling load needed by the occupants.

(2) The best option of fin was selected based on four types of fin shapes. Future researchers should also consider shapes, dimensions and arrangements other than those mentioned in this thesis. With this research, the PVT unit condenser with fins can be further optimized and improve the performance.

(3) The use of phase change material (PCM) and a combination of fins and PCM on the absorber of PVT unit condenser are other methods to enhance the heat transfer characteristics and which should be considered by future researchers. PCM has been shown to be a thermal

energy management due to its ability to absorb heat and release it whenever needed. Integrating PCM with PVT unit condenser would be more beneficial in perspective of avoiding heat island and storing heat which can be used in other application purposes, when solar energy is not enough. In addition, many more channel structures should be developed and incorporated in the absorber of PVT unit condenser with the objective to further enhance flow uniformity and the residence time of fluid flow.

(4) To fully explore the benefits of using nano-fluids in the PVT unit, future researchers should consider two phase change of nano-fluids and also the impact of some other nano-fluids apart from those used in the current research (Al_3O_2 and Ag). The use of two phase nanofluid has been demonstrated to result in a significant improvement in heat transfer. Therefore, introducing this concept in the research of PVT unit under cooling condition would increase its performance.

(5) Having the results of the above stated suggestions, further studies should be conducted in perspective of both economy and CO_2 emissions reduction in order to determine the contribution of the new unit to the goal set by the United Nations about global warming. In addition, all the aforementioned ideas should be implemented experimentally by the future researchers to provide cooling load to the society in hot climatic zone.

References

- [1] Buker M S, Riffat S B. Solar assisted heat pump systems for low temperature water heating applications: A systematic review [J]. *Renewable and Sustainable Energy Reviews*. 2016, 55: 399-413.
- [2] Emmi G, Bordignon S, Zarrella A, et al. A dynamic analysis of a SAGSHP system coupled to solar thermal collectors and photovoltaic-thermal panels under different climate conditions [J]. *Energy Conversion and Management*. 2020, 213: 112851.
- [3] Boden T, Andres R, Marland G: *Environmental System Science Data Infrastructure for a Virtual Ecosystem ...*, 2017.
- [4] Hoegh-Guldberg O, Bruno J F. The impact of climate change on the world's marine ecosystems [J]. *Science*. 2010, 328(5985): 1523-8.
- [5] Morton J F. The impact of climate change on smallholder and subsistence agriculture [J]. *Proceedings of the national academy of sciences*. 2007, 104(50): 19680-5.
- [6] Berrittella M, Bigano A, Roson R, et al. A general equilibrium analysis of climate change impacts on tourism [J]. *Tourism management*. 2006, 27(5): 913-24.
- [7] Koetse M J, Rietveld P. The impact of climate change and weather on transport: An overview of empirical findings [J]. *Transportation Research Part D: Transport and Environment*. 2009, 14(3): 205-21.
- [8] Üрге-Vorsatz D, Eyre N, Graham P, et al. Chapter 10-Energy End-Use: Building. In *Global Energy Assessment-Toward a Sustainable Future* [M]. Cambridge university press. 2012.
- [9] Urge-Vorsatz D, Petrichenko K, Staniec M, et al. Energy use in buildings in a long-term perspective [J]. *Current Opinion in Environmental Sustainability*. 2013, 5(2): 141-51.
- [10] Somu N, Mr G R, Ramamritham K. A hybrid model for building energy consumption forecasting using long short term memory networks [J]. *Applied Energy*. 2020, 261: 114131.
- [11] Commission C E. California Commercial End-Use Survey (CEUS) [J]. Database. 2006.
- [12] Ashrae A H. *Hvac systems and equipment*, American society of heating [J]. Refrigeration and Air-conditioning Engineers, Atlanta, GA. 2012.
- [13] Ma Z, Ren H, Lin W. A review of heating, ventilation and air conditioning technologies and innovations used in solar-powered net zero energy Solar Decathlon houses [J]. *Journal of Cleaner Production*. 2019, 240: 118158.
- [14] Pérez-Lombard L, Ortiz J, Pout C. A review on buildings energy consumption information [J]. *Energy and buildings*. 2008, 40(3): 394-8.
- [15] Zhou C, Liang R, Zhang J, et al. Experimental study on the cogeneration performance of roll-bond-PVT heat pump system with single stage compression during summer [J]. *Applied Thermal Engineering*. 2019, 149: 249-61.
- [16] Zhou C, Liang R, Riaz A, et al. Experimental investigation on the tri-generation performance of roll-bond photovoltaic thermal heat pump system during summer [J]. *Energy Conversion and Management*. 2019, 184: 91-106.
- [17] Abd Alla S, Bianco V, Marchitto A, et al. Impact of the utilization of heat pumps for buildings heating in the Italian power market [C]; 2018 15th International Conference on the European Energy Market (EEM), 2018. IEEE.

- [18] Brockway A M, Delforge P. Emissions reduction potential from electric heat pumps in California homes [J]. *The Electricity Journal*. 2018, 31(9): 44-53.
- [19] Yunna W, Ruhang X. Green building development in China-based on heat pump demonstration projects [J]. *Renewable energy*. 2013, 53: 211-9.
- [20] Brumbaugh J E. HVAC Fundamentals. Volume 3: Air Conditioning, Heat Pumps and Distribution Systems [J]. 2004.
- [21] Renaldi R, Kiprakis A, Friedrich D. An optimisation framework for thermal energy storage integration in a residential heat pump heating system [J]. *Applied energy*. 2017, 186: 520-9.
- [22] Aguilar F, Aledo S, Quiles P. Experimental study of the solar photovoltaic contribution for the domestic hot water production with heat pumps in dwellings [J]. *Applied Thermal Engineering*. 2016, 101: 379-89.
- [23] Bellos E, Tzivanidis C, Moschos K, et al. Energetic and financial evaluation of solar assisted heat pump space heating systems [J]. *Energy Conversion and Management*. 2016, 120: 306-19.
- [24] Weeratunge H, De Hoog J, Dunstall S, et al. Life Cycle Cost Optimization of a Solar Assisted Ground Source Heat Pump System [C]; 2018 IEEE Power & Energy Society General Meeting (PESGM), 2018. IEEE.
- [25] Kern Jr E, Russell M: Massachusetts Inst. of Tech., Lexington (USA). Lincoln Lab., 1978.
- [26] Bazilian M D, Kamalanathan H, Prasad D. Thermographic analysis of a building integrated photovoltaic system [J]. *Renewable Energy*. 2002, 26(3): 449-61.
- [27] Tiwari A, Sodha M. Performance evaluation of solar PV/T system: an experimental validation [J]. *Solar energy*. 2006, 80(7): 751-9.
- [28] Zondag H A, De Vries D D, Van Helden W, et al. The thermal and electrical yield of a PV-thermal collector [J]. *Solar energy*. 2002, 72(2): 113-28.
- [29] Tong Y, Lee H, Kang W, et al. Energy and exergy comparison of a flat-plate solar collector using water, Al₂O₃ nanofluid, and CuO nanofluid [J]. *Applied Thermal Engineering*. 2019, 159: 113959.
- [30] Reddy Penaka S, Kumar Saini P, Zhang X, et al. Digital Mapping of Techno-Economic Performance of a Water-Based Solar Photovoltaic/Thermal (PVT) System for Buildings over Large Geographical Cities [J]. *Buildings*. 2020, 10(9): 148.
- [31] Michael J J, Iniyar S, Goic R. Flat plate solar photovoltaic–thermal (PV/T) systems: A reference guide [J]. *Renewable and sustainable energy reviews*. 2015, 51: 62-88.
- [32] Lari M O, Sahin A Z. Design, performance and economic analysis of a nanofluid-based photovoltaic/thermal system for residential applications [J]. *Energy Conversion and Management*. 2017, 149: 467-84.
- [33] Kandilli C. Performance analysis of a novel concentrating photovoltaic combined system [J]. *Energy Conversion and Management*. 2013, 67: 186-96.
- [34] Babu C, Ponnambalam P. The role of thermoelectric generators in the hybrid PV/T systems: A review [J]. *Energy conversion and management*. 2017, 151: 368-85.
- [35] Kern Jr E C, Russell M C: Massachusetts Inst. of Tech., Lexington (USA). Lincoln Lab., 1978.
- [36] Al Harbi Y, Eugenio N, Al Zahrani S. Photovoltaic-thermal solar energy experiment in Saudi Arabia [J]. *Renewable energy*. 1998, 15(1-4): 483-6.
- [37] Huang B, Lin T, Hung W, et al. Solar photo-voltaic/thermal co-generation collector [C]; Proceedings of the ISES 1999 Solar World Congress, Jerusalem, Israel, 1999.

- [38] Huang B, Lin T, Hung W, et al. Performance evaluation of solar photovoltaic/thermal systems [J]. *Solar energy*. 2001, 70(5): 443-8.
- [39] Ibrahim A, Othman M Y, Ruslan M H, et al. Recent advances in flat plate photovoltaic/thermal (PV/T) solar collectors [J]. *Renewable and sustainable energy reviews*. 2011, 15(1): 352-65.
- [40] Chow T. Performance analysis of photovoltaic-thermal collector by explicit dynamic model [J]. *Solar Energy*. 2003, 75(2): 143-52.
- [41] Florschuetz L. On heat rejection from terrestrial solar cell arrays with sunlight concentration [J]. *pvs*. 1975: 318-26.
- [42] Florschuetz L. Extension of the Hottel-Whillier model to the analysis of combined photovoltaic/thermal flat plate collectors [J]. *Solar energy*. 1979, 22(4): 361-6.
- [43] Hendrie S: Massachusetts Inst. of Tech., Lexington (USA). Lincoln Lab., 1982.
- [44] Tiwari A, Sodha M. Parametric study of various configurations of hybrid PV/thermal air collector: experimental validation of theoretical model [J]. *Solar Energy Materials and Solar Cells*. 2007, 91(1): 17-28.
- [45] Garg H, Adhikari R S. Conventional hybrid photovoltaic/thermal (PV/T) air heating collectors: steady-state simulation [J]. *Renewable energy*. 1997, 11(3): 363-85.
- [46] Zondag H. Flat-plate PV-Thermal collectors and systems: A review [J]. *Renewable and Sustainable Energy Reviews*. 2008, 12(4): 891-959.
- [47] Zondag H, De Vries D, Van Helden W, et al. The yield of different combined PV-thermal collector designs [J]. *Solar energy*. 2003, 74(3): 253-69.
- [48] Charalambous P, Maidment G G, Kalogirou S A, et al. Photovoltaic thermal (PV/T) collectors: A review [J]. *Applied thermal engineering*. 2007, 27(2-3): 275-86.
- [49] Tripanagnostopoulos Y, Nousia T, Souliotis M, et al. Hybrid photovoltaic/thermal solar systems [J]. *Solar energy*. 2002, 72(3): 217-34.
- [50] Tonui J, Tripanagnostopoulos Y. Air-cooled PV/T solar collectors with low cost performance improvements [J]. *Solar energy*. 2007, 81(4): 498-511.
- [51] Tiwari A, Sodha M. Performance evaluation of hybrid PV/thermal water/air heating system: a parametric study [J]. *Renewable energy*. 2006, 31(15): 2460-74.
- [52] Karwa R, Karwa N, Misra R, et al. Effect of flow maldistribution on thermal performance of a solar air heater array with subcollectors in parallel [J]. *Energy*. 2007, 32(7): 1260-70.
- [53] Yin J M, Bullard C W, Hrnjak P S. Single-phase pressure drop measurements in a microchannel heat exchanger [J]. *Heat Transfer Engineering*. 2002, 23(4): 3-12.
- [54] Fabbri G. Heat transfer optimization in corrugated wall channels [J]. *International Journal of Heat and Mass Transfer*. 2000, 43(23): 4299-310.
- [55] Kandlikar S G, Joshi S, Tian S. Effect of channel roughness on heat transfer and fluid flow characteristics at low Reynolds numbers in small diameter tubes [J]. *Atmosphere*. 2001, 4(7).
- [56] Amador C, Gavriilidis A, Angeli P. Flow distribution in different microreactor scale-out geometries and the effect of manufacturing tolerances and channel blockage [J]. *Chemical Engineering Journal*. 2004, 101(1-3): 379-90.
- [57] Ramos-Alvarado B, Li P, Liu H, et al. CFD study of liquid-cooled heat sinks with microchannel flow field configurations for electronics, fuel cells, and concentrated solar cells [J]. *Applied Thermal Engineering*. 2011, 31(14-15): 2494-507.

- [58] Liu H, Li P, Van Lew J. CFD study on flow distribution uniformity in fuel distributors having multiple structural bifurcations of flow channels [J]. *International Journal of Hydrogen Energy*. 2010, 35(17): 9186-98.
- [59] Eastman J A, Phillpot S, Choi S, et al. Thermal transport in nanofluids [J]. *Annu Rev Mater Res*. 2004, 34: 219-46.
- [60] Keblinski P, Phillpot S, Choi S, et al. Mechanisms of heat flow in suspensions of nano-sized particles (nanofluids) [J]. *International journal of heat and mass transfer*. 2002, 45(4): 855-63.
- [61] Teng K-L, Hsiao P-Y, Hung S-W, et al. Enhanced thermal conductivity of nanofluids diagnosis by molecular dynamics simulations [J]. *Journal of nanoscience and nanotechnology*. 2008, 8(7): 3710-8.
- [62] Levin M, Miller M. Maxwell's" *Treatise on Electricity and Magnetism*" [J]. *Soviet Physics Uspekhi*. 1981, 24(11): 904.
- [63] Das S K, Choi S U, Patel H E. Heat transfer in nanofluids—a review [J]. *Heat transfer engineering*. 2006, 27(10): 3-19.
- [64] Choi S U, Eastman J A: Argonne National Lab.(ANL), Argonne, IL (United States), 1995.
- [65] Wang J, Zheng R, Gao J, et al. Heat conduction mechanisms in nanofluids and suspensions [J]. *Nano Today*. 2012, 7(2): 124-36.
- [66] Saidur R, Meng T, Said Z, et al. Evaluation of the effect of nanofluid-based absorbers on direct solar collector [J]. *International Journal of Heat and Mass Transfer*. 2012, 55(21-22): 5899-907.
- [67] Tyagi H, Phelan P, Prasher R. Predicted efficiency of a low-temperature nanofluid-based direct absorption solar collector [J]. *Journal of solar energy engineering*. 2009, 131(4).
- [68] Yazdanifard F, Ameri M, Ebrahimnia-Bajestan E. Performance of nanofluid-based photovoltaic/thermal systems: A review [J]. *Renewable and Sustainable Energy Reviews*. 2017, 76: 323-52.
- [69] Al-Shamani A N, Alghoul M, Elbreki A, et al. Mathematical and experimental evaluation of thermal and electrical efficiency of PV/T collector using different water based nano-fluids [J]. *Energy*. 2018, 145: 770-92.
- [70] Al-Waeli A H, Chaichan M T, Kazem H A, et al. Comparative study to use nano-(Al₂O₃, CuO, and SiC) with water to enhance photovoltaic thermal PV/T collectors [J]. *Energy Conversion and Management*. 2017, 148: 963-73.
- [71] Sardarabadi M, Passandideh-Fard M. Experimental and numerical study of metal-oxides/water nanofluids as coolant in photovoltaic thermal systems (PVT) [J]. *Solar Energy Materials and Solar Cells*. 2016, 157: 533-42.
- [72] Menon G S, Murali S, Elias J, et al. Experimental investigations on unglazed photovoltaic-thermal (PVT) system using water and nanofluid cooling medium [J]. *Renewable Energy*. 2022, 188: 986-96.
- [73] Karaaslan I, Menlik T. Numerical study of a photovoltaic thermal (PV/T) system using mono and hybrid nanofluid [J]. *Solar Energy*. 2021, 224: 1260-70.
- [74] Mohanraj M, Belyayev Y, Jayaraj S, et al. Research and developments on solar assisted compression heat pump systems—A comprehensive review (Part A: Modeling and modifications) [J]. *Renewable and sustainable energy reviews*. 2018, 83: 90-123.
- [75] Sporn P, Ambrose E. The heat pump and solar energy [C]; *Proceedings of the world symposium on applied solar energy*, 1955.

- [76] Cervantes J G, Torres-Reyes E. Experiments on a solar-assisted heat pump and an exergy analysis of the system [J]. *Applied Thermal Engineering*. 2002, 22(12): 1289-97.
- [77] Huang B, Chyng J. Performance characteristics of integral type solar-assisted heat pump [J]. *Solar Energy*. 2001, 71(6): 403-14.
- [78] Tsai H-L. Modeling and validation of refrigerant-based PVT-assisted heat pump water heating (PVTa-HPWH) system [J]. *Solar Energy*. 2015, 122: 36-47.
- [79] Zhang X-R, Yamaguchi H, Uneno D. Experimental study on the performance of solar Rankine system using supercritical CO₂ [J]. *Renewable Energy*. 2007, 32(15): 2617-28.
- [80] Marion M, Voicu I, Tiffonnet A-L. Study and optimization of a solar subcritical organic Rankine cycle [J]. *Renewable Energy*. 2012, 48: 100-9.
- [81] Hawlader M, Chou S, Ullah M. The performance of a solar assisted heat pump water heating system [J]. *Applied Thermal Engineering*. 2001, 21(10): 1049-65.
- [82] Kuang Y, Wang R, Yu L. Experimental study on solar assisted heat pump system for heat supply [J]. *Energy Conversion and Management*. 2003, 44(7): 1089-98.
- [83] Li Y, Wang R, Wu J, et al. Experimental performance analysis and optimization of a direct expansion solar-assisted heat pump water heater [J]. *Energy*. 2007, 32(8): 1361-74.
- [84] Dikici A, Akbulut A. Performance characteristics and energy-exergy analysis of solar-assisted heat pump system [J]. *Building and Environment*. 2008, 43(11): 1961-72.
- [85] Bi Y, Guo T, Zhang L, et al. Solar and ground source heat-pump system [J]. *Applied Energy*. 2004, 78(2): 231-45.
- [86] Han Z, Zheng M, Kong F, et al. Numerical simulation of solar assisted ground-source heat pump heating system with latent heat energy storage in severely cold area [J]. *Applied Thermal Engineering*. 2008, 28(11-12): 1427-36.
- [87] Hepbasli A. Exergetic modeling and assessment of solar assisted domestic hot water tank integrated ground-source heat pump systems for residences [J]. *Energy and buildings*. 2007, 39(12): 1211-7.
- [88] Mohanraj M, Jayaraj S, Muraleedharan C. Performance prediction of a direct expansion solar assisted heat pump using artificial neural networks [J]. *Applied Energy*. 2009, 86(9): 1442-9.
- [89] Wang H, Qi C, Wang E, et al. A case study of underground thermal storage in a solar-ground coupled heat pump system for residential buildings [J]. *Renewable energy*. 2009, 34(1): 307-14.
- [90] Alaghmand S. New windcatcher as natural ventilation in sustainable architecture [J]. *NATIONALPARK-FORSCHUNG IN DER SCHWEIZ (Switzerland Research Park Journal)*. 2014, 103(1).
- [91] Hughes B R, Chaudhry H N, Ghani S A. A review of sustainable cooling technologies in buildings [J]. *Renewable and Sustainable Energy Reviews*. 2011, 15(6): 3112-20.
- [92] Santamouris M, Kolokotsa D. Passive cooling dissipation techniques for buildings and other structures: The state of the art [J]. *Energy and Buildings*. 2013, 57: 74-94.
- [93] Foruzanmehr A. The wind-catcher: users' perception of a vernacular passive cooling system [J]. *Architectural Science Review*. 2012, 55(4): 250-8.
- [94] Hughes B R, Calautit J K, Ghani S A. The development of commercial wind towers for natural ventilation: A review [J]. *Applied energy*. 2012, 92: 606-27.

- [95] Kantzioura A, Kosmopoulos P, Dimoudi A, et al. Experimental investigation of microclimatic conditions in relation to the built environment in a central urban area in Thessaloniki (Northern Greece): A case study [J]. *Sustainable Cities and Society*. 2015, 19: 331-40.
- [96] Oke T, Johnson G, Steyn D, et al. Simulation of surface urban heat islands under 'ideal' conditions at night part 2: Diagnosis of causation [J]. *Boundary-Layer Meteorology*. 1991, 56(4): 339-58.
- [97] Santamouris M, Cartalis C, Synnefa A, et al. On the impact of urban heat island and global warming on the power demand and electricity consumption of buildings—A review [J]. *Energy and Buildings*. 2015, 98: 119-24.
- [98] Maragogiannis K, Kolokotsa D, Maria E-A. Study of night ventilation efficiency in urban environment: technical and legal aspects [J]. *Environmental and Climate Technologies*. 2011, 6(1): 49-56.
- [99] Georgakis C, Zoras S, Santamouris M. Studying the effect of “cool” coatings in street urban canyons and its potential as a heat island mitigation technique [J]. *Sustainable Cities and Society*. 2014, 13: 20-31.
- [100] Kolokotsa D, Santamouris M, Zerefos S. Green and cool roofs' urban heat island mitigation potential in European climates for office buildings under free floating conditions [J]. *Solar Energy*. 2013, 95: 118-30.
- [101] Saffari M, De Gracia A, Ushak S, et al. Passive cooling of buildings with phase change materials using whole-building energy simulation tools: A review [J]. *Renewable and Sustainable Energy Reviews*. 2017, 80: 1239-55.
- [102] Koronaki I. The impact of configuration and orientation of solar thermosyphonic systems on night ventilation and fan energy savings [J]. *Energy and buildings*. 2013, 57: 119-31.
- [103] Lain M, Hensen J. The optimization of the mechanical night cooling system in the office building [C]; Proc proceedings of the 6th int conf on compressors and coolants, casta papiernicka, slovakia, 2006.
- [104] Liu Y, Yang L, Hou L, et al. A porous building approach for modelling flow and heat transfer around and inside an isolated building on night ventilation and thermal mass [J]. *Energy*. 2017, 141: 1914-27.
- [105] Solgi E. Optimizing thermal mass in night ventilation [D]; Master Thesis), Art University, 2014.
- [106] Santamouris M, Sfakianaki A, Pavlou K. On the efficiency of night ventilation techniques applied to residential buildings [J]. *Energy and Buildings*. 2010, 42(8): 1309-13.
- [107] Leenknecht S, Wagemakers R, Bosschaerts W, et al. Numerical study of convection during night cooling and the implications for convection modeling in Building Energy Simulation models [J]. *Energy and buildings*. 2013, 64: 41-52.
- [108] Gratia E, Bruyere I, De Herde A. How to use natural ventilation to cool narrow office buildings [J]. *Building and environment*. 2004, 39(10): 1157-70.
- [109] Landsman J. Performance, prediction and optimization of night ventilation across different climates [J]. 2016.
- [110] Geros V, Santamouris M, Karatasou S, et al. On the cooling potential of night ventilation techniques in the urban environment [J]. *Energy and Buildings*. 2005, 37(3): 243-57.
- [111] Givoni B. Performance and applicability of passive and low-energy cooling systems [J]. *Energy Build*. 1991, 17: 177-99.

- [112] Givoni B. Comfort, climate analysis and building design guidelines [J]. *Energy and buildings*. 1992, 18(1): 11-23.
- [113] Shaviv E, Yezioro A, Capeluto I G. Thermal mass and night ventilation as passive cooling design strategy [J]. *Renewable energy*. 2001, 24(3-4): 445-52.
- [114] Dreau J L, Heiselberg P, Jensen R L. Experimental investigation of convective heat transfers during night cooling with different ventilation systems and surface emissivities [J]. *Energy Build*. 2013, 61: 308-17.
- [115] Breesch H, Janssens A. Reliable design of natural night ventilation using building simulation [C]; 10th Thermal Performance of the Exterior Envelopes of Whole Buildings Conference: 30 years of research, 2007. American Society of Heating, Refrigerating and Air-Conditioning Engineers.
- [116] Artmann N, Gyalistras D, Manz H, et al. Impact of climate warming on passive night cooling potential [J]. *Building Research & Information*. 2008, 36(2): 111-28.
- [117] Breesch H. Natural night ventilation in office buildings: performance evaluation based on simulation, uncertainty and sensitivity analysis [D]; Ghent University, 2006.
- [118] Artmann N, Jensen R L, Manz H, et al. Experimental investigation of heat transfer during night-time ventilation [J]. *Energy and buildings*. 2010, 42(3): 366-74.
- [119] Breesch H, Janssens A. Performance evaluation of passive cooling in office buildings based on uncertainty and sensitivity analysis [J]. *Solar energy*. 2010, 84(8): 1453-67.
- [120] Goethals K, Couckuyt I, Dhaene T, et al. Sensitivity of night cooling performance to room/system design: surrogate models based on CFD [J]. *Building and Environment*. 2012, 58: 23-36.
- [121] Liddament M W, Agency I E. Low energy cooling: annex 28 technical synthesis report based on: Review of low energy cooling technologies, contributing authors: M. Kolokotroni..., Selection guidance for low energy cooling technologies by N. Barnard..., Low energy cooling, early design guidance by J. Huang [M]. ESSU, 2000.
- [122] Blondeau P, Spérandio M, Allard F. Night ventilation for building cooling in summer [J]. *Solar energy*. 1997, 61(5): 327-35.
- [123] Chaudhry H N, Calautit J K, Hughes B R. Computational analysis of a wind tower assisted passive cooling technology for the built environment [J]. *Journal of Building Engineering*. 2015, 1: 63-71.
- [124] Duffie John A, Beckman William A. *Solar engineering of thermal processes* [M]. New York: John Wiley & Sons. 2006.
- [125] Del Col D, Padovan A, Bortolato M, et al. Thermal performance of flat plate solar collectors with sheet-and-tube and roll-bond absorbers [J]. *Energy*. 2013, 58: 258-69.
- [126] Bliss Jr R W. Atmospheric radiation near the surface of the ground: a summary for engineers [J]. *Solar Energy*. 1961, 5(3): 103-20.
- [127] Juchau B. Nocturnal and conventional space cooling via radiant floors [C]; International Passive and Hybrid Cooling Conference, Miami Beach, 1981.
- [128] Erell E, Etzion Y. A radiative cooling system using water as a heat exchange medium [J]. *Architectural Science Review*. 1992, 35(2): 39-49.
- [129] Cavelius R, Isaksson C, Perednis E, et al. Passive cooling technologies [J]. Austrian Energy Agency. 2005: 125.
- [130] Dimoudi A, Androutsopoulos A. The cooling performance of a radiator based roof component [J]. *Solar energy*. 2006, 80(8): 1039-47.

- [131] Farahani M F, Heidarinejad G, Delfani S. A two-stage system of nocturnal radiative and indirect evaporative cooling for conditions in Tehran [J]. *Energy and Buildings*. 2010, 42(11): 2131-8.
- [132] Lin W, Ma Z, Sohel M I, et al. Development and evaluation of a ceiling ventilation system enhanced by solar photovoltaic thermal collectors and phase change materials [J]. *Energy conversion and management*. 2014, 88: 218-30.
- [133] Hu M, Pei G, Wang Q, et al. Field test and preliminary analysis of a combined diurnal solar heating and nocturnal radiative cooling system [J]. *Applied energy*. 2016, 179: 899-908.
- [134] Pean T Q, Gennari L, Olesen B W, et al. Nighttime radiative cooling potential of unglazed and PV/T solar collectors: parametric and experimental analyses [C]; Proceedings of the 8th Mediterranean Congress of Heating, Ventilation and Air-Conditioning (CLIMAMED 2015), 2015.
- [135] Nwaji G, Okoronkwo C, Ogueke N, et al. Investigation of a hybrid solar collector/nocturnal radiator for water heating/cooling in selected Nigerian cities [J]. *Renewable Energy*. 2020, 145: 2561-74.
- [136] Hu M, Zhao B, Ao X, et al. Performance assessment of a trifunctional system integrating solar PV, solar thermal, and radiative sky cooling [J]. *Applied Energy*. 2020, 260: 114167.
- [137] Liang R, Zhou C, Zhang J, et al. Characteristics analysis of the photovoltaic thermal heat pump system on refrigeration mode: An experimental investigation [J]. *Renewable Energy*. 2020, 146: 2450-61.
- [138] Lu S, Zhang J, Liang R, et al. Refrigeration characteristics of a hybrid heat dissipation photovoltaic-thermal heat pump under various ambient conditions on summer night [J]. *Renewable Energy*. 2020, 146: 2524-34.
- [139] Misha S, Abdullah A L, Tamaldin N, et al. Simulation CFD and experimental investigation of PVT water system under natural Malaysian weather conditions [J]. *Energy Reports*. 2019.
- [140] Arslan E, Aktaş M, Can Ö F. Experimental and numerical investigation of a novel photovoltaic thermal (PV/T) collector with the energy and exergy analysis [J]. *Journal of Cleaner Production*. 2020, 276: 123255.
- [141] Yu C, Li H, Chen J, et al. Investigation of the thermal performance enhancement of a photovoltaic thermal (PV/T) collector with periodically grooved channels [J]. *Journal of Energy Storage*. 2021, 40: 102792.
- [142] Ramdani H, Ould-Lahoucine C. Study on the overall energy and exergy performances of a novel water-based hybrid photovoltaic-thermal solar collector [J]. *Energy Conversion and Management*. 2020, 222: 113238.
- [143] Teymori-Omran M, Motevali A, Seyedi S R M, et al. Numerical simulation and experimental validation of a photovoltaic/thermal system: Performance comparison inside and outside greenhouse [J]. *Sustainable Energy Technologies and Assessments*. 2021, 46: 101271.
- [144] Yao J, Liu W, Zhao Y, et al. Two-phase flow investigation in channel design of the roll-bond cooling component for solar assisted PVT heat pump application [J]. *Energy Conversion and Management*. 2021, 235: 113988.
- [145] Salari A, Parcheforosh A, Hakkaki-Fard A, et al. A numerical study on a photovoltaic thermal system integrated with a thermoelectric generator module [J]. *Renewable Energy*. 2020, 153: 1261-71.

- [146] Khanjari Y, Kasaeian A, Pourfayaz F. Evaluating the environmental parameters affecting the performance of photovoltaic thermal system using nanofluid [J]. *Applied Thermal Engineering*. 2017, 115: 178-87.
- [147] Wilkinson S, Hanna S, Hesselgren L, et al. Inductive aerodynamics' computation and performance [C]; *Proceedings of the 31st eCAADe Conference*, 2013.
- [148] Aziz A. Optimum dimensions of extended surfaces operating in a convective environment [J]. 1992.
- [149] Kraus A D, Aziz A, Welty J, et al. Extended surface heat transfer [J]. *Appl Mech Rev*. 2001, 54(5): B92-B.
- [150] Hosseinirad E, Khoshvaght-Aliabadi M, Hormozi F. Effects of splitter shape on thermal-hydraulic characteristics of plate-pin-fin heat sink (PPFHS) [J]. *International Journal of Heat and Mass Transfer*. 2019, 143: 118586.
- [151] Khoshvaght-Aliabadi M, Deldar S, Hassani S. Effects of pin-fins geometry and nanofluid on the performance of a pin-fin miniature heat sink (PFMHS) [J]. *International Journal of Mechanical Sciences*. 2018, 148: 442-58.
- [152] Ali H M, Arshad W. Effect of channel angle of pin-fin heat sink on heat transfer performance using water based graphene nanoplatelets nanofluids [J]. *International Journal of Heat and Mass Transfer*. 2017, 106: 465-72.
- [153] Yao J, Chen E, Dai Y, et al. Theoretical analysis on efficiency factor of direct expansion PVT module for heat pump application [J]. *Solar Energy*. 2020, 206: 677-94.
- [154] Page R P R. THERMOPHYSICAL PROPERTIES OF REFRIGERANTS [J]. 2009.
- [155] Kell G S. Density, thermal expansivity, and compressibility of liquid water from 0. deg. to 150. deg.. Correlations and tables for atmospheric pressure and saturation reviewed and expressed on 1968 temperature scale [J]. *Journal of Chemical and Engineering data*. 1975, 20(1): 97-105.
- [156] Shang D. Free convection film flows and heat transfer [M]. Springer, 2006.
- [157] Khanjari Y, Pourfayaz F, Kasaeian A. Numerical investigation on using of nanofluid in a water-cooled photovoltaic thermal system [J]. *Energy Conversion and Management*. 2016, 122: 263-78.
- [158] Ögüt E B. Natural convection of water-based nanofluids in an inclined enclosure with a heat source [J]. *International Journal of Thermal Sciences*. 2009, 48(11): 2063-73.
- [159] Kakaç S, Pramuanjaroenkij A. Review of convective heat transfer enhancement with nanofluids [J]. *International journal of heat and mass transfer*. 2009, 52(13-14): 3187-96.
- [160] Mishra P C, Mukherjee S, Nayak S K, et al. A brief review on viscosity of nanofluids [J]. *International nano letters*. 2014, 4(4): 109-20.
- [161] Yu W, Choi S. The role of interfacial layers in the enhanced thermal conductivity of nanofluids: a renovated Hamilton–Crosser model [J]. *Journal of Nanoparticle Research*. 2004, 6(4): 355-61.
- [162] Ansys I. ANSYS FLUENT Theory Guide: Release 14.0. 2011 [J]. Ansys Inc Canonsburg^ ePA PA.
- [163] Brackbill J U, Kothe D B, Zemach C. A continuum method for modeling surface tension [J]. *Journal of computational physics*. 1992, 100(2): 335-54.
- [164] Yakhot V, Orszag S A. Renormalization group analysis of turbulence. I. Basic theory [J]. *Journal of scientific computing*. 1986, 1(1): 3-51.

- [165] Versteeg H K, Malalasekera W. An introduction to computational fluid dynamics: the finite volume method [M]. Pearson education, 2007.
- [166] Argiriou A, Santamouris M, Assimakopoulos D. Assessment of the radiative cooling potential of a collector using hourly weather data [J]. *Energy*. 1994, 19(8): 879-88.
- [167] Duffie J. a., Beckman W a., Worek WM. Solar Engineering of Thermal Processes [J]. *Journal of Solar Energy Engineering*. 1994.
- [168] Erell E, Etzion Y. Radiative cooling of buildings with flat-plate solar collectors [J]. *Building and environment*. 2000, 35(4): 297-305.
- [169] Madams W. Heat Transmission, 1954 [M]. McGraw-Hill.
- [170] Aste N, Del Pero C, Leonforte F. Thermal-electrical optimization of the configuration a liquid PVT collector [J]. *Energy Procedia*. 2012, 30: 1-7.
- [171] Gaba V K, Tiwari A K, Bhowmick S. A report on performance of annular fins having varying thickness [J]. *ARNP J Eng Appl Sci*. 2016, 11(8): 5120-5.
- [172] Shah R K. Extended surface heat transfer [J]. *Thermopedia*, Feb. 2011, 14: 1-8.
- [173] Joshi A S, Tiwari A. Energy and exergy efficiencies of a hybrid photovoltaic–thermal (PV/T) air collector [J]. *Renewable Energy*. 2007, 32(13): 2223-41.
- [174] Hosseinzadeh M, Salari A, Sardarabadi M, et al. Optimization and parametric analysis of a nanofluid based photovoltaic thermal system: 3D numerical model with experimental validation [J]. *Energy Conversion and Management*. 2018, 160: 93-108.
- [175] Demir H, Dalkilic A, Kürekci N, et al. Numerical investigation on the single phase forced convection heat transfer characteristics of TiO₂ nanofluids in a double-tube counter flow heat exchanger [J]. *International Communications in Heat and Mass Transfer*. 2011, 38(2): 218-28.
- [176] Mahmoudi A H, Shahi M, Shahedin A M, et al. Numerical modeling of natural convection in an open cavity with two vertical thin heat sources subjected to a nanofluid [J]. *International Communications in Heat and Mass Transfer*. 2011, 38(1): 110-8.
- [177] Chiu C-H. A decomposition method for solving the convective longitudinal fins with variable thermal conductivity [J]. *International Journal of Heat and Mass Transfer*. 2002, 45(10): 2067-75.
- [178] Huang Y, Li X-F. Exact and approximate solutions of convective-radiative fins with temperature-dependent thermal conductivity using integral equation method [J]. *International Journal of Heat and Mass Transfer*. 2020, 150: 119303.
- [179] Miansari M, Ganji D, Miansari M. Application of He's variational iteration method to nonlinear heat transfer equations [J]. *Physics Letters A*. 2008, 372(6): 779-85.
- [180] Rajabi A. Homotopy perturbation method for fin efficiency of convective straight fins with temperature-dependent thermal conductivity [J]. *Physics Letters A*. 2007, 364(1): 33-7.
- [181] Kern D, Kraus A. Extended surface heat transfer, 1972 [M]. McGraw-Hill, New York, NY.
- [182] Boumaaraf B, Touafek K, Ait-Cheikh M S, et al. Comparison of electrical and thermal performance evaluation of a classical PV generator and a water glazed hybrid photovoltaic–thermal collector [J]. *Mathematics and Computers in Simulation*. 2020, 167: 176-93.
- [183] Bruus H. Theoretical microfluidics [M]. Oxford university press, 2007.
- [184] Kong X, Li Y, Lin L, et al. Modeling evaluation of a direct-expansion solar-assisted heat pump water heater using R410A [J]. *International Journal of Refrigeration*. 2017, 76: 136-46.

- [185] Lenz J. Polytropic exponents for common refrigerants [J]. 2002.
- [186] Karassik I J. Pump Handbook Fourth Edition, Dec. 18, 2007 [M]. McGraw Hill, New York, NY.
- [187] Taler D, Taler J. Simple heat transfer correlations for turbulent tube flow [C]; E3S Web of conferences, 2017. EDP Sciences.
- [188] Selmi M, Al-Khawaja M J, Marafia A. Validation of CFD simulation for flat plate solar energy collector [J]. Renewable energy. 2008, 33(3): 383-7.

Publications and projects during PhD Period

I. Publications

1. **Pie Basalike**, Wang Peng, Jili Zhang, Shixiang Lu. Numerical analysis of Roll Bond Photovoltaic Thermal working as a condenser during nighttime. **Renewable Energy** (SCI, IF: 8.634), 194-206 (2022).
2. **Pie Basalike**, Wang Peng, Jili Zhang, Shixiang Lu. Numerical investigation on the performance and environmental aspect of roll bond photovoltaic thermal unit condenser incorporating fins on the absorber [J]. **Energy** (SCI, IF: 8.857), 123915 (2022)
3. **Pie Basalike**, Wang Peng, Jili Zhang, Shixiang Lu. Numerical investigation on the performance characteristics of Photovoltaic Thermal refrigerator integrating phase change material and with water/nanofluid as fluid medium (J). **Journal of Energy Storage** (SCI, IF: 8.907), 103453 (2021).
4. **Pie Basalike**, Wang Peng, Jili Zhang, Shixiang Lu, Ahmad Riaz. Numerical investigation on the performance characteristics and sustainability of dual function roll bond photovoltaic thermal unit integrating a novel channel(J). **Energy**. Under review
5. **Pie Basalike**, Wang Peng, Jili Zhang. Numerical study on the performance of roll bond photovoltaic thermal unit condenser with water/nanofluids as fluids medium (J). **Renewable Energy** (SCI, IF: 8.634), 606-616 (2022).
6. Youhua Han, Yang Liu, Shixiang Lu, **Pie Basalike**, Jili Zhang. Electrical performance and power prediction of a roll-bond photovoltaic thermal array under dewing and frosting conditions (J). **Energy** (SCI, IF: 8.857), 121758 (2021).

II. Projects

1. Science and technology assistance project of the Ministry of science and technology to developing countries in 2020 (KY20202012): key technology of low-energy solar photovoltaic photothermal building integration, 2.7million yuan RMB, from September 1, 2020 to August 31,2023, led by Zhang Jili.
2. The innovation leading talents project of Liaoning Province's "rejuvenating Liaoning Talents Program" in 2020: key technology of solar photovoltaic solar heat pump cogeneration (XLYC1902068), 1million yuan RBM, from January 1, 2020 to December 31, 2022, let by Zhang Jili.

Acknowledgement

First and foremost, I say a very big thanks to my supervisor Professor Dr. Jili Zhang for accepting me in his research group. I would like to thank him for encouraging my research and for allowing me to grow as a research scientist. His advices on both research as well as on career have been invaluable.

I would also wish to express my gratitude to Dr. Peng Wang for extended discussions and valuable suggestions which have contributed to the improvement of the thesis.

This thesis has been written during my stay at the Dalian university of technology, Institute of Building Energy (IBE). I would like to thank all the staff members of IBE; Dr. Liangdong Ma, Dr. Tianyi Zhao, Dr. Ruobing Liang and Dr. Zhao Yu.

I would like to acknowledge my best friends who supported me during my time here. First and foremost, I would like to thank Dr. Chao Zhou, Luonan Li, Xiaochao Guo, Li Zhiwei and Dr. Ahmad Riaz for your friendship, love and unyielding support.

I cannot forget a good time I spent with friends and Building Energy lab colleagues. In particular, I would like to thank Dr. Shixiang Lu, Dr. Li Wei, Dr. Keyan Ma, Dr. Nina Shao, Tianjiao Zhang and Youhua Han for their encouragement and valuable time.

Without financial support it couldn't be easier for me to get all the necessary means and complete this PhD. In this regard, I would like to thank the Chinese Scholarship Council (CSC), Science Technology Partnership Program (Supported by Science and Technology Partnership Program, Ministry of Science and Technology of China (KY20202012)), Liao Ning Revitalization Talents Program (Supported by Liao Ning Revitalization Talents Program (XLYC1902068)) and the National Key Research and Development Project of China.

Finally, a special thanks goes to my family. Words cannot express how grateful I am to my Mother, Father, brothers and sisters for all the sacrifices you've made on my behalf. Your prayer for me was what sustained thus far.

Pie Basalike

Date: 19/09/2022

Curriculum Vitae

Name: Pie Basalike

Gender: Male

Date of Birth: 1985-06-01

Nationality: Rwandan



Research Area: PVT heat Pump system, PVT units working as a condenser during night

Educational Experience:

B.Sc. (Mechanical engineering) (2006-2011)

Kigali Institute of Science and Technology (KIST), Kigali, Rwanda

M.Sc. (Sustainable Energy Systems) (2013-2015)

Mälardalen University, Sweden

Ph.D. (Heating, Ventilation and Air Conditioning Engineering) (2017-2022)

Institute of Building Energy, Dalian University of Technology, Dalian, PR China

Dalian University of Technology Doctoral Dissertation

Copyright Use Authorization

I fully understand relevant regulations regarding university dissertation copyright. Copyright of theses at university during PhD period belongs to Dalian University of Technology, allowing theses to be consulted and borrowed. University has right to retain theses and submit copies and electronic editions to national departments and institutions concerned. University can index relevant database for retrieval using part or the whole of this dissertation. University can photocopy, print in reduced format or scan to keep and compile this dissertation.

Dissertation Title: Numerical Simulation of Enhanced Heat Transfer of PVT Unit Under
Condensation and Cooling Conditions

Author's Signature:  Date: 2022/09/19

Supervisor's Signature:  Date: 2022/09/21

Chairman's Signature:  Date: 2022/09/22

大连理工大学学位论文版权使用授权书

本人完全了解学校有关学位论文知识产权的规定，在校攻读学位期间论文工作的知识产权属于大连理工大学，允许论文被查阅和借阅。学校有权保留论文并向国家有关部门或机构送交论文的复印件和电子版，可以将本学位论文的全部或部分内容编入有关数据库进行检索，可以采用影印、缩印、或扫描等复制手段保存和汇编本学位论文。

学位论文题目 : 冷凝与冷却条件下 PVT 组件强化传热数值模拟研究

作者签名 :  日期 : 2022 年 09 月 19 日

导师签名 :  日期 : 2022 年 09 月 21 日

答辩委员会主席 :  日期 : 2022 年 09 月 22 日